sIHF IS A NOVEL NUCLEOID-ASSOCIATED PROTEIN SPECIFIC TO THE ACTINOBACTERIA

sIHF IS A NOVEL NUCLEOID-ASSOCIATED PROTEIN SPECIFIC TO THE ACTINOBACTERIA

By

JULIA PATRYCJA SWIERCZ, B.Sc. (H)

A Thesis
Submitted to the School of Graduate Studies
In Partial Fulfillment of the Requirements
Of the Degree
Doctor of Philosophy

McMaster University

DOCTOR OF PHILOSOPHY (2013) McMaster University

(Biology) Hamilton, Ontario

TITLE: sIHF is a novel nucleoid-associated protein specific to the actinobacteria

AUTHOR: Julia Patrycja Swiercz, B.Sc. (H) (McMaster University)

SUPERVISOR: Dr. Marie A. Elliot

NUMBER OF PAGES: xii, 133

ABSTRACT

The relatively recent discoveries of bacterial small RNAs (sRNAs) and their important regulatory functions prompted us to conduct a genome wide survey for sRNAs in *Streptomyces coelicolor*. We used a combined bioinformatics and experimental approach to identify and characterize six sRNAs. sRNA expression profiles were determined throughout *S. coelicolor* development, including vegetative and reproductive growth, during growth on minimal and rich media. Additionally, we also tested sRNA expression in various *S. coelicolor* developmental mutants. Two sRNAs were expressed exclusively during growth on one medium type and all but one were expressed constitutively throughout growth apart from the late sporulation timepoint. One of the identified sRNAs, scr1906, appeared to be closely associated with development. scr1906 was only expressed in nutrient limiting conditions just prior to aerial development and sporulation. Expression of scr1906 was abolished in a mutant that was defective in sporulation (due to a mutation in the sporulation sigma factor gene, *whiG*); however, expression was detected in mutants of both known σ^{WhiG} target genes, *whiH* and *whiI*, which encode sporulation transcription factors. Intriguingly, *in silico* analysis predicted *whiH* to be a direct target for scr1906-mediated regulation based on potential nucleotide binding sites. The effects of deletion and overexpression of *scr1906* on WhiH levels were tested, but require further experimentation.

In a separate line of investigation, we sought to characterize a novel actinobacterial-specific protein named sIHF. The *sIHF* mutant strain revealed that sIHF influenced DNA compaction and segregation during *S. coelicolor* sporulation and also affected antibiotic production. sIHF associated with the nucleoid, and *in vitro*, it bound to DNA non-specifically in a length dependent manner, although it was determined to have a preference for three distinct DNA motifs. Like most nucleoid-associated proteins, sIHF affected gene expression indicating the potential for an additional role as a transcription factor. Interestingly, sIHF impacted the activity of topoisomerase. Leveraging information that we have gained from the sIHF-DNA co-crystal complex, studies aimed at characterizing the sIHF regions that are important for DNA interaction and topoisomerase modulation are currently underway.

ACKNOWLEDGEMENTS

First and foremost, I want to thank Dr. Marie Elliot for being an incredible supervisor and inspirational mentor to me during my Ph.D. training. Dr. Elliot encouraged me to never give up and was always tremendously patient with me when I needed help. Without question, Dr. Elliot's guidance and support throughout these years were instrumental to the success of this thesis.

I would like to thank the members of my supervisory committee, Dr. Turlough Finan and Dr. Eric Brown, for helpful discussions and for continually challenging me to think about my research from different perspectives. Thank you to our collaborators, Dr. Alba Guarné, Tamiza Nanji and Melanie Gloyd, for their invaluable contributions to this work and for our engaging scientific discussions. I would also like to thank the members of the Li lab, specifically Dr. Simon McManus and Dr. Wendy Mok, for their time and willingness to help me with my work.

My graduate school experience would not have been the same without the group of individuals I was fortunate to work with over the past six years. I would like to thank all the members of the Elliot lab, past and present, for filling these years with unforgettable memories. In particular, I would like to thank: Dave Capstick (for always helping me and making me laugh), Daphne Gao (for advice and encouragement), Henry Haiser (for coffee break chats and for always being thoughtful), Hindra (for always being willing to help), Emma Sherwood (for all the 'pep' talks), Mary Yousef (for being incredibly caring and inspirational), Andrew Duong (for his warm heart and generosity), Matthew Moody (for being a '*moo moo*' and a support system when times were tough), Stephanie Jones and Danielle Sexton (for being the world's best 'baby' grad students), Renee St-Onge (for being the only other member of the 'early morning club'), and Rachel Young (for always siding with me!).

Additionally, I would like to thank all my friends that supported me outside of school. In particular, many thanks go to Chantal Januszkiewicz and Julia Stegner, for being caring friends and for always making sure I enjoyed my life outside of the lab. Thank you to Emilia Stpicki for being exceedingly helpful and my first STM friend! Also, thank you to my life-long friends, Anna and Justyna Terlecka, for all our keepsake memories and for those to come. Thanks to my sister, Marta Swiercz, for her unconditional friendship and wise-beyond-her-years advice. The end of this long journey has included one of the most important people in my life, Jonathan Beardall, who has been incredibly understanding and supportive throughout this process.

Finally, I would like to thank my parents. They provided an environment in which I could follow my dreams and were supportive and encouraging. I hope to always strive to be as amazing as my parents are – to them I dedicate this thesis.

TABLE OF CONTENTS

Chapter 3: Small RNA Regulators in *S. coelicolor*

LIST OF FIGURES

LIST OF TABLES

LIST OF ABBREVIATIONS

^{32}P	phosphorous-32 isotope
6×-His	hexa-histidine
A	adenine
Å	Angstrom
aa	amino acid
ATP	adenosine triphosphate
ATPase	adenosine triphosphatase
B2H	bacterial two-hybrid
bld	bald
bp	base pair
BSA	bovine serum albumin
C	cytosine or
C	carboxyl or
C	Celsius
CDA	calcium-dependent antibiotic
cDNA	complementary DNA
ChIP-Seq	chromatin-immunoprecipitation sequencing
cm	centimetre
dATP	2′-deoxyadenosine-5′-triphosphate
DAPI	4',6-diamidino-2-phenylindole
dCTP	2′-deoxycytosine 5′-triphosphate
dGTP	2′-deoxyguanosine 5′-triphosphate
dH_20	distilled water
DMSO	dimethyl sulfoxide
DNA	deoxyribonucleic acid or
DNA	Difco nutrient agar
DNase	deoxyribonuclease
dNTP	deoxyribonucleotide
Dps	DNA-binding protein from starved cells
dsDNA	double stranded DNA
DTT	dithiothreitol
dTTP	2′-deoxythymine 5′-triphosphate
eGFP	enhanced green fluorescent protein
EDTA	ethylenediaminetetraacetic acid
EMSA	electrophoretic mobility shift assay
Fis	factor for inversion stimulation
FLP	flippase
FRT	FLP recognition target
fwd	forward
G	guanine or
g	grams or
g	gravity
H-NS	heat stable nucleoid-structuring protein

HU	heat unstable protein
IHF	integration host factor
IPTG	isopropyl β-D-1-thiogalactopyranoside
kb	kilo base pair
kDa	kilo Daltons
L	litre
LB	Luria Bertani
Lrp	leucine responsive regulatory protein
M	molar
Mb	mega base pairs
mg	milligram
ml	millilitre
mm	millimetre
MM	minimal medium
mM	millimolar
mRNA	messenger RNA
MS	mannitol soy flour agar
NAP(s)	nucleoid-associated protein(s)
ng	nanogram
Ni-NTA	nickel-nitrilotriacetic acid
nm	nanometre
nM	nanomolar
nt	nucleotide
OD	optical density
P buffer	protoplast buffer
PAGE	polyacrylamide gel electrophoresis
PBS	phosphate buffered saline
PCR	polymerase chain reaction
PEG	polyethylene glycol
pH	potential of hydrogen
pI	isoelectric point
pmol	picomole
poly (dI-dC)	poly(deoxyinosinic-deoxycytidylic) acid sodium salt
PVDF	polyvinylidene fluoride
RT-qPCR	Reverse transcription, quantitative PCR
RBS	ribosome binding site
rev	reverse
RLM-RACE	FirstChoice® RNA ligase mediated 5′-rapid amplification of cDNA ends
RM	rich medium
RNA	ribonucleic acid
RNA-Seq	RNA sequencing
Rpf	resuscitation promoting factor
RNase	ribonuclease
rpm	revolutions per minute

rRNA	ribosomal RNA
SALP	SsgA-like proteins
SASP	small acid-soluble protein
Scp	segregation and condensation proteins
SDS	sodium dodecyl sulfate
SELEX	systematic evolution of ligands by exponential enrichment
SMC	structural maintenance of chromosomes
sRNA	small RNA
SSC	saline sodium citrate
ssDNA	single stranded DNA
Swl	*Streptomyces* cell wall lytic enzyme
T	thymine
TBS	Tris-buffered saline
TBST	Tris-buffered saline and Tween 20
TEG	Tris-EDTA-glucose
TEM	transmission electron microscopy
TES	N-Tris(hydroxymethyl)methyl-2-aminoethanesufonic acid
tRNA	transfer RNA
Tris	Tris(hydroxymethyl)aminomethane
TSB	tryptone soy broth
UV	ultra-violet
U	units
V	volts
whi	white
WT	wild type
X-gal	5-bromo-4-chloro-3-indolyl-β-D-galactopyranoside
YEME	yeast extract-malt extract
YT	yeast tryptone broth
Z-ring	FtsZ-ring
µg	microgram
µl	microlitre
µM	micromolar

CHAPTER 1

GENERAL INTRODUCTION

1.1 The actinomycetes

The actinomycetes are a group of Gram-positive bacteria that constitute the order *Actinomycetales*, a major subdivision of the Eubacteria. Initially, these microorganisms were erroneously considered to be fungi due to their filamentous and sporogenic life cycle and, consequently, their name was derived from the Greek words meaning 'ray fungus' (Hopwood, 1999). Despite being first described in 1877 (Harz, 1877), it was not until the 1950s that *Streptomyces*, an actinomycete, was discovered to be a bacterium: it possesses a cell wall characteristic of Gram-positive bacteria and lacks a nuclear envelope (Hopwood, 2007a).

The actinomycetes are well represented in the soil but can also be found in freshwater and marine environments (Goodfellow and Williams, 1983). Most actinomycetes are saprophytes that contribute to the breakdown of complex organic matter into readily available nutrients. In addition to these ecological benefits, some actinomycetes, namely the *Streptomyces*, are producers of numerous bioactive compounds with pharmaceutical and agricultural significance (Bérdy, 2005). A small proportion of actinomycetes are pathogenic; these include the causative agents of tuberculosis (*Mycobacterium tuberculosis*), leprosy (*M. leprae*), and diphtheria *(Corynebacterium diphtheriae*) (Stackebrandt and Woese, 1981).

1.1.1 The genus *Streptomyces*

In the 1940s, one of the first medically relevant antibiotics, streptomycin, was isolated from *Streptomyces griseus* (Jones *et al.*, 1944). This discovery prompted the search for other compounds of clinical and biotechnological importance produced by the actinomycetes. Today, two-thirds of all the antibiotics produced by microorganisms come from the actinomycetes (Kieser *et al.*, 2000), and 80% of these are produced by the streptomycetes (Kieser *et al.*, 2000). *Streptomyces* are also producers of other medically relevant compounds, including fungicides, anti-cancer agents and immune-suppressants (Kieser *et al.*, 2000; Bérdy, 2005; Hopwood, 2007b). Intriguingly, analysis of *Streptomyce*s genome sequences has revealed large numbers of previously unidentified gene clusters resembling those of known secondary metabolite biosynthetic pathways. For example, before the *S. coelicolor* genome was sequenced, only four clusters involved in antibiotic production had been characterized (Hopwood *et al.*, 1995; Chong *et al.*, 1998; Bentley *et al.*, 2002); however, analysis of the sequenced genome revealed 28 additional clusters that appeared to direct the synthesis of novel secondary metabolites (Bentley *et al.*, 2002; Nett *et al.*, 2009), implying that *S. coelicolor* likely produces many more compounds than previously recognized. Understanding the regulation of these clusters in *S. coelicolor* and those in other actinomycetes might permit the identification of novel compounds with medical significance (Challis and Hopwood, 2003). This is of major importance due to the dramatic increase in the numbers of antibiotic resistant microbial pathogens and a corresponding decline in

antibiotic discovery (Wright, 2007).

S. coelicolor is a model streptomycete, and has been the most thoroughly studied genetically (Hopwood, 1999). Historically, *S. coelicolor* produces four known antibiotics: actinorhodin, undecylprodigiosin, methylenomycin and calcium-dependent lipopeptide antibiotic (CDA). Actinorhodin and undecylprodigiosin are pigmented blue and red, respectively, making it easy to study the genetics of these two systems, given the ease of identifying mutations that impact (positively or negatively) the production of these two pigmented compounds. CDA, which is closely related to the clinical antibiotic daptomycin (Enoch *et al.*, 2007), has antimicrobial activity against a wide range of Gram-positive bacteria (Lakey *et al.*, 1983), whereas undecylprodigiosin has anti-cancer activity (Ho *et al.*, 2007). Methylenomycin has antibiotic activity against Gram-positive and Gram-negative bacteria (Haneishi *et al.*, 1974), as does actinorhodin based on preliminary results (Nodwell lab, unpublished).

S. coelicolor contains a linear 8.7 Mb chromosome with an approximate 70% G+C content (Bentley *et al.*, 2002). It also harbours two plasmids (Bibb *et al.*, 1977; Bentley *et al.*, 2002), SCP1 (linear and 365 Kb) and SCP2 (circular and 31 kb), in addition to a third plasmid integrated into the chromosome, SLP1 (17 kb) (Bibb and Hopwood, 1981; Omer *et al.*, 1988). The linear chromosome comprises two chromosome "arms" flanking a central "core". This core region extends from ~1.5 Mb to 6.4 Mb (Bentley *et al.*, 2002), and contains genes that code for essential proteins, such as those required for DNA replication, transcription and translation, whereas genes encoding non-essential proteins, like those involved in secondary metabolism, are typically found within the "arms" (Kirby, 2011). Out of the predicted 7,825 protein-encoding genes, 12.3% are expected to encode regulators (Bentley *et al.*, 2002) reflecting the complex networks likely needed to regulate the elaborate *Streptomyces* life cycle.

1.2 Life cycle of *Streptomyces coelicolor*

The *S. coelicolor* life cycle (Figure 1.1) is characterized by its progression through distinct differentiated stages. Growth initiates with the germination of a free spore. The initial germ tubes grow via hyphal tip extension. These hyphal filaments subsequently branch, and this repeated extension and branching ultimately leads to the formation of a dense mycelial network of vegetative hyphae termed the vegetative mycelium. Vegetative hyphae have relatively sparse and irregularly positioned cross walls, which creates compartments of varying size, each of which carry multiple copies of uncondensed chromosomes. Complex regulatory networks, which have yet to be fully elucidated, are involved in the morphological transition from vegetative growth to reproductive development. Nutrient depletion, and possibly other stimuli, is thought to trigger the emergence of a second cell type, the aerial hyphae, from the vegetative milieu. These aerial hyphae must first break through the air-water interface at the surface of a developing colony, before extending into the air. Secondary metabolite production, and in particular antibiotic production, is intimately associated with the onset of aerial growth (Elliot *et al.*, 2008).

Like the vegetative hyphae, aerial hyphae grow via hyphal tip extension, but they do not branch (Flärdh, 2003b). An unknown signal arrests aerial hyphae elongation prior to converting the aerial hyphae into spore chains. This process involves a synchronized round of septation and chromosome segregation (Chater, 2001). Prespore compartments are created when sporulation septa are laid down at regularly spaced intervals within the aerial hyphae, resulting in about 50 prespore compartments per aerial cell. Coinciding with septation, chromosomes are condensed and segregated such that each compartment receives an equivalent amount of chromosomal DNA (typically thought to be a single chromosome, although unpublished work from the laboratory of Dr. Joseph McCormick has suggested that spores may be diploid). To develop into spores, each prespore compartment must undergo a number of maturation steps, culminating with the assembly of a thick spore wall, deposition of a grey spore pigment and rounding of the spore. Mature spores have low metabolic activity and during the final stages of the life cycle, cell separation results in the release of individual spores into the environment.

1.2.1 Vegetative growth

Streptomyces germination is not well understood; only a few parallels can be drawn from the well-characterized germination process of the Gram-positive endospore-forming bacterium *Bacillus subtilis*. During *Streptomyces* germination, germ tubes extend from spores and grow by apical tip extension, a process that completely depends on DivIVA, an essential coiled-coil protein that directs the deposition of new cell material at the cell pole (Flärdh, 2003a; Flärdh, 2003b). This is in contrast to most rod-shaped bacteria, where the cytoskeletal protein MreB directs this deposition to the lateral wall (Carballido-López and Errington, 2003). As vegetative cells elongate, DivIVA aggregates can 'break off' of the tip complex, and accumulate at new sites, effectively marking the site of future branch formation (Hempel *et al.*, 2012). This leads to the formation of a dense network of vegetative cells. Cell division is infrequent during vegetative growth with cross walls occasionally forming within hyphae to create long multi-genomic cells.

1.2.2 Aerial growth

Aerial hyphae formation depends on a group of proteins encoded by the '*bld*' (for bald) genes, as determined by the fact that colonies lacked 'fuzzy' aerial hyphae when these genes were mutated (Figure 1.2). Antibiotic production is also impaired in many *bld* mutants, highlighting the shared regulatory connections between aerial development and secondary metabolite production (Chater, 1993). There are 12 classic *bld* genes that have been described (named *bldA*-*D*, *G*-*N*). Mutants of these genes are further subdivided into two groups: conditional and non-conditional mutants. Normal aerial mycelium formation is rescued in conditional mutants under certain growth conditions, whereas non-conditional mutants are defective in aerial hyphae formation under all growth conditions. An example of a conditional mutant is Δ*bldA*. Unlike most *bld* genes, which encode regulatory proteins, *bldA* encodes the only tRNA specific for the rare UUA leucine codon in *S. coelicolor* (Leskiw *et al.*, 1991). Out of the 7,827 predicted *S. coelicolor* genes, ~146 contain TTA codons,

including *bldH* and several genes encoding pathway-specific antibiotic regulators, rendering the *bldA* mutant unable to raise aerial hyphae (Takano *et al.*, 2003; Nguyen *et al.*, 2003) or produce antibiotics (Lawlor *et al.*, 1987). Aerial hyphae formation is rescued in the *bldA* mutant during growth on media containing mannitol or maltose as a carbon course (Kelemen and Buttner, 1998); however, antibiotic production is not restored (Merrick, 1976; Champness, 1988). An example of a non-conditional mutant is Δ*bldB*, which is also defective in antibiotic production (Pope *et al.*, 1998; Eccleston *et al.*, 2002) . The function of BldB is unknown; however, overexpression of a mutant BldB protein (dimerization competent but functionally defective), results in an accelerated sporulation phenotype (Eccleston *et al.*, 2006). Further investigation is required to elucidate the implications of this result.

The *bld* gene products are required for the production of structural molecules, including the SapB surfactant peptide and eight hydrophobic proteins designated the 'chaplins' (Elliot *et al.*, 2003; Elliot and Talbot, 2004; Claessen *et al.*, 2006), which are also required for aerial hyphae development. By coating the nascent aerial hyphae, these molecules lower the surface tension at the air-water interface, thereby allowing aerial cells to emerge from the aqueous soil environment into the air. The chaplins are essential for aerial hyphae formation on minimal and rich media, while SapB appears to be required only during growth on the latter (Capstick *et al.*, 2007).

As aerial hyphae cells elongate, there are regulatory mechanisms in place so as to prevent premature sporulation. For instance, the integral membrane protein CrgA (for **c**oordination of **r**eproductive **g**rowth) inhibits sporulation septation prior to the growth arrest of aerial hyphae. CrgA is an integral membrane protein and its expression peaks at the start of aerial development, and declines in the lead-up to sporulation (Del Sol *et al.*, 2006). The loss of functional CrgA results in accelerated aerial hyphae formation and enhanced septation (Del Sol *et al.*, 2003), while its overexpression prevents FtsZ-ring (Z-ring) formation, leading to a sporulation deficient phenotype (Del Sol *et al.*, 2006). These defects are only observed when the *crgA* mutants are grown on rich media, implying that something else coordinates Z-ring formation during growth on minimal media.

1.2.3 Sporulation

Proteins involved in initiating sporulation septation are considered to be 'early' regulators of sporulation and are crucial for the normal development of spores. Strains bearing mutations in these genes are termed "*whi*" (white) mutants, due to the absence of the grey spore-associated pigment deposited on mature spores – the final stage in sporulation (Figure 1.2). Those characterized in *S. coelicolor* include: *whiA*, *whiB, whiG, whiH* and *whiI*, along with *ssgA* and *ssgB*. WhiG, a sporulation-specific sigma factor, is the earliest acting Whi regulator and is therefore a key activator of sporulation (Mendez and Chater, 1987; Chater *et al.*, 1989). The only known targets of σ^{WhiG} are *whiH* and *whiI*, encoding a GntR family transcription factor and an atypical response regulator, respectively (Ryding *et al.*, 1998; Aínsa *et al.*, 1999). *whiG* mutants form aerial hyphae with widely spaced vegetative-like cross walls (Flärdh *et al.*, 1999) and exhibit no obvious chromosome

condensation. In contrast, chromosome condensation has been detected in a *whiH* mutant (Ryding *et al.*, 1998). The aerial hyphae erected by *whiG, whiH* and *whiI* mutants are all of roughly equivalent length to those observed in wild type strains. This is not, however, the case for *whiA* and *whiB* mutants, which develop abnormally long aerial hyphae and exhibit no chromosome condensation. This may indicate that these strains are unable to sense whatever signals the arrest of aerial hyphae growth prior to sporulation septation (Flärdh *et al.*, 1999). WhiA is a sporulation-specific transcription factor (Kaiser and Stoddard, 2011) conserved among Gram-positive bacteria, whereas WhiB is a small, Fe-S cluster-containing actinomycete-specific protein that may function as a putative transcription factor (Davis and Chater, 1992; Aínsa *et al.*, 1999). SsgA and SsgB are also essential for sporulation septation (van Wezel *et al.*, 2000; Keijser *et al.*, 2003), but will be discussed in more detail below.

Other *whi* genes whose products act during in the later stages of sporulation have also been identified. Although their corresponding mutants still exhibit a white phenotype (due to the lack of spore-associated pigment), these *whi* mutants nevertheless develop spores, albeit abnormal ones. A deletion mutant of the late sporulation-specific sigma factor, SigF, develops irregular, thin-walled spores with uncondensed chromosomes (Potúcková *et al.*, 1995). A *whiD* mutant - where WhiD belongs to the same protein family as WhiB - develops thin-walled spores of varying shapes and sizes due to abnormal septal placement (Molle *et al.*, 2000). Finally, WhiE is involved in the synthesis of the grey polyketide spore pigment of mature spores. One of the last steps in spore maturation is considered to be the deposition of the grey polyketide pigment onto the spore coat and, therefore, the spores of *whiE* mutants remain white, but are not actually morphologically defective (McVittie, 1974; Davis and Chater, 1990).

In addition to the Whi proteins, there are a number of other proteins that contribute to *Streptomyces* sporulation. Among these is the tubulin-like FtsZ protein that polymerizes into a ring-like structure termed the 'Z-ring', at future sites of cell division (Margolin, 2005; Adams and Errington, 2009). In most bacteria, FtsZ is essential; however, in *S. coelicolor*, it is dispensable for vegetative growth and is only critical for sporulation (McCormick *et al.*, 1994). Upregulation of *ftsZ* expression in aerial hyphae is thought to produce the necessary levels of FtsZ to enable Z-ring 'ladder' assembly, which initiates the sporulation process (Flärdh *et al.*, 2000). None of the early *whi* mutants show increased *ftsZ* transcription during aerial development (Flärdh *et al.*, 2000), suggesting that inadequate FtsZ levels contribute to their failure to form sporulation septa.

During the onset of sporulation, FtsZ first forms helical filaments along the length of the aerial hyphae. These filaments are later resolved into regularly spaced Z-rings that define the future spore compartments (Schwedock *et al.*, 1997; Grantcharova *et al.*, 2005). A number of proteins contribute to proper Z-ring formation and localization. In mutants of the cell division genes *ftsW* and *ftsI*, FtsZ fails to form Z-rings, with only occasional spirals being detected after an extended growth period (Mistry *et al.*, 2008; Bennett *et al.*, 2009). *ftsW* and *ftsI* are located immediately upstream of *ftsZ* and both encode membrane proteins, where FtsW is associated with cell **s**hape, **e**longation, **d**ivision and **s**porulation (SEDS) (Henriques

et al., 1998), and FtsI is involved in peptidoglycan remodeling (Botta and Park, 1981). Although direct interactions between FtsZ, FtsW and FtsI have not been shown in *S. coelicolor*, FtsW was revealed to interact directly with FtsZ (Datta *et al.*, 2002) and FtsI (Datta *et al.*, 2006) in *M. tuberculosis*. Loss of equivalent interactions in *S. coelicolor* could be responsible for the lack of Z-ring assembly in the *ftsW* and *ftsI* mutants.

Two other proteins having a crucial role in Z-ring formation are SsgA and SsgB. SsgA first localizes to future division sites, where it then recruits SsgB. SsgB in turn interacts with the N-terminus of FtsZ to promote Z-ring assembly (Willemse *et al.*, 2011). Although an *ssgA* mutant develops a *whi* mutant phenotype, limited sporulation is observed upon prolonged incubation on mannitol-containing medium (van Wezel *et al.*, 2000), suggesting that other proteins could be compensating for SsgA. Candidate compensatory proteins include the other five SALPs (**S**sg**A**-**l**ike **p**roteins) encoded by *S. coelicolor* (Noens *et al.*, 2005; Traag and van Wezel, 2008).

After successful placement of Z-rings within the aerial hyphae, septation is needed to define the spore compartments. This involves invagination of the membrane, which is coordinated by several membrane proteins, including FtsL, DivIC and FtsQ, which form a complex in *Escherichia coli* and *B. subtilis* (Buddelmeijer and Beckwith, 2002a; Errington *et al.*, 2003). FtsL and DivIC are small proteins that are predicted to form a heterodimer in the membrane (Sievers and Errington, 2000), and it is proposed that FtsL recruits other members of the cell division machinery to the division site (Gonzalez *et al.*, 2010); however, the precise roles played by these proteins in cell division have not been confirmed. Unlike in *E. coli* (Guzman *et al.*, 1992; Buddelmeijer *et al*., 2002b) and *B. subtilis* (Levin and Losick, 1994; Daniel *et al.*, 1996), FtsL and DivIC are not essential for viability in *S. coelicolor* (Bennett *et al.*, 2007). In single or double mutants of *ftsL* and/or *divIC*, occasional spore chains are detected; however, the majority of septating aerial hyphae exhibit shallow constrictions at regularly spaced intervals, suggesting a failure in complete septation (Bennett *et al.*, 2007). This indicates that Z-ring formation is unaffected in these mutants but that septum synthesis is obstructed. The septal defect is more pronounced when either single mutant is grown on a high osmolarity, rich medium (Bennett *et al.*, 2007), indicating that septation could be regulated differently during stress. An *ftsQ* mutant exhibits a similar phenotype as the *ftsL* and *divIC* mutants in *S. coelicolor* (Mistry *et al.*, 2008) indicating the complex in *B. subtilis* and *E. coli* could be conserved in *S. coelicolor*.

1.2.4 Spore maturation

Following prespore compartment delineation by sporulation septa, the next stage of sporulation involves spore maturation, which includes generating a thick spore coat and rounding out of each spore compartment within spore chains. Although the composition of the *Streptomyces* spore coat is not well defined, analogies based on the *Bacillus* spore wall (Atrih and Foster, 1999) infer it to contain spore-specific proteins and a thick layer of peptidoglycan with a different structure compared with the vegetative and aerial hyphae walls.

In rod-shaped bacteria, MreB, an actin-like cytoskeletal protein, determines cell shape (van den Ent *et al.*, 2001). In spore-forming actinomycetes, MreB is instead

important during sporulation, and in particular, is important for spore wall development. Although, vegetative growth is unimpeded in an *S. coelicolor mreB* mutant, aerial hyphae are prone to lysis, spores are susceptible to heat and detergent and furthermore germinate prematurely (Mazza *et al.*, 2006). MreB localizes dynamically throughout *S. coelicolor* aerial cell development (Mazza *et al.*, 2006): it is first located at future sites of septa formation and then at the poles of spore compartments following septation. MreB appears to coat the interior of developing spores prior to loss of localization within mature spores (Mazza *et al.*, 2006). *mreB* is found in an operon with two other genes, *mreC* and *mreD*. Strains bearing mutations in these genes and in *pbp2* and *sfr*, two genes that are independently transcribed and found immediately downstream of the *mreBCD* cluster, exhibit the same phenotype as an *mreB* mutant (Kleinschnitz *et al.*, 2011) suggesting that the products of these genes act in the same pathway. *mreC*, *mreD* and *sfr* encode integral membrane proteins, while *pbp2* encodes an extracytoplasmic peptidoglycan biosynthesis protein (PBP2). Interestingly, MreB likely interacts with RodZ, another integral protein, which in turn has been shown to interact with MreC, MreD, PBP2, Sfr and FtsI (Kleinschnitz *et al.*, 2011), implying a direct connection between cell division and spore maturation. The effects of these interactions have yet to be tested directly.

The final stage in the developmental process involves the release of mature spores from the spore chain. Detachment of spores appear to involve the autolytic activity of RpfA (**r**esuscitation **p**romoting **f**actor **A**) and Swl (***S****treptomyces* cell **w**all **l**ytic enzyme) hydrolase proteins (Haiser *et al.*, 2009) along with two SALPs (**S**sg**A**-**l**ike **p**roteins), SsgE and SsgF. Rfp and Swl proteins are implicated in spore wall remodeling; however, the exact function of each is unknown (Haiser *et al.*, 2009). Deletion strains of all these hydrolases result in spores of variable sizes with thinner cell walls and increased heat sensitivity as compared to wild type (Haiser *et al.*, 2009), reflecting the importance of proper hydrolase activity to remodel the cell wall and maintain its integrity. Three of these mutants, *rpfA*, *swlB*, and *swlC*, are also impaired in spore separation indicating their contribution to producing free-living spores. Similar observations have been made for strains with mutations in *ssgE* and *ssgF*, which show premature spore separation and ineffective release of spores (Noens *et al.*, 2005), respectively.

1.2.5 Novel regulators in *S. coelicolor*

During the past several decades, much headway has been made in uncovering the regulators directing *S. coelicolor* development. Many genes involved in morphogenesis have now been identified and a lot of progress has been made in understanding their roles in *S. coelicolor* development. To further genetically define the regulation of this process, roles of novel small RNA (sRNA) regulators are being investigated.

1.2.5.1 RNA-based regulation

Proteins are classical regulators of gene expression; however, RNA molecules are now recognized as having important roles in mediating transcript stability and translation efficiency, processes which significantly impact gene expression. Non-

coding sRNAs, amongst others, are RNA molecules with regulatory functions. sRNAs were initially characterized as being novel regulators in bacteriophages, transposons and plasmids (Mizuno *et al.*, 1983; Mizuno *et al.*, 1984). In these contexts, sRNAs typically act on mRNA targets encoded in *cis,* on the opposite strand, and consequently these sRNAs share complete complementarity with their mRNA target (Itoh and Tomizawa, 1980; Krinke and Wulff, 1987; Takayama *et al.*, 1987; Klein *et al.*, 2002). sRNAs encoded on bacterial chromosomes now have been discovered in a multitude of different species; however, the majority of chromosomally-encoded sRNAs that have been characterized act by base pairing with mRNA targets encoded in *trans.* This makes identifying sRNA targets difficult, since these sRNAs interact with their targets through base pairing, but with imperfect sequence complementarity.

The majority of sRNAs studied to date are involved in post-transcriptional target interactions that either modulate mRNA stability by inhibiting/promoting ribonuclease activity, or impact translation by interacting with the target mRNA to block the ribosome binding site or melt inhibitory secondary structures that sequester the ribosome binding site (Storz *et al.*, 2004). sRNAs, however, do not always target mRNAs. For example, the target of the 6S RNA is the σ^{70}- RNA polymerase complex (Trotochaud and Wassarman, 2004; Trotochaud and Wassarman, 2005), while the two sRNAs CsrB and CsrC directly bind the global post-transcriptional regulator CsrA (Romeo, 1998; Weilbacher *et al.*, 2003). sRNA investigations have revealed sRNAs to be crucial regulators of processes such as outer membrane protein biogenesis (Vogel and Papenfort, 2006), iron homeostasis (Massé and Gottesman, 2002; Lenz *et al.*, 2004), quorum sensing (Wilderman *et al.*, 2004; Tu and Bassler, 2007) and sugar metabolism (Vanderpool and Gottesman, 2004). In general, it appears that sRNAs are important in mediating cellular stress responses.

To carry out their function, the majority of *trans*-acting sRNAs in *E. coli* require Hfq, an sRNA-binding chaperone-like protein (Zhang *et al.*, 2003). Typically, Hfq associates with sRNAs, increasing their stability and facilitating the base pairing interactions between sRNAs and their mRNA targets (Maki *et al.*, 2010; Fender *et al.*, 2010; Hopkins *et al.*, 2011; Hwang *et al.*, 2011). The *hfq* mutant phenotype in *E. coli* includes decreased growth rate and increased sensitivity to environmental stress (Tsui *et al.*, 1994), and this is thought to directly stem from the loss of normal sRNA activity (Valentin-Hansen *et al.*, 2004). Despite the importance of Hfq in mediating sRNA-dependent regulation, not all bacteria appear to encode Hfq-like proteins, as is the case with *Streptomyces* (Bentley *et al.*, 2002).

1.3 DNA dynamics during *S. coelicolor* sporulation

Typically, bacterial cells contain one circular chromosome packaged into a nucleoid, and DNA replication, chromosome condensation and chromosome segregation occur simultaneously. Those chromosome-associated proteins that contribute to these processes have been mostly studied in simple model organisms like *E. coli, B. subtilis* and *Caulobacter crescentus* (Errington *et al.*, 2003; Thanbichler and Shapiro, 2006); chromosome dynamics and chromosome organization are expected to be correspondingly more complex in bacteria like *Streptomyces,* which

have more complicated developmental cycles. In *Streptomyces*, synchronous septation serves to initiate sporulation. After septal constriction begins, approximately 50 copies of the linear chromosome are precisely aligned along the septating cell such that equal chromosomal DNA content will be present in each prespore compartment. Complete septation results in the formation of prespore compartments, and this is then followed by chromosomal DNA condensation. The coordination of these processes is vital, so as to ensure that prespore compartments inherit complete chromosomes. It is clear that the processes of spore septation, chromosome segregation and chromosome condensation are necessarily intertwined. Significant progress has been make in understanding this intricate system in *S. coelicolor* and these processes will likely be well understood in the near future.

1.3.1 Chromosome segregation during *S. coelicolor* sporulation

DNA segregation in most bacteria is governed by the mitosis-like ParAB system. This system includes the ATPase ParA and the DNA binding protein ParB, which binds to centromere-like DNA sequences (referred to as '*parS*' sequences) that flank the origin of replication (Fogel and Waldor, 2006; Ptacin *et al.*, 2010). ParB binding to *parS* sites seeds nucleoprotein complex formation. ParA then interacts with ParB and facilitates chromosome segregation either through polymerizing or oscillating between independent chromosomes (Leonard *et al.*, 2005). *S. coelicolor* encodes a typical *parAB* operon and has 24 *parS* sites situated around the origin region (Kim *et al.*, 2000; Jakimowicz *et al.*, 2002). Two promoters control the expression of *parAB*: one promoter is constitutively active at a low level, whereas expression from the second promoter is strongly upregulated prior to aerial hyphae septation (Kim *et al.*, 2000). Unlike in *C. crescentus* (Mohl and Gober, 1997), ParA and ParB are not essential for *S. coelicolor* growth; however, deletion of their corresponding genes results in significantly increased numbers of anucleate spores relative to wild type (Kim *et al.*, 2000). This suggests that chromosome segregation is a critical process during sporulation.

In aerial hyphae, *parAB* expression is upregulated prior to sporulation (Jakimowicz *et al.*, 2006). As with FtsZ, this likely increases the local ParA/B concentration, facilitating chromosome segregation. Initially, ParA aggregates at the tips of aerial hyphae and adopts what appears to be a double helical filament structure down the length of the aerial hyphae (Jakimowicz *et al.*, 2007). Concomitant with ParA helix formation in the aerial hyphae, ParB complexes - which initially appear diffuse - assemble into regularly spaced foci positioned between the Z-rings that mark future prespore compartments; these ParB foci disappear only after septation has occurred (Jakimowicz *et al.*, 2007). Unlike in other bacteria, a ParA mutant defective in ATP-binding can still assemble into a helical filament, but ParB localization is lost in such a strain (Jakimowicz *et al.*, 2007), suggesting that ParA ATPase activity is required for ParB positioning.

Recently, a new protein (ParJ) has been found to interact with ParA and appears to regulate ParA depolymerization. ParJ encodes an unusual ATPase, lacking any recognizable ATP-binding motifs. This protein promotes ParA filament disassembly *in vitro* (Ditkowski *et al.*, 2010). Like ParB, ParJ localizes as foci along

the aerial hyphae; however, unlike ParB, this placement is independent of ParA. Deletion of *parJ*, like deletion of *parAB*, leads to increased numbers of anucleate spores and mini-compartments, suggesting that ParJ is required for both efficient chromosome partitioning and septal placement.

Although ParA, ParB and ParJ are clearly involved in DNA segregation, the majority of spore compartments contain complete chromosomes in the *parAB* mutant suggesting that there are other systems that contribute to chromosomal segregation during sporulation. An additional level of complexity that needs to be considered is that the chromosomes are segregated into prespore compartments during the late stages of sporulation septation (Schwedock *et al.*, 1997; Miguélez *et al.*, 1998). Consequently, it is possible for chromosomes to be 'guillotined' by the closing septum. In other bacteria like *E. coli* and *B. subtilis*, a 'nucleoid occlusion' mechanism is used to prevent septum formation over nucleoids (Wu and Errington, 2004; Bernhardt and de Boer, 2005); however, such a phenomenon does not appear to exist in *Streptomyces,* as septum formation often initiates over uncondensed chromosomes. Most bacteria also possess a membrane-bound 'DNA pump' known as FtsK (Iyer *et al.*, 2004) that further prevents DNA guillotining by a closing septum. FtsK localizes to the invaginating septum and is thought to translocate residual DNA from the septal region into adjacent progeny cells (Pease *et al.*, 2005) prior to septation. In *S. coelicolor,* an *ftsk* mutation does not affect cell division or lead to increased numbers of anucleate cells (Wang *et al.*, 2007; Dedrick *et al.*, 2009); however, in such a strain, 15-20% of spores contain large terminal fragment deletions from one or both chromosome ends (Wang *et al.*, 2007). Colonies that develop from spores with these truncations display abnormal phenotypes (Wang *et al.*, 2007), likely due to the loss of genetic information important for normal development. Like in other bacteria, FtsK is found at the sporulation septa in aerial hyphae (Wang *et al.*, 2007), where it likely also serves a DNA 'pumping' role.

It is notable that in both the ParAB and FtsK systems, there appears to be some redundancy, in that there is not a complete loss of chromosome segregation (Δ*parAB*), and not all chromosomes are truncated (Δ*ftsK*). In the latter instance, this may be circumvented by additional proteins belonging to the FtsK/SpoIIIE family. To date, the only other characterized FtsK-like system comprises two proteins: SffA (for **S**poIIIE/**F**tsK **f**amily) and SmeA, a small putative membrane protein (Ausmees *et al.*, 2007). Deletion of the *smeA-sffA* operon results in reduced spore-specific pigmentation, defects in chromosome compaction and segregation, thinner spore walls, uneven spore sizes, an inability to liberate free spores and higher spore susceptibility to heat. SffA localizes to the septa of developing aerial hyphae prior to Z-ring formation. The specific localization of SffA in sporulating cells requires SmeA, which is solely expressed in the aerial hyphae. Although SffA shares similar features with FtsK, the *sffA* mutant phenotype does not suggest a shared function.

1.3.2 Chromosome condensation during *S. coelicolor* sporulation

Following chromosome segregation and completion of septation, the DNA within the prespore compartments is condensed. Nucleoid-associated proteins play an important role in this process, and at least three classes of these proteins exist in the *Streptomyces*: the SMC, HU-like and Dps-like proteins.

SMC (**s**tructural **m**aintenance of **c**hromosomes) proteins are found in eukaryotes, archaea and bacteria, where they are responsible for chromosome organization and higher order chromosome structure (Hirano, 1998; Soppa, 2001). SMC proteins are large (110 – 170 kDa) and exhibit ATPase activity, which is required for DNA interaction. An *S. coelicolor smc* mutant shows defects in nucleoid compaction, as has been seen in other bacteria (Graumann, 2000); however, it also exhibits defects in chromosome segregation, with there being 7% more anucleate spores in the mutant compared to wild type (Dedrick *et al.*, 2009; Kois *et al.*, 2009). Interestingly an *smc parB* double mutant had greater numbers of anucleate spore compartments than expected based on the additive effects of each single mutant (Dedrick *et al.*, 2009). In addition, ParB foci are smaller and less prominent in an *smc* mutant (Kois *et al.*, 2009), suggesting that there is a functional overlap between DNA segregation and condensation systems mediated by the Par and SMC systems. Perhaps unexpectedly, SMC localization does not mirror that of ParB; it forms clusters of irregularly spaced foci in pre-divisional aerial hyphae prior to the assembly of ParB complexes, and then disappears following the completion of sporulation septation (Kois *et al.*, 2009). SMC functions in complexes with other proteins including ScpA and ScpB (**s**egregation and **c**ondensation **p**roteins). A similar phenotype to that of the *smc* mutant has been observed following deletion of *scpA* and *scpB*; however, chromosome segregation is less affected and instead, approximately 25% of chromosomes adopt a 'bilobed' structure that is not seen in the *smc* mutant (Dedrick *et al.*, 2009).

In addition to the SMC complex, another nucleoid-associated protein - one of the HU-like (for **h**eat **u**nstable) proteins - is involved in chromosome condensation during sporulation in *S. coelicolor*. Unlike many DNA binding proteins including ParB, HU–like proteins strongly prefer to bind structurally distorted DNA rather than a specific DNA sequence (Castaing *et al.*, 1995; Kamashev *et al.*, 1999; Kamashev and Rouvière-Yaniv, 2000). Upon binding DNA, HU induces DNA bending at variable bend angles ranging from 105˚ to ~140˚, which contributes to its ability to promote DNA compaction (Swinger *et al.*, 2003). *S. coelicolor* encodes two HU-like proteins (Bentley *et al.*, 2002): HupA and HupS. Expression of both coding sequences is developmentally regulated: *hupA* expression is detected predominately during vegetative growth, while *hupS* expression is upregulated during aerial hyphae development and sporulation (Salerno *et al.*, 2009). Increased *hupS* expression is not observed in early *whi* mutants (*whiA*, *whiI* and *whiG)* and is only seen in occasional spore-like aerial hyphae fragments of a *whiH* mutant, suggesting that *hupS* upregulation may be subject to the same sporulation-specific checkpoint(s) as *ftsZ* and *parAB*. HupS localizes to the nucleoid and *hupS* deletion leads to reduced chromosome compaction (Salerno *et al.*, 2009). *hupS* mutant spores are less grey than their wild type counterparts and are more sensitive to heat (Salerno *et al.*, 2009), suggesting that DNA compaction is an important step in establishing spore dormancy. Effects of *hupA* deletion have not been investigated.

The final group of proteins known to impact chromosome condensation during *S. coelicolor* sporulation is the Dps (for **D**NA-binding **p**rotein from **s**tarved cells)-like proteins. These proteins are well conserved in bacteria, bind DNA in a sequence-independent manner and ultimately shield DNA from environmental

stress (Almirón *et al.*, 1992). DNA binding by Dps-like proteins causes 'hyper compaction' of the chromosome, which contributes to DNA protection. The Dps proteins also possess ferroxidase activity, which further protects DNA from oxidative damage (Nair and Finkel, 2004). Dps has been extensively studied in *E. coli* and *B. subtilis*, where it is important in the general stress response during the stationary phase of growth. *S. coelicolor* encodes three *dps* genes: *dpsA*, *dpsB*, and *dpsC*. *dpsA* is expressed more highly than either *dpsB* or *dpsC* throughout development, with its expression further increasing during sporulation (Facey *et al.*, 2009). Deletion of each *dps* gene revealed their products to have different roles during sporulation (Facey *et al*., 2009). The *dpsA* mutant forms irregularly sized spore compartments that frequently contain more than one nucleoid, suggesting a role in spore septum placement and chromosome segregation. In contrast, the *dpsB* mutant displays enhanced nucleoid compaction, whereas the *dpsC* mutant most closely resembles its wild type parent. Unexpectedly, the irregular DNA content in the *dpsA* mutant is eliminated in *dpsAB* or *dpsAC* mutants, suggesting that DspB or DspC counteract the effect of the *dpsA* deletion; however, more work is required to understand these protein relationships (Facey *et al.*, 2009).

1.4 Nucleoid-associated proteins

Nucleoid-associated proteins (NAPs) modulate the dynamic structure of the nucleoid and contribute to chromosome compaction through bending, bridging and wrapping of chromosomal DNA (Luijsterburg *et al.*, 2006); they further affect DNA supercoiling (Dorman, 2013), which impacts DNA replication and transcription. Nucleoid structure is influenced by cell growth conditions, as the pool of available NAPs fluctuates depending on growth phase and culture conditions (Almirón *et al.*, 1992). While most bacteria share a conserved subset of NAPs, other NAPs are specific to particular bacterial groups. *S. coelicolor* encodes three well characterized NAPs that are involved in chromosome condensation during sporulation (discussed above in section 1.3.2).

1.4.1 NAPs and the effects of their binding

NAPs can either bind DNA non-specifically or can recognize a specific target sequence. Examples of well-characterized sequence-specific NAPs include Fis (for **f**actor for **i**nversion **s**timulation), Lrp (for **l**eucine **r**esponsive regulatory **p**rotein) and IHF (for **i**ntegration **h**ost **f**actor) (Pan *et al.*, 1994; Hales *et al.*, 1994; Cui *et al.*, 1995), none of which are encoded by *S. coelicolor*. Fis and Lrp from *E. coli* recognize their respective binding sequences through helix-turn-helix (HTH) domains that contact the major groove of DNA (Willins *et al.*, 1991; de los Rios and Perona, 2007; Stella *et al.*, 2010). IHF also recognizes a specific sequence, but contrary to Fis and Lrp, it binds to the minor groove of DNA (Hales *et al.*, 1994). This is uncommon, as direct interaction with nucleotides in the minor groove can be challenging due to its narrow structure. The structural flexibility of the preferred IHF binding sequence, coupled with additional interactions with the DNA phosphate backbone, suggests that IHF preferentially recognizes a specific target DNA structure rather than a specific sequence *per se* – this is known as an 'indirect readout' mechanism for DNA binding (Aeling *et al.*, 2006). Other NAPs that bind DNA non-specifically include Dps

and H-NS (**h**eat stable **n**ucleoid-**s**tructuring protein). H-NS is generally correlated with binding to AT-rich DNA sequences and is suggested to prefer curved DNA (Navarre *et al.*, 2006; Lucchini *et al.*, 2006; Oshima *et al.*, 2006; Gordon *et al.*, 2011); however, this interpretation is confounded by the general curvature or flexibility of AT-rich DNA.

The effect of DNA binding by different NAPs differs significantly. DNA binding by Fis, IHF and HU results in DNA bending by 50-90˚ (Fis), 160-180˚ (IHF) and 105-140˚ (HU), respectively (Pan *et al.*, 1996; Rice *et al.*, 1996; Swinger *et al.*, 2003). In contrast, H-NS bridges DNA, whereas Dps condenses DNA by forming extremely stable and large complexes (Almirón *et al.*, 1992). NAPs frequently bind – at a minimum - hundreds of sites in the chromosome. For example, Fis interacts with approximately 600 intergenic regions in the *E. coli* genome (Cho *et al.*, 2008), and similar observations have been made for H-NS and Lrp (Grainger *et al.*, 2006). Changes to nucleoid structure have profound and widespread impacts on global gene expression, and consequently NAPs can also be considered global transcription regulators. For instance, *E. coli* IHF affects the expression of anywhere between 150 and 500 genes, while HU impacts the expression of over 900 genes (Gama-Castro *et al.*, 2008; Prieto *et al.*, 2011). In contrast to IHF and HU, Dps does not appear to regulate gene expression and instead seems to have a purely structural role in promoting DNA compaction and protection against damage and oxidative stress. NAP-mediated global transcription regulation is controlled by the dynamic expression profiles of the various NAP genes throughout growth (Luijsterburg *et al.*, 2006). In *E. coli,* Fis and HU are expressed in early lag phase, while IHF appears in exponential phase, peaking during the transition to stationary phase. Lrp peaks at the same time as IHF, while Dps is most highly expressed during stationary phase. Unusually, H-NS is constantly expressed throughout growth (Dillon and Dorman, 2010).

1.4.2 Topoisomerase and its influence on nucleoid structure

DNA topoisomerases are among the most conserved proteins in all organisms and regulate the topological state of the chromosome. This is accomplished by introducing either negative (DNA gyrase) or positive supercoils (reverse gyrase) into DNA, resulting in altered levels of chromosome supercoiling (Travers and Muskhelishvili, 2005). There are two major types of topoisomerases: those that pass one strand of DNA through a break in the opposing strand (type I), and those that pass duplex DNA from the same or different DNA molecule through a double-stranded break (type II).

In addition to modulating DNA supercoiling, topoisomerases also promote catenation and decatenation of circular chromosomes and help in untangling linear chromosomes (Champoux, 2001). *E. coli* possesses two type I (I and III) and two type II (gyrase and IV) topoisomerases, whereas *S. coelicolor* encodes only one type I (I) and one type II (gyrase) enzyme (Bentley *et al.*, 2002).

When considering their complementary roles in chromosome organization, it is not surprising that functional interactions between NAPs and topoisomerases have been reported. In *E. coli*, HU functions to maintain a balance between the supercoiling activity of gyrase and the relaxing activity of topoisomerase I by

constraining supercoils and, therefore regulating the global level of DNA supercoiling (Bensaid *et al.*, 1996). Additionally, suppressor mutations in topoisomerase I rescue the effects of MukB (SMC equivalent) deficiencies in *E. coli* by increasing the levels of negative supercoils (Sawitzke and Austin, 2000).

1.5 Aims of this work

At a time when sRNAs were first being discovered in bacteria, our group conducted a systematic search for these RNA species in *S. coelicolor*. We confirmed six sRNAs that were predicted using a comparative genomics approach and identified an sRNA that was tightly linked with sporulation. The characterization of this sporulation-specific sRNA is described in Chapter 3. Due to technical difficulties the sRNA project was not continued.

Chapter 4 details the examination of an actinomycetes-specific NAP termed sIHF. The phenotype of the *sIHF* deletion strain revealed that sIHF is involved in septal placement, spore maturation, antibiotic production and chromosomal segregation and condensation during sporulation. sIHF was shown to bind DNA non-specifically with a preference for three specific DNA motifs that were identified using *in vitro* selection. Notably, sIHF influenced the relaxing activity of topoisomerase, which has provided insight into its function within the cell.

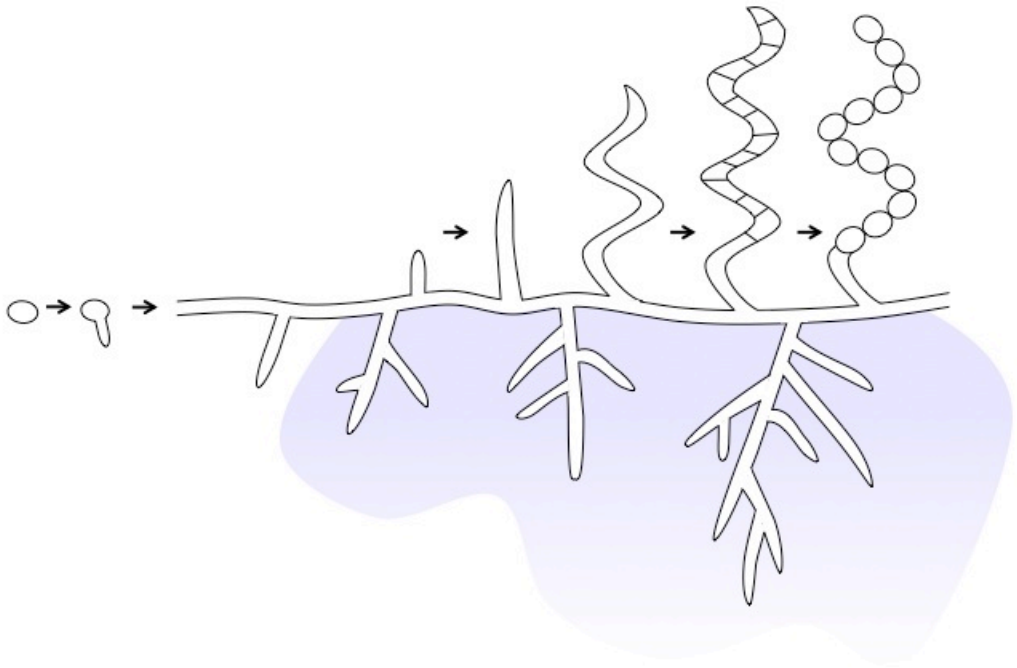

Figure 1.1 The *Streptomyces coelicolor* life cycle. The *S. coelicolor* life cycle initiates with spore germination followed by vegetative growth through tip extension and hyphal branching into the soil (or lab agar media), eventually forming a vegetative mycelium. This is followed by the emergence of aerial hyphae from the surface of the developing colony and their extension into the air. Aerial hyphae formation coincides with the onset of secondary metabolite production (indicated in purple). Aerial hyphae undergo a synchronous round of cell division, after which the resulting compartments mature, forming chains of reproductive spores. Image adapted from: (Swiercz and Elliot, 2012)

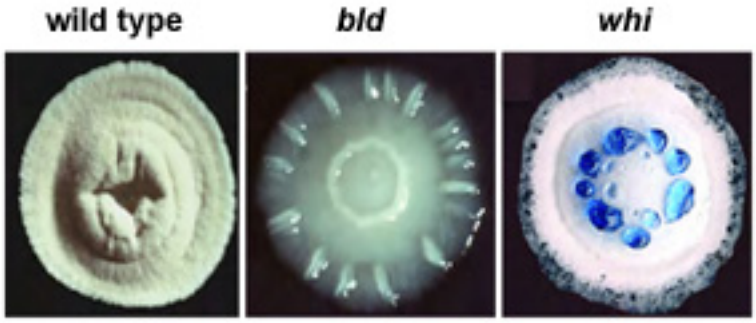

Figure 1.2 Comparison of wild type, *whi* and *bld S. coelicolor* colonies. The 'fuzzy' and grey appearance of wild type *S. coelicolor* colonies (left panel) represents aerial hyphae and spore formation, respectively. In contrast, '*bld*' colonies (middle panel) do not develop past the vegetative stage and appear shiny instead of 'fuzzy' due to the lack of aerial hyphae formation, whereas '*whi*' colonies (right panel) develop aerial hyphae and appear 'fuzzy', but do not sporulate and lack the grey spore-associated pigment. The blue droplets on the surface of the '*whi*' colony are actinorhodin – one of the antibiotics produced by *S. coelicolor*. Image adapted from http://spider.science.strath.ac.uk/sipbs/staff/Paul_Hoskisson.html, with photo credit to Brenda Leskiw for the left and middle panels.

CHAPTER 2

MATERIALS AND METHODS

2.1 Bacterial strains and growth conditions

2.1.1 Bacterial strains and plasmids

The bacterial strains and plasmids used throughout this work are outlined in Tables 2.1 – 2.3. To create *S. coelicolor* spore stocks, cells were streaked for single colonies on mannitol-soy flour (MS) agar medium and grown for 4-5 days at 30˚C. A single colony was streaked for lawns on MS agar medium overlaid with cellophane discs, and grown for 4-5 days or until sporulation was obvious. Spores were removed using the flat end of a sterilized metal spatula and were added to ~10 ml of sterilized water in a glass "universal" vial. The mixture was water bath sonicated and vortexed until spore clumps were no longer visible. The suspension was passed through a cotton filter in a 10 ml syringe and the resulting spore-containing filtrate was centrifuged at 1,248 × g for 5 minutes. The supernatant was discarded and the spore pellet was resuspended in 40% glycerol. *S. coelicolor* developmental mutants that do not sporulate were harvested in a similar manner, only instead of sonicating and vortexing, cells were homogenized in 10 ml of sterilized water with a 15 ml Pyrex® homogenizer (Corning). *S. coelicolor* stocks were stored at -20˚C. *E. coli* stocks were created by mixing equal volumes of overnight cultures with 40% glycerol and were stored at -80˚C.

2.1.2 Bacterial culture conditions

S. coelicolor strains were grown on MS agar, rich (glucose-containing) R2YE agar, minimal medium (MM) agar supplemented with 0.5% mannitol (w/v), Difco nutrient agar (DNA), or in a 1:1 mixture of yeast extract–malt extract and tryptic soy broth (YEME-TSB) complex liquid medium (Kieser *et al.*, 2000). Unless otherwise indicated, antibiotics added to media were used at the following final concentrations (μg/ml): apramycin, 50; hygromycin B, 50; kanamycin sulfate, 50; nalidixic acid, 25; thiostrepton, 50. Solid cultures were grown in petri plates and incubated in a 30˚C stationary incubator for up to 5 days. Liquid cultures were grown in glass "universal" vials or 250 ml baffled flasks containing stainless steel springs (to reduce cell clumping) in a 30˚C shaking (200 rpm) incubator for up to 6 days.

E. coli strains were typically grown in liquid or on agar Luria Bertani (LB) media (Miller, 1972); they were grown in super optimal broth (SOB) liquid or on DNA solid media when hygromycin, a salt sensitive antibiotic, was used for strain selection. Unless otherwise indicated, antibiotics added to media were used at the following final concentrations (μg/ml): ampicillin, 100; apramycin, 50; chloramphenicol, 25; hygromycin B, 50; kanamycin sulfate, 50. Liquid *E. coli* strains were grown overnight in a shaking 37˚C incubator at 200 rpm, while solid cultures were grown in a stationary 37˚C incubator. The only exceptions were *E. coli* BW25113/pIJ790 cultures, which were grown at 30˚C, and BT340, which were grown at either 30˚ or 42˚C.

2.2 Oligonucleotides

All oligonucleotides used in the sRNA and sIHF studies are summarized in Tables 2.4 and 2.5, respectively.

2.3 Genetic and molecular biology techniques

2.3.1 Introducing and isolating DNA into/from *Escherichia coli*

Plasmid DNA was introduced into *E. coli* by transformation or electroporation (Sambrook and Russell, 2001).

2.3.1.1 Introducing DNA into *E. coli* by transformation

DNA transformations were completed using *E. coli* Subcloning Efficiency™ DH5α™ Competent Cells (Invitrogen) or chemically competent cells. Chemically competent *E. coli* cells were prepared as described elsewhere (Sambrook and Russell, 2001). Briefly, an overnight liquid culture of *E. coli* DH5α grown at 37˚C was sub-cultured in a 250 ml flask containing 50 ml of LB medium and grown at 37˚C until an OD_{600} of ~0.4 was reached. The culture was centrifuged at 1,248 × g at 4˚C for 5 minutes and the resulting cell pellet was washed with 15 ml of ice-cold $MgCl_2/CaCl_2$ (80 mM $MgCl_2$, 20 mM $CaCl_2$) twice and resuspended in 2 ml of ice-cold 0.1 M $CaCl_2$ containing 15% glycerol. Cell aliquots of 100 µl were prepared in 1.5 ml microfuge tubes and stored at -80˚C.

For the transformation reaction, 5-10 ng of plasmid DNA was added to either a 50 µl aliquot of Subcloning Efficiency™ DH5α™ Competent Cells (Invitrogen™) *E. coli* cells or a 100 µl aliquot of chemically competent *E. coli* cells, which were previously thawed on ice. The mixture was incubated on ice for 30 minutes before heat shocking in a 37˚C water bath for 30 seconds. Heat shocked cells were immediately placed on ice for 2 minutes before adding 700 µl of LB liquid medium, and incubating at 37˚C in a shaking incubator for 45-60 minutes. The cell culture was plated onto LB agar medium containing the appropriate antibiotics for plasmid selection, and incubated at 37˚C overnight.

2.3.1.2 Introducing DNA into *E. coli* by electroporation

Electroporating plasmid DNA into *E. coli* was completed using freshly prepared electrocompetent cells. Electrocompetent *E. coli* cells were prepared by sub-culturing an overnight *E. coli* culture (1/100) grown in 5 ml of LB into a 250 ml flask containing 50 ml of LB liquid medium. Once an OD_{600} of ~0.4 was reached, the culture was centrifuged and the resulting cell pellet was washed three times with 10 ml of chilled 10% glycerol before being resuspended in 100 µl of 10% glycerol. One or two microliters (~100 ng) of plasmid DNA was mixed with 50 µl of freshly prepared electrocompetent *E. coli* cells and transferred into a chilled 0.2 mm electroporation cuvette (Bio-Rad). After electroporation using a Bio-Rad MicroPulser™ (2.5 kV), 1 ml of ice-cold liquid LB medium was immediately added to the cell mixture and this was then transferred into a 1.5 ml microfuge tube. The electroporated cells were incubated at 37˚C for 60 minutes, and the cells were later plated onto LB agar medium containing the appropriate antibiotics for plasmid selection and incubated at 37˚C overnight.

2.3.1.3 Isolating DNA (plasmid or cosmid) from *E. coli*

DNA extractions (plasmid or cosmid) from *E. coli* were completed as described previously (Sambrook and Russell, 2001). Briefly, overnight *E. coli* cultures containing the plasmid/cosmid of interest, which were grown in 5 ml of LB liquid medium at 37˚C, were centrifuged at 2,218 × g for 5 minutes at 4˚C. The resulting cell pellet was resuspended in 100 µl TEG (50 mM Tris-HCl, 20 mM EDTA, 1% glucose, pH 8). Lysis buffer (0.2 mM NaOH, 1% SDS) was added to the mixture and incubated at room temperature for 5 minutes. The lysed products were then precipitated by adding 150 µl of NaOAc (3 M, pH 4.8) and centrifuged at 2,218 × g for 10 minutes at 4˚C. The supernatant, containing the soluble fraction, was transferred to a 1.5 ml microfuge tube and an equal volume of phenol:chloroform (1:1) was added. The mixture was vortexed until the solution appeared homogeneous and then was centrifuged at 2,218 × g for 5 minutes at 4˚C. The supernatant was transferred to a 1.5 ml microfuge tube and the DNA was precipitated by adding 2.5 volumes of ice-cold 95% ethanol and incubated on ice for 30 minutes. The mixture was centrifuged at 2,218 × g for 10 minutes at 4˚C and the resulting pellet was dried at room temperature before being resuspended in 40 µl of sterile water. To obtain ultra pure DNA suitable for sequencing, plasmids were extracted using the PureLink™ Quick Plasmid Miniprep kit (Invitrogen) or the QIAprep® Miniprep kit (Qiagen) as per the manufacturer's instructions. Plasmid/cosmid DNA concentrations were measured with an Ultrospec™ 3100 Pro (Biochrom Ltd.) or NanoDrop 1000 (Thermo Scientific) spectrophotometer, or approximate concentrations were obtained by separating a fraction of plasmid/cosmid DNA on a 1% agarose gel containing ethidium bromide using electrophoresis, and comparing DNA intensity to a quantified marker.

2.3.2 Introducing and isolating DNA into/from *S. coelicolor*

Plasmid or cosmid DNA containing an origin of transfer (*oriT*) was conjugated into *S. coelicolor*, while other constructs (such as plasmids lacking an *oriT*) were introduced into *S. coelicolor* by protoplast transformation.

2.3.2.1 Introducing DNA into *S. coelicolor* by conjugation

Conjugations were completed as outlined previously (Kieser *et al.*, 2000). Plasmid or cosmid DNA was first introduced into *E. coli* ET12567 (methylation deficient) containing the pUZ8002 mobilizing plasmid (a strain termed 'ET/pUZ') via transformation, as described previously in 2.3.1.1. A liquid culture of ET/pUZ, containing the plasmid/cosmid of interest, was grown overnight in LB liquid medium at 37˚C. This overnight culture was then sub-cultured into a 250 ml flask containing 25 ml of LB liquid medium and grown at 37˚C until reaching an OD_{600} of ~0.4. After centrifugation at 2,218 × g at 4˚C, the resulting cell pellets were washed with 10 ml of LB liquid medium three times and then resuspended in 1 ml of LB liquid medium. During this time, ~10^8 *S. coelicolor* spores (from a spore stock), were added to 500 µl of 2× YT medium, heat shocked for 12 minutes in a 50˚C heating block and allowed to cool to room temperature. The heat shocked *S. coelicolor* recipient cells were combined with 500 µl of the prepared *E. coli* donor cells in a 1.5

ml microfuge tube, which was inverted several times to mix the strains. The mixture was briefly centrifuged to pellet the cells and the supernatant was discarded, with the residual liquid being used to resuspend the cell pellet. The resuspended cells were plated on MS agar medium supplemented with 10 mM $MgCl_2$ and incubated at 30˚C. After 16 hours of growth, the conjugants were overlayed with 1 ml of sterile water containing 20 µl of nalidixic acid (25 mg/ml) and 25 µl of apramycin or hygromycin (50 mg/ml).

2.3.2.2 Introducing DNA into *S. coelicolor* by protoplast transformation

Protoplasts and protoplast transformations were completed as described previously (Kieser *et al.*, 2000). To prepare protoplasts, *S. coelicolor* was grown in 10 ml of YEME:TSB liquid medium overnight. The overnight culture was transferred into a 250 ml baffled flask containing 30 ml of YEME:TSB liquid medium and grown for ~2 days or until a slight red pigmentation was evident. The culture was centrifuged at 1,218 × g for 5 minutes at 4˚C and the resulting cell pellet was washed with 5 ml of ice-cold 10.3% sucrose twice and then resuspended in 4 ml P buffer ([g/800 ml]: sucrose, 103; K_2SO_4, 0.25; $MgCl_2 \cdot 6H_20$, 2.02; supplemented with 2 ml of trace element solution [per L: $ZnCl_2$, 40 mg; $FeCl_3 \cdot 6H_2O$, 200 mg; $CuCl_2 \cdot 2H_2O$, 10 mg; $MnCl_2 \cdot 4H_2O$, 10 mg; $Na_2B_4O_7 \cdot 10H_2O$, 10 mg; $(NH_4)_6Mo_7O_{24} \cdot 4H_2O$, 10 mg] and after autoclaving modified by adding [ml/80ml]: KH_2PO_4 (0.5%), 1; $CaCl_2 \cdot 2H_20$ (3.68%), 10; TES buffer (5.73%, pH 7.2), 10]). The mixture was transferred into a glass "universal" vial and incubated in a 30˚C water bath for 45-60 minutes. The cell mixture was removed from the water bath three times throughout the incubation period to mechanically separate the protoplasts from the cell wall by drawing the cell mixture in and expelling it out of a 5 ml pipette several times. The cell mixture was then diluted by adding 5 ml of P buffer and passing it through a cotton syringe filter. The flow-through, containing the protoplasts, was collected in a 15 ml conical tube and centrifuged at 1000 × g for 10 minutes. The protoplast pellet was resuspended in 1 ml of P buffer and 100 µl of these cells were mixed with 5 µl of cosmid/plasmid DNA, which had been isolated from the methylation-deficient *E. coli* strain (ET/pUZ), as described in 2.3.2.1. After adding DNA, 200 µl of P buffer containing 0.25% PEG 1000 was immediately added to the sample and mixed by pipetting up and down several times. The mixture was plated on R2YE agar medium and grown for 16-20 hours at 30˚C before the plates were overlayed with 1 ml of sterile water containing 25 µl of apramycin (50 mg/ml) or 100 µl of kanamycin (50 mg/ml) and incubated for an additional 4-5 days until colonies were detected.

2.3.2.3 Isolating genomic DNA from *S. coelicolor*

An overnight culture containing *S. coelicolor* in a glass "universal" vial containing 10 ml of liquid YEME:TSB media was transferred into a 250 ml baffled flask with a metal spring containing 50 ml YEME:TSB and grown for 1-2 days at 30˚C. The culture was centrifuged at 1,248 × g for 10 minutes at 4˚C, and the resulting cell pellet was washed with 10 ml of ice-cold 10% glycerol. Washed pellets were resuspended in 6 ml of P buffer containing 3 mg/ml lysozyme, transferred into a glass "universal" vial and incubated in a 37˚C water bath for 1 hour. The mixture

was additionally incubated for 10 minutes after adding EDTA (0.5 M, pH 8) to a final concentration of 0.1 M and subsequently incubated for 10 minutes at 60˚C after adding SDS (20%) to a final concentration of 1%. The mixture was diluted with 4 ml P buffer and two to three phenol:chloroform (1:1) extractions were completed, which involved adding an equal volume of phenol:chloroform (1:1), vortexing the mixture, centrifuging for 15 minutes at 11,950 × g at 4˚C and recovering the upper liquid phase. The purified DNA was precipitated overnight at -20˚C by adding 3 volumes of ice-cold 95% ethanol. The precipitated DNA was physically removed from the mixture using a sterilized glass Pasteur pipette and was transferred to a 1.5 ml microfuge tube before being resuspended in 500 µl of sterile water overnight at 4˚C. RNase A was added (final concentration: 30 µg/ml) to the resuspended DNA and incubated in a 37˚C water bath for 1 hour. Genomic DNA quality was assessed using electrophoresis on a 0.8% agarose gel containing ethidium bromide.

2.3.5 Amplifying DNA by PCR

PCR checks were completed using *Taq* DNA polymerase (Norgen Biotek Corp.) in a total volume of 25 µl, using the reaction and cycling conditions described in Tables 2.6 and 2.7. High-fidelity amplification was performed with Phusion High-Fidelity DNA polymerase (Thermo Scientific) in a total volume of 50 µl, using the reaction and cycling conditions described in Tables 2.8 and 2.9.

2.3.6 Creating deletion mutants in *S. coelicolor*

Deletion strains were generated using the ReDirect system (Gust *et al.*, 2003) using cosmids from an *S. coelicolor* library (with the SuperCos-1 backbone conferring kanamycin-resistance (Redenbach *et al.*, 1996)). The sIHF-coding sequence (from start codon to stop codon) or the majority of the intergenic region encompassing the *scr1906* specific sequence was initially replaced by an *oriT*-containing apramycin resistance cassette (*acc*(3)IV; from pIJ773). Cosmids carrying the genes of interest were introduced into *E. coli* BW25113 (Datsenko and Wanner, 2000) by electroporation, as described in 2.3.1.2. The apramycin knockout cassette with target gene-specific extensions on its 5′ and 3′ ends was electroporated into *E. coli* BW25113 carrying the appropriate cosmid, resulting in replacement of the gene of interest with the apramycin cassette. The cosmid carrying the gene knockout was introduced by electroporation into ET/pUZ *E. coli* cells and the resulting strain was used to conjugate the mutant cosmid into *S. coelicolor*, as described in 2.3.2.1. Transconjugants were screened for double-crossovers between the mutant cosmid and *S. coelicolor* chromosomal DNA by replica-plating the cells onto DNA agar containing kanamycin or apramycin. Strains that were kanamycin sensitive and apramycin resistant were considered to have lost the cosmid and had their target genes replaced by the apramycin cassette. PCR was used to confirm the location of the apramycin cassette and loss of the target gene sequence, using primer combination SCO1480 k/o 1 with SCO1480 down and SCO1480 up with SCO1480 internal (Table 2.5).

Unmarked mutants of Δ*sIHF* (bearing no selectable marker) were created by removing the apramycin cassettes using FLP-mediated recombination. The

knockout cosmids were electroporated into *E. coli* BT340 (Datsenko and Wanner, 2000), which harbours a temperature sensitive plasmid encoding the FLP recombinase gene. At 30˚C, this plasmid replicates and at 42˚C FLP recombinase is expressed before the plasmid is eventually lost (Cherepanov and Wackernagel, 1995). FLP recombinase recognizes the FLP recognition target (FRT) sites that flank the apramycin cassette and its binding results in cassette removal, leaving an in-frame 81 bp sequence lacking any stop codons (Gust *et al.*, 2003). After an overnight incubation at 42˚C, replica plating onto DNA agar medium containing kanamycin or apramycin was completed to screen for the loss of the apramycin resistance cassette. Cassette removal was confirmed by PCR using primer combinations: SCO1480 up with SCO1480 down and SCO1480 up with SCO1480 internal (Table 2.5). The mutant cosmid was then introduced into *S. coelicolor* by protoplast transformation as described in 2.3.2.2, initially selecting for kanamycin resistance, and then screening for kanamycin and apramycin sensitivity. The unmarked mutants were verified by PCR, as described above.

2.3.7 Complementing deletion strains

Complementation strains were only created when phenotypic differences were observed for mutant strains as compared to their wild type parent strains. Complementation of the Δ*scr1906* strain was not attempted due to discontinuation of the scr1906 research project.

2.3.7.1 Creating an *sIHF* mutant complementation strain

To complement the Δ*sIHF*-mutant phenotype, the sIHF-coding sequence was amplified, together with additional upstream (284 nt) and downstream (156 nt) sequences, using primers SCO1480 up and SCO1480 down (Table 2.5). The PCR-amplified product was agarose gel extracted using the PureLink™ Gel Extraction kit (Invitrogen), as per manufacturer's instructions, and phosphorylated. The final product was introduced into the *Eco*RV-digested and dephosphorylated integrating vector pIJ82. The resulting construct was introduced into *E. coli* ET/pUZ, as described in 2.3.1.1. This strain was used to conjugate the complementation construct into the Δ*sIHF*-mutant strain, as described in 2.3.2.1. The empty plasmid was also introduced into both the mutant- and wild type M600 strains as a control.

2.3.8 Creating an scr1906 overexpressing *S. coelicolor* strain

A small RNA (sRNA) overexpression cloning vector, termed pMC500, was engineered using the *E. coli* pUC57 backbone (Yanisch-Perron *et al.*, 1985). pMC500 (Figure 2.1) was designed to include a multiple cloning site downstream of the constitutive *ermE** promoter (Schmitt-John and Engels, 1992) and terminator sequences both upstream of the *ermE** promoter - to prevent read through from upstream genes - and downstream of the multiple cloning site, to effectively terminate sRNA/mRNA expression. The sequence of the smaller scr1906 transcript was PCR amplified using primers 'small 1906 upstream' and 'small 1906 downstream' (Table 2.4), purified and cloned downstream of the *ermE** promoter in the *Eco*RV digested and dephosphorylated pMC500 vector. The entire P_{ermE*}-*scr1906* fragment was excised from pMC500 using *Bgl*II sites flanking all engineered

elements, and cloned into the *Bam*HI digested integrating pRT801 vector (Gregory *et al.*, 2003). The resulting construct was introduced into wild type *S. coelicolor* to create an scr1906 overexpression strain. Northern blot analysis, described below in 2.4.2, was used to confirm overexpression of the smaller scr1906 transcript.

2.3.9 Creating tagged protein fusions

2.3.9.1 Creating WhiH-3× FLAG tag

A 3× FLAG tag (DYKDHDGDYKDHDDIDYKDDDDK) was introduced at the 3′ end of the WhiH coding sequence, before the stop codon. To generate this construct, *whiH* was initially PCR amplified as two fragments. The first fragment, generated using primers whiH upstream and whiH/XhoI (Table 2.4), included the *whiH* coding sequence with 319 nt of upstream sequence and an in frame *Xho*I site prior to the stop codon. The second fragment, generated using primers whiH/stop/XhoI and whiH downstream (Table 2.4), overlapped with the first fragment at the *Xho*I-end and extended 385 nt downstream. The PCR products were both digested with *Xho*I and ligated together. The resulting product was PCR amplified using primers whiH upstream and whiH downstream (Table 2.4), purified and introduced into the *Eco*RV digested and dephosphorylated integrating pIJ82 vector. The 3× FLAG tag, which was prepared by annealing two complementary 3× FLAG tag sequence-specific oligonucleotides (FLAG plus and FLAG minus; see Table 2.4) with *Xho*I-specific overhangs, was cloned into the *Xho*I site engineered upstream of the *whiH* stop codon. The desired products were identified using colony PCR with whiH/stop/XhoI and whiH down primers (Table 2.4). The directionality of the FLAG fragment was checked by sequencing the insert with the M13 Reverse primer (Table 2.4). The resulting construct could therefore express WhiH with a C-terminal 3× FLAG tag, and we expected to be able to detect this protein using FLAG tag-specific antibodies. The final product was passaged through ET/pUZ, as described in 2.3.1.1 and introduced into *S. coelicolor* as described in 2.3.2.1.

2.3.9.2 Creating sIHF-eGFP

The sIHF-coding sequence, including 284 nt of upstream sequence, was PCR amplified using primers fuse 1 and fuse 2 (Table 2.5). The primers used for the amplification included *Nde*I and *Bam*HI sites within their 5′-ends to facilitate digestion of the resulting amplified product and cloning into the equivalent sites upstream of the enhanced green fluorescent protein (eGFP) gene in pIJ8660 (Sun *et al.*, 1999). The downstream primer also included an extra 30 nt encoding a flexible linker peptide (LPGPELPGPE) to facilitate proper folding and functioning of both sIHF and eGFP within the fusion protein. This translational fusion was passaged through ET/pUZ, as described in 2.3.1.1 and introduced into the Δ*sIHF*-mutant strain by conjugation, as described in 2.3.2.1, and was determined to function in place of the wild type sIHF by testing for complementation of the mutant phenotype (antibiotic production, spore pigmentation and spore size).

2.3.10 Antibiotic production assays

Equal numbers of wild type and mutant spores were used to inoculate 10 ml YEME:TSB liquid starter cultures in glass 'universal' vials that were grown for 2 days at 30°C. An equivalent amount of biomass (~0.25 g) was transferred to a 250 ml flask containing 100 ml of YEME-TSB liquid medium and incubated at 30˚C for up to 6 days. Levels of actinorhodin and undecylprodigiosin were measured, as described elsewhere (Kang *et al.*, 1998; Kieser *et al.*, 2000), every 24 hours after inoculation for 6 days. To quantify actinorhodin levels, 0.5 ml of culture was transferred to a 1.5 ml microfuge tube and centrifuged at 2,218 × g for 5 minutes. The supernatant was transferred to a fresh 1.5 ml microfuge tube and an equal volume of NaOH was added to a final concentration of 1 M. The absorbance of the solution was measured at 633 nm using an Ultrospec 3100 pro (Biochrom). To quantify levels of undecylprodigiosin, a similar procedure was followed; however, the cell pellet of the centrifuged sample was resuspended in acidified methanol overnight, at room temperature, after which the absorbance was measured at 530 nm. To ensure results were reproducible, three cultures were set up per strain and two aliquots of each culture was tested.

Calcium-dependent antibiotic (CDA) was measured using a plate-based bioassay, as described previously (Kieser *et al.*, 2000) with minor modifications. *S. coelicolor* was grown on nutrient agar plates for 24-48 hours at 30˚C to produce a lawn of confluent growth. A sterile glass Pasteur pipette was used to remove agar plugs from this lawn and the plug was then transferred into an empty Petri plate. The plate was then filled with soft nutrient agar (1.15% [w/v] nutrient agar, 0.4% [w/v] nutrient broth) supplemented with 12 mM $CaCl_2$ and $1/100^{th}$ volume of overnight *S. aureus* ATCC 29213 cells. Control plates were treated the same, only $CaCl_2$ was omitted from the plates. Zones of growth inhibition were measured after two days of growth at 37˚C. To ensure results were reproducible, the assay was performed in triplicate on three separate occasions.

2.3.11 Bacterial-two-hybrid assay

To determine whether sIHF interacts with TopA, the bacterial two-hybrid assay was used (Karimova *et al.*, 1998). The *sIHF* and *topA* genes were PCR amplified with primers (Table 2.5) that introduced *Kpn*I and *Xba*I or *Bam*HI and *Eco*RI restriction sites at the 5′ and 3′ ends of the resulting PCR products. The PCR products were digested with these restriction enzymes and introduced into similarly digested pKT25/pKNT25 or pUT18/pUT18C (Table 2.3). Pairs of plasmids, including constructs containing each of the T18 and T25 fragments of *Bordetella pertussis* adenylate cyclase gene fused to *sIHF* or *topA*, were introduced into *E. coli* DHM1, as described in 2.3.1.1. Resulting strains were plated on LB agar containing 40 µg/ml X-gal and 0.5 mM IPTG and incubated at 37˚C overnight. Blue/white selection was used to screen colonies, with blue colonies indicating interaction between the two proteins. Negative controls included *E. coli* carrying plasmid pairs containing only one fusion so that no interaction could occur and as a positive control, pKNT25 and pUT18C carrying the leucine zipper of the yeast protein GCN4, which is known to dimerize, were used (Karimova *et al.*, 1998).

2.4 RNA techniques

2.4.1 Isolating RNA from *S. coelicolor*

RNA extractions from *S. coelicolor* were completed as described previously (Hopwood *et al.*, 1985) with minor modifications. *S. coelicolor* was spread on MS or R2YE agar media overlaid with cellophane discs and grown at 30˚C for up to 4 days. At defined timepoints, cells were removed using the flat end of a sterilized spatula and added into 15 ml conical tubes containing 5 ml of modified Kirby's mixture (1% w/v N-lauroylsarcosine sodium salt, 6% w/v sodium 4-amino salicylate, 6% v/v phenol mixture, pH 7.9) and ~10 glass beads (4 mm in diameter). Samples were mechanically disrupted by vortexing for 2 minutes, after which 5 ml of phenol:chloroform (1:1) was added. The mixture was repeatedly vortex mixed for 30 seconds and incubated on ice for 30 seconds, until it appeared homogenous. After centrifuging at 7798 × g for 5 minutes at 4˚C, the upper phase of the separated sample was transferred to a new 15 ml conical tube and the sample was extracted again using 5 ml of phenol:chloroform (1:1). Phenol-chloroform extractions were repeated until little to no interface was remained between the organic and aqueous layers. The upper aqueous phase of the final extraction was then transferred to a fresh 15 ml conical tube and precipitated by adding 0.1 volumes of ice-cold 3 M NaOAc (pH 6) and an equal volume of ice-cold isopropanol and then stored at -20˚C overnight. The samples were centrifuged at 7798 × g for 20 minutes at 4˚C, and the resulting pellets were washed with 1 ml of 80% ice-cold ethanol and air dried before resuspending in 500 µl of sterile water at 4˚C overnight. RNA was next treated with DNase I (6 rounds of one hour incubations using 10 U DNase I per round), extracted with phenol:chloroform (1:1) and precipitated, as described above, before being resuspended in 40 µl of sterile water. RNA sample concentrations were measured with an Ultrospec™ 3100 Pro (Biochrom Ltd.) or a NanoDrop 1000 (Thermo Scientific) spectrophotometer and RNA sample quality was determined by separating the samples on 1% agarose gels using electrophoresis.

2.4.2 Northern blot analysis

Northern blots were prepared as described previously (Haiser *et al.*, 2008), with minor modifications. Total RNA (40 µg) was mixed with a formamide-based loading dye and heated at 95˚C for 10 minutes before being loaded onto a 12.5% Tris-borate-EDTA (TBE)-based denaturing polyacrylamide gel. Gels were run in 1× TBE buffer at 100 V for 30-60 minutes. Gels containing the separated RNA samples were transferred to Zeta probe nylon membranes (Bio-Rad) using a semi-dry transfer apparatus (Trans-Blot® Semi-dry, Bio-Rad) at 15 V for 45-60 minutes. RNA was cross-linked to the nylon membranes by UV-light treatment using a UV crosslinker (Spectrolinker XL-1000, Spectronics Corporation).

Hybridization probes were prepared by 5′ end labeling 2 pmol of the desired single stranded primer with [γ-^{32}P] ATP (Perkin Elmer) using 10 U T4 polynucleotide kinase (Invitrogen), as per the manufacturer's instructions. 5′ end labeled probes were purified using the MinElute® Reaction Cleanup kit (Qiagen)

and eluted with 50 µl of sterilized water. Prior to probe hybridization, RNA-bound membranes were pre-hybridized with 15 ml of hybridization buffer (Ultrahyb®-oligo, Ambion) in a hybridization tube (Techne) rotating in a hybridization oven (HB-1D, Techne) at 42˚C for at least 30 minutes. Half of the purified probe was added to the hybridization buffer and incubated (as above) overnight. Membranes were washed twice for 5 minutes with low stringency buffer (2× SSC, 0.1% [v/v] SDS), followed by one wash for 5 minutes with high stringency buffer (0.2× SSC, 0.1% [v/v] SDS). Membranes were exposed to X-ray film (Kodak) or phosphorscreens (Molecular Dynamics) for a few hours and developed or scanned using a phosphorimager (Molecular Dynamics), respectively. Northern blots were conducted a minimum of three times, using RNA isolated from at least two independent time courses. Any comparisons of transcript abundance between different RNA isolations were done using RNA transferred to the same (single) membrane, hybridized with the same labeled oligonucleotide probe, and exposed to X-ray film for the same length of time.

2.4.3 5′ and 3′ transcript end mapping

5′-rapid amplification of cDNA ends (RACE) was carried out using the FirstChoice® RNA Ligase Mediated (RLM)-RACE kit (Ambion), following the manufacturer's instructions, but adjusted for use with bacterial RNA. Briefly, 10 µg of total RNA extracted from *S. coelicolor* at specific timepoints, as described in 2.4.1, was treated with tobacco acid pyrophosphatase (TAP) before being ligated to a 5′-RACE adapter using T4 RNA ligase. This ligated product was then used as template for reverse transcription using a primer complementary to the sRNA sequence (Table 2.4), together with SuperScript™ III reverse transcriptase (Invitrogen). The resulting cDNA then served as template for 5′-end PCR amplification, using an adaptor-specific oligonucleotide (Table 2.4) and the same oligonucleotide used to prime the reverse transcription reaction. The resulting PCR product was then used as template for an additional round of PCR amplification using a second 'nested' adaptor-specific oligonucleotide, and a nested sRNA-specific oligonucleotide (Table 2.4). The PCR products from the second reaction were resolved on an agarose gel, excised, and purified using the MinElute PCR purification kit (Qiagen). The purified products were cloned into the TOPO® vector using TOPO TA Cloning® (Invitrogen) and transformed into One Shot® DH5α-TOP10F′ competent cells (Invitrogen). Colony PCR using vector specific primers (and *E. coli* colonies themselves as template), was conducted to identify those colonies containing cDNA inserts, which were then grown overnight. Plasmid DNA was extracted using the QIAprep® Miniprep kit (Qiagen), and the cloned inserts were sequenced using the M13 reverse primer (Table 2.4). 3′-RACE was conducted using the same kit as the 5′-RACE, following the manufacturer's instructions. Prior to initiating the 3′-RACE protocol, however; 40 µg of total RNA was polyadenylated by treatment with 5 U of poly(A) polymerase (2 U/ml, Ambion) at 37˚C for 1 h. The 3′-RACE adapter was then annealed to ~50 ng poly(A)-RNA, and this RNA was reverse transcribed using Moloney Murine Leukemia Virus (M-MLV) reverse transcriptase (Ambion) for 1 h at 42˚C. PCR, cloning and sequencing were conducted as described for 5′-RACE.

2.4.4 Semi-quantitative reverse transcription – PCR (RT-PCR)

Five micrograms of RNA, 2 pmol of gene-specific reverse primer (to prime the reverse transcription; Table 2.4) and 0.5 mM dNTPs were mixed together, heated at 95˚C for 10 minutes, then immediately placed on ice. RNA was reverse transcribed into cDNA by adding first strand buffer, DTT, RNase OUT (40 U; Invitrogen) and SuperScript® III reverse transcriptase (Invitrogen), as described in the manufacturer's instructions. Reactions were incubated at 42˚C for 50 minutes, before being terminated by incubating at 70˚C for 15 minutes. The resulting PCR product was used as template to check for the presence of the desired products with gene specific primers (Table 2.4). To ensure that no residual DNA was contaminating the RNA samples, a PCR control was completed using RNA (without a reverse transcription step) as template. Any amplification signal in these controls suggested potential DNA contamination, which resulted in sample re-treatment with DNase I. PCR products were resolved on a 2% agarose gel using electrophoresis.

2.4.5 Reverse transcription, quantitative PCR (RT-qPCR)

Three sets of RNA time courses were prepared from wild type and Δ*sIHF* mutant strains grown on MS medium. All RNA samples were reverse transcribed as described in 2.4.4, with reverse primers corresponding to the nucleoid-associated protein- (NAP-) encoding genes of interest (Table 2.5). cDNA generated during the RT reaction was amplified using the PerfeCta®SYBR®Green SuperMix (Quanta Biosciences) using 0.2 mM of each forward and reverse primers specific to the genes of interest (Table 2.5). In addition to the NAP-encoding genes, an endogenous reference gene, *rpoB*, was included to obtain relative levels of NAP gene expression throughout the time course. Quantitative PCR was completed in duplicate in 96-well optical plates with a CFX96 Touch™ Real-Time PCR Detection System (Bio-Rad) using the thermal cycling conditions described by the manufacturer, with 50 amplification cycles. Negative control reactions (using RNA samples that were not subjected to RT as template) were conducted for all RNA samples, and four 'no template' (water alone) controls were included on each 96-well plate. The data from each replicate were processed separately as follows: baseline-corrected fluorescence data (ΔR_n) was exported from Bio-Rad CFX Manager 2.1 (Bio-Rad) and analyzed using Data Analysis for Real-Time PCR (DART-PCR) (Peirson *et al.*, 2003). The average midpoint and average amplification efficiency of each data set, which comprised the amplification curves of one gene, were determined and used to calculate a gene expression value (R_0) per sample. R_0 values of target genes were normalized to total RNA.

2.4.6 Analyzing RNA-RNA interactions using electrophoretic mobility shift assays (EMSAs)

In vitro transcription of scr1906 and *whiH* was completed using the components of the MEGAshortscript kit (Invitrogen) with *scr1906* and *whiH* DNA template sequences prepared by PCR or oligonucleotide annealing. These templates were designed so as to include a T7 promoter upstream of the sequence to be transcribed. The *whiH* template was created by PCR amplifying *whiH* with an

upstream primer containing the T7 promoter sequence (T7 whiH up; Table 2.4). In contrast, complementary oligonucleotides (T7 scr1906 plus and T7 scr1906 minus; Table 2.4) containing the T7 promoter sequence upstream of the *scr1906* specific sequence were annealed together to create the scr1906 template. After incubating the *in vitro* transcription reaction at 37˚C for 4 hours, the transcribed RNA was precipitated by adding 0.1 volume of ammonium acetate stop solution (Invitrogen) and 2 volumes of ice-cold ethanol. The mixture was incubated on ice for 20 minutes before centrifuging at ~15,700 × g for 15 minutes at 4˚C. The RNA pellet was air dried, resuspended in sterile water and purified from a native polyacrylamide gel. RNA was [γP^{32}] 5′ end-labeled and unincorporated [γP^{32}] was removed using Nuc-away spin columns (Ambion) as per the manufacturer's instructions. The RNA molecules were folded to their native conformation, either together or in separate reactions, and then incubated together at 30˚C for 30 minutes to allow for any RNA-RNA interactions to occur. RNA folding was completed by incubating RNA with 40 mM $MgCl_2$ in structure buffer (Ambion) at 95˚C for 5 minutes and cooling to room temperature. The mixtures were loaded onto a 12.5% native polyacrylamide gel and electrophoresis was performed in 1× TBE buffer at 100 V for 45-90 minutes. Gels were exposed to Biomax XAR film (Kodak) at room temperature for ~20 min before being developed.

2.5 Protein biochemical techniques

2.5.1 Protein overexpression and purification

2.5.1.1 sIHF overexpression and purification

sIHF was PCR amplified from chromosomal DNA using primers SCO1480 Nde and SCO1480 Bam (Table 2.5) and purified using the PureLink™ Gel Extraction kit (Invitrogen), as per manufacturer's instructions. The purified product was introduced into *Sma*I-digested and dephosphorylated pIJ2925 (Table 2.3). *sIHF* was then excised following digestion with *Nde*I and *Bam*HI and cloned into a similarly digested pET15b vector (Table 2.3). The resulting product was sequenced and introduced into *E. coli* Rosetta cells (Table 2.2), as described in 2.3.1.1. A flask containing 250 ml LB liquid medium was inoculated with 1/100 volume of an overnight culture of the sIHF overexpression strain. Overexpression of 6×His-sIHF was achieved by growing this culture at 37°C to mid-exponential phase (OD_{600} ~0.4-0.6), before adding 1 mM isopropyl β-D-1-thiogalactopyranoside (IPTG) and growing it overnight at 26°C. Cultures were centrifuged at 2,218 × g for 5 minutes and the cell pellet was resuspended in lysis buffer (50 mM NaH_2PO_4, 300 mM NaCl and 10 mM imidazole, pH 8.0) containing 1 mg/ml lysozyme and one complete mini EDTA-free protease inhibitor pellet (Roche). The mixture was incubated on ice for 30 min before being lysed by sonication (Branson®, Sonifier Cell Disrupter 350) at 50% power for repeated cycles of 15 seconds sonication on ice, followed by 15 seconds of incubation on ice until the lysate appeared translucent. RNase A (80 µg/ml) and DNase I (40 U/ml) were then added to the cell lysate and incubated on ice for 20 minutes before centrifuging at ~15,700 × g for 30 minutes at 4˚C. The supernatant was transferred to a fresh 15 ml conical tube and mixed with 1 ml Ni-

nitrilotriacetic acid (Ni-NTA) agarose resin (Qiagen) and rotated for 1 hour at 4˚C. 6×His-sIHF was purified by passing the mixture over a PolyPrep chromatography column (Bio-Rad) and washing with 5 ml wash buffer (20 mM Tris-HCl pH 7.5, 250 mM NaCl) supplemented with increasing concentrations of imidazole and eluting with 1 ml 150 mM imidazole into a tube containing 10 ml of sterile water. The eluted protein was then washed with phosphate buffered saline (PBS) (pH 7.4) using Macrosep Advance Centrifugal Devices (PALL) with a 10 kDa cutoff and concentrated to a 500 µl total volume.

2.5.1.2 TopA overexpression and purification

TopA was purified in a similar manner as sIHF, with some modifications. Briefly, *topA* was PCR amplified from chromosomal DNA using primers topA1 and topA2 (Table 2.5). The PCR product was digested with *Nde*I and *Bam*HI and cloned into a similarly digested pET11a vector (Table 2.3). The resulting product was sequenced and introduced into *E. coli* BL21(DE3) (Table 2.2), as described in 2.3.1.1. TopA overexpression was induced in a culture at OD_{600} of 0.7 and further incubated for 3 hours at 37˚C. Cell pellets were resuspended in lysis buffer (20 mM Tris-HCl pH 7.5, 25 mM KCl, 1.4 mM β-mercaptoethanol and 5% glycerol), lysed by sonication and cleared by centrifugation at 40,000 × g for 40 minutes. The supernatant was loaded onto a HiTrap SP HP column (GE Healthcare) equilibrated with lysis buffer. TopA was eluted using a linear gradient to 500 mM KCl. Fractions containing TopA were pooled together and concentrated to 3.5 mg/ml.

2.5.2 Antibody purification

Purified 6×His-sIHF was dialyzed into storage buffer (50 mM Tris-HCl pH 7.5, 150 mM NaCl and 1 mM dithiothreitol [DTT]) and used for polyclonal antibody generation (Cedarlane Labs; Burlington, ON). Prior to using the sIHF antibody that was received from Cedarlane Labs, 6×His-reactive molecules from the crude antiserum were removed. First, a 6×His-tagged protein from another bacterial species (6×His-VirB8 from *Brucella suis*) was overexpressed and immobilized on a PolyPrep column containing Ni-NTA agarose resin, as described in 2.5.1. After several 5 ml washes (20 mM Tris-HCl pH 7.5, 250 mM NaCl), 5 ml crude antiserum was passed through the column, with the flow-through containing an antiserum cleared of 6×His-reactive species. This pre-cleared antiserum was then incubated with 6×His-sIHF, which had been previously bound to Ni-NTA beads. The beads were then washed several times with wash buffer (as above), followed by equilibration buffer (50 mM Tris-HCl pH 7.4, 150 mM NaCl,), and rotated overnight at 4˚C. The mixture was loaded onto a PolyPrep column and washed with 5 ml equilibration buffer and then 5 ml equilibration buffer supplemented with 2 M NaCl. Next, 2 ml of 4 M $MgCl_2$ was added to the column and the flow-through was collected in a 50 ml conical tube containing 20 ml of sterilized water. The mixture was passed through a Macrosep Advance Centrifugal Device (PALL) with a 10 kDa cutoff and subjected to buffer exchange with PBS, as described in 2.5.1. After concentrating the purified antibody, glycerol was added (50%) and the mixture was stored at -20˚C. Sodium dodecyl sulphate–polyacrylamide gel electrophoresis (SDS-PAGE) and

Coomassie Brilliant Blue (0.1% Coomassie Brilliant Blue R-250, 50% methanol, 10% acetic acid) staining were used to check for the presence of purified antibody.

2.5.3 Protein-DNA EMSAs

Electrophoretic mobility shift assays (EMSAs) were performed using 8–15% native polyacrylamide gels and [γ-^{32}P] ATP 5′-end-labelled probes. Probes were created by first 5′ end-labeling 50 pmol of a single stranded primer using 10 U T4 polynucleotide kinase (Invitrogen) and 4.76 pmol [γ -^{32}P] ATP (Perkin Elmer) as per the manufacturer's instructions. Labeled products were purified using the MinElute® Reaction Cleanup kit (Qiagen) and eluted with 50 µl of sterilized water. The same concentration of cold complementary primer was mixed with the purified, labeled primer in an oligonucleotide annealing buffer (10 mM Tris-HCl pH 7.5–8.0, 50 mM NaCl, 1 mM EDTA) up to a volume of 100 µl. The mixture was heated at 95˚C for 5 minutes and allowed to cool to room temperature overnight to allow the oligonucleotides to anneal. Probes larger than 200 bp were first PCR amplified (Table 2.5) and a fraction of the purified PCR products were separated on a 1% agarose gel containing ethidium bromide using electrophoresis, and DNA intensity was compared to a quantified marker to estimate its concentration. The PCR product was then labeled as described above.

Increasing concentrations of purified sIHF (0–100 µM), isolated as described in 2.5.1, were combined with 0.1 µM probe, 1 mg/ml bovine serum albumin (BSA) and binding buffer (10 mM Tris-HCl pH 7.8, 5 mM $MgCl_2$, 60 mM KCl and 10% glycerol), incubated at room temperature for 10 min and then on ice for 30 minutes prior to adding loading dye (250 mM Tris-HCl pH 7.8, 0.2% bromophenol blue, 40% glycerol). To test binding specificity, increasing concentrations of poly(dI-dC) (0–5 µg; Roche) were added together with 10 µM sIHF to the EMSA reactions described above. The mixtures were loaded onto a native polyacrylamide gel and electrophoresis was performed in 1× TBE buffer at 100 V for 45-90 minutes. Gels were exposed to Biomax XAR film (Kodak) at room temperature for ~20 min before being developed.

2.5.4 Cell extract preparation, SDS-PAGE and immunoblotting

S. coelicolor was grown on MS agar overlaid with cellophane discs at 30˚C for up to 4 days. Samples were harvested at various timepoints by scraping cells off cellophane discs using the flat end of a sterilized metal spatula. Lysis buffer (10 mM Tris-HCl pH 7.5, 1 mM EDTA, 1 mM DTT, 10% [v/v] glycerol, 150 mM NaCl) supplemented with lysozyme (2 mg/ml) and one cOmplete, mini, EDTA-free™ protease inhibitor pellet (Roche) was added to the cells in a 1.5 ml microfuge tube. The mixture was incubated at 37˚C for 30 minutes or until lysis was evident, and was then sonicated (Branson®, Sonifier Cell Disrupter 350) at 50% power for cycles of 15 seconds sonication, 15 seconds of incubation on ice until the lysate appeared translucent. The soluble fraction was removed after centrifugation at ~15,700 × g for 30 minutes at 4˚C and an equal volume of 2× Laemmli buffer was added (Laemmli, 1970). Protein samples were heated at 95˚C for 5 minutes before being resolved by SDS-PAGE and were either visualized by staining with Coomassie Brilliant Blue to ensure equal sample loading, or were transferred to a 0.45 µm

polyvinylidene difluoride (PVDF) membrane (GE). PVDF membranes were first soaked in methanol for 15 minutes and equilibrated with transfer buffer (25 mM Tris (pH 7.6), 192 mM Gly, 10% methanol) for an additional 15 minutes. Protein samples were transferred onto the treated PVDF membranes between two filter papers soaked with transfer buffer in a semi-dry transfer apparatus (Trans-Blot® semi-dry, Bio-Rad) at 15 V for 1 hour. Membranes were blocked for 3 hours at room temperature with Tris-buffered saline, with added Tween detergent (TBST; 10 mM Tris-HCl pH 8.0, 100 mM NaCl and 0.05% Tween 20) containing 6% fat-free skim milk and subsequently incubated overnight at 4°C in TBST/6% skim milk containing crude polyclonal sIHF antibody (1:7000 dilution). The membrane was then washed three times with TBST, incubated for 30 min in TBST/6% skim milk containing goat anti-rabbit IgG horseradish peroxidase-linked secondary antibody (1:3500 dilution; Cell Signaling) before again being washed three times with TBST. Signals were detected using Amersham ECL™ Western Blotting Detection reagents (GE Healthcare) and Biomax XAR film (Kodak).

2.5.5 Topoisomerase activity assays

The effect of sIHF on plasmids *ex vivo* was assayed using *E. coli* Rosetta cells (Table 2.2) containing the 6×His-sIHF overexpression plasmid. An overnight culture of this strain, grown in 5 ml LB liquid medium, was sub-cultured (1/100) into a 500 ml flask containing 100 ml LB medium and grown to an OD_{600} of ~0.4, at which point 1 mM IPTG was added to induce expression of the sIHF fusion. As a negative control, equivalent cultures were grown without IPTG induction. To test whether general protein overexpression led to changes in plasmid structure, the same experiment was conducted using *E. coli* Rosetta cells containing the same overexpression plasmid (pET15b), only with *srtA* in place of *sIHF* [pMC141; (Duong *et al.*, 2012)]; *srtA* encodes an endopeptidase used to anchor proteins to the surface of Gram-positive cells. Plasmid DNA from overexpression and control cultures was extracted using the PureLink™ Quick Plasmid Miniprep Kit (Invitrogen) 8 hours after induction, and the resulting DNA was resolved by electrophoresis on a 0.8% agarose gel. Cell-free extracts for each culture (induced and uninduced) were also prepared and were resolved using electrophoresis on 12–18% SDS-PAG stained with Coomassie Brilliant Blue to ensure both sIHF and SrtA were effectively expressed after 8 hours of induction.

The effects of sIHF or a negative control protein (lysozyme) on the activity of TopA was tested by incubating the purified proteins with supercoiled plasmid DNA to assess plasmid relaxation. Reactions were set up in a total volume of 15 µl containing 8 ng of TopA, 64 nM of a supercoiled form of a plasmid (pUC19) and reaction buffer (50 mM Tris-HCl pH 7.5, 50 mM KCl, 10 mM $MgCl_2$, 0.1 mM EDTA, 0.5 mM DTT and 0.06 mg/ml BSA) with either sIHF or lysozyme at the following final concentrations (µM): 8.64, 17.28 or 34.56 (1:135, 1:270 and 1:540 [DNA:protein] molar excess, respectively). To demonstrate that sIHF or lysozyme alone did not affect plasmid mobility; reactions were also conducted as described above, only replacing TopA with storage buffer. Additional reactions at lower DNA:sIHF molar excesses were conducted using sIHF at lower concentrations (1:17, 1:34, 1:68, 1:135, 1:270 and 1:540). Reactions were incubated at room temperature for 30 minutes

and stopped with 5 µl of stop buffer (6% SDS, 30% glycerol, 10 mM EDTA and 0.25% bromophenol blue). Reaction products were resolved on 1% agarose gels stained with ethidium bromide using electrophoresis.

2.5.6 Systematic Evolution of Ligands by Exponential Enrichment (SELEX)

A single stranded library containing ~10^8 random 20 nt sequences flanked by 14 nt primer sites (Table 2.5) was ordered from Integrated DNA Technologies. A Klenow reaction was completed to generate a double stranded library by mixing 1 µg of single stranded library DNA with 8 U of Klenow (New England Biolabs), 100 µM SELEX rev primer (Table 2.5), reaction buffer (50 mM Tris-HCl pH 8, 10 mM $MgCl_2$, 50 mM NaCl), 1 mM of each dATP, dCTP, dTTP and [αP^{32}]dGTP, along with and 0.1 mM dGTP. The mixture was incubated at room temperature for 10 minutes and precipitated by adding 0.1 volume of NaOAc (pH 7) and 2.5 volumes of ice-cold ethanol before incubating on ice for at least 20 minutes and then centrifuging at ~15,700 × g for 20 minutes at 4˚C. The resulting DNA pellet was air dried, re-suspended in 10 µl of sterile water, purified from a 10% native polyacrylamide gel and concentrated by precipitation.

The sIHF concentration used for all SELEX experiments was equivalent to the sIHF minimal concentration required to shift a 42 bp probe in an EMSA, and then reduced 5-fold. The first SELEX round was performed using the purified double stranded library and 1 µM sIHF incubated with components as described in section 2.5.3 for 10 minutes at room temperature, followed by 40 minutes on ice. Protein-DNA complexes were isolated by incubating the mixture with 1 ml Ni-nitrilotriacetic acid (Ni-NTA) agarose resin (Qiagen) and incubated, while inverting, at 4˚C for 30 minutes. The complexes were then loaded onto a PolyPrep chromatography column (Bio-Rad) and washed with binding buffer until the radioactivity in the flow-through was the equivalent of background levels. sIHF-DNA complexes were eluted from the column using 500 µl 150 mM imidazole. The relative amount of DNA eluted, compared to nonspecific DNA in the flow-through, was measured using a scintillation counter. After precipitating the eluted sample, imidazole was removed by washing it with binding buffer in a Micro Bio-Spin column (Bio-Rad). The eluted sample was used as template for subsequent PCR using SELEX fwd and SELEX rev primers (Table 2.5), which are specific to the known sequences flanking the library DNA, together with the same dNTP preparation as described above. PCR products were purified on a 10% native polyacrylamide gel, as above, and the protocol was repeated up to six times. PCR products from the 2^{nd} and 6^{th} selection rounds were cloned into pTZ57R/T (Fermentas) and transformed into *E. coli*. Plasmid DNA from 100 colonies from each selection was sequenced with a plasmid-specific primer – M13 forward (Table 2.5). From these, sequences were obtained for 50 (selection #2) and 71 (selection #6) clones. These sequences were analyzed using MEME (Bailey and Elkan, 1994).

2.5.7 Fluorescence resonance energy transfer (FRET)

Complementary plus and minus strand oligonucleotides (dsDNA FRET 1 and dsDNA FRET 2; Table 2.5) that were 5′ end-labeled with TAMRA (fluorophore

acceptor) or Fluorescin (fluorophore donor) were obtained from Integrated DNA Technologies. The oligonucleotides were annealed to create double stranded molecules by incubating 100 pmol of each oligonucleotide in annealing buffer (10 mM Tris-HCl pH 8.0, 50 mM NaCl, 1 mM EDTA) up to a volume of 100 µl. The mixture was heated at 95˚C for 5 minutes and allowed to cool to room temperature overnight.

FRET studies were performed using donor-acceptor labeled oligonucleotides, alongside donor or acceptor only labeled oligonucleotides as controls. Oligonucleotides (100 nM) were combined with 50 µM sIHF, 10 mg/ml BSA and binding buffer (10 mM Tris-HCl pH 7.8, 5 mM $MgCl_2$, 60 mM KCl and 15% glycerol) in a total volume of 100 µl and incubated at room temperature for 10 minutes and then on ice for 30 minutes. Fluorescence measurements were taken using a microplate reader (Tecan). Raw FRET was first measured by exciting the donor fluorophore (495 nm) and measuring the emission of the acceptor fluorophore (584 nm). The background fluorescence of each fluorophore was corrected in the raw FRET data with the measurements obtained from measuring the fluorescence after exciting the donor and acceptor fluorophores and measuring the emission of each separately. Each reaction was preformed in triplicate to ensure the reproducibility of the results. Four water samples served as additional background fluorescence controls. Background corrected raw FRET data was used to determine the distance between the fluorophores and bend angle. The calculations are described in detail here: (Kugel, 2008).

2.6 Microscopy techniques

2.6.1 Light and fluorescence microscopy

Samples for light and fluorescence microscopy were obtained by growing *S. coelicolor* along the underside of a sterile coverslip inserted into MS agar at a 45° angle at 30˚C. After 5 days, the coverslip was removed from the agar and adherent cells were stained with 4′,6-diamidino-2-phenylindole (DAPI) diluted in a SlowFade solution (1:250; Invitrogen) and mounted onto a microscope slide. All images were obtained with a Leica DMI 6000 B wide-field deconvolution microscope using the Leica HCS Plan Apo oil immersion objective (magnification: ×100; numerical aperture: 1.4; Leica Microsystems, Wetzlar, Germany). Spore lengths, nucleoid areas and nucleoid fluorescence were all determined using ImageJ software (Abramoff *et al.*, 2004). When visualizing eGFP, control strains (harbouring empty pIJ8660; Table 2.3) were first examined to adjust fluorescence levels such that there was no detectable GFP signal, before imaging the experimental strains.

2.6.2 Scanning electron microscopy

Samples were prepared for scanning electron microscopy (SEM) as described previously (Haiser *et al.*, 2009). *S. coelicolor* strains were streaked for single colonies on MS agar medium and grown for 5 days at 30˚C. Individual colonies were excised from the plate using a sterilized razor and submerged in 2% glutaraldehyde solution overnight at 4˚C. The fixed samples were rinsed in sterilized water twice and post-fixed in 1% osmium tetroxide for 1 hour. Samples were then dehydrated using an

ethanol gradient (50%, 70%, 95%, 100%) after which they were dried using a critical point dryer before being mounted onto SEM stubs and coated with gold. Samples were visualized using a JEOL JSM840 SEM. Images were analyzed using ImageJ software (Abramoff *et al.*, 2004).

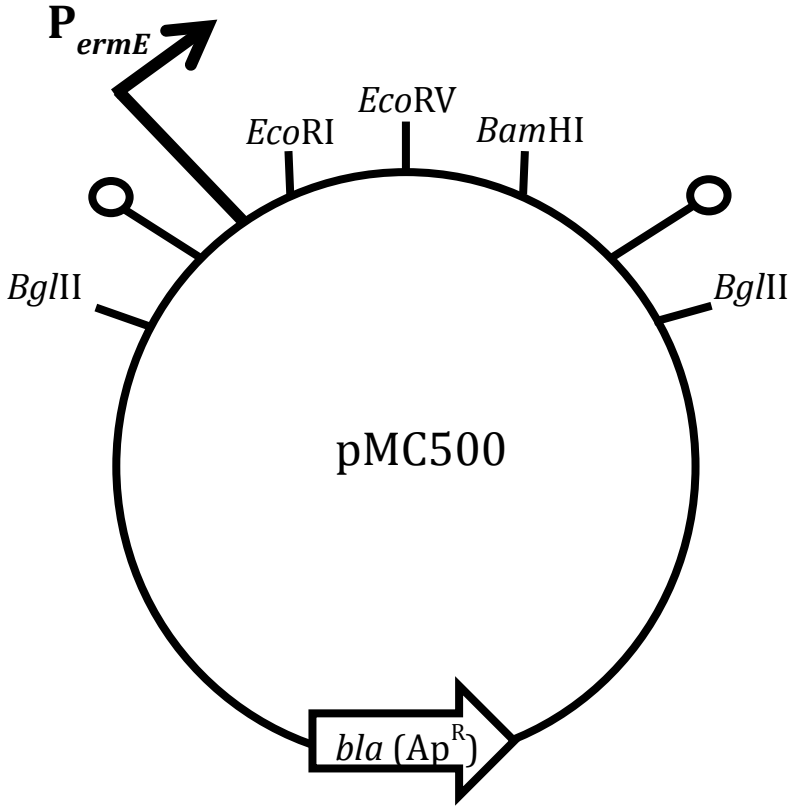

Figure 2.1 Map of pMC500. RNA overexpression vector, pMC500, contains a constitutive *ermE* promoter (Schmitt-John and Engels, 1992) upstream of a multiple cloning site. The region containing the promoter and multiple cloning site is flanked by terminator sequences, represented by the circles attached to lines, to prevent readthrough from upstream genes, and to effectively terminate the expression of the sRNA/RNA. This entire region is also flanked by *Bgl*II sites for the option of excising and cloning the region into a *Bam*HI site of another vector of choice. The backbone of pMC500 is pUC57.

Table 2.1: *Streptomyces* strains used in this work

Streptomyces strains	Genotype	Reference
M600	SCP1- SCP2-	(Chakraburtty and Bibb, 1997)
N985	M145 *bldB*::*aphI*	(Eccleston *et al.*, 2002)
J1700	J1501 *bldA39*	(Piret and Chater, 1985)
J2400	M145 *whiG*::*hyg*	(Flärdh *et al.*, 1999)
J2402	M145 *whiG*::*hyg*	(Flärdh *et al.*, 1999)
E309	M600 *scr1906*::[*acc(3)IV*)-*oriT*]	(Swiercz *et al.*, 2008)
E309a	M600 *scr1906*::*FRT*	(Swiercz *et al.*, 2008)
E310	M600 *sIHF*::[*acc(3)IV)-oriT*]	(Swiercz *et al.*, 2013)
E310a	M600 *sIHF*::*FRT*	(Swiercz *et al.*, 2013)

Table 2.2: *E. coli* strains used in this work

E. coli strains	Use	Reference
DH5a	Plasmid construction and general sub-cloning	(Hanahan, 1983)
ET12567/pUZ8002	Generation of methylation-free plasmid DNA	(Paget *et al.*, 1999)
BW25113	Construction of cosmid-based knockouts	(Gust *et al.*, 2003)
BT340	DH5a carrying 'FLP recombination' plasmid	(Datsenko and Wanner, 2000)
BL21 DE3 pLysS Rosetta	Protein overexpression	Novagen
BL21 DE3	Protein overexpression	Novagen
TOP10F′	Transformation of TOPO vector	Invitrogen
DHM1	Protein-protein interaction (bacterial two-hybrid)	(Karimova *et al.*, 2005)

Table 2.3: Plasmids used in this work

Name	Use	Reference
pIJ2925	General cloning vector	(Janssen and Bibb, 1993)
pCR2.1-TOPO	TOPO cloning vector used for cloning 5′ and 3′ RACE products	Invitrogen
pIJ773	Plasmid carrying apramycin knockout cassette	(Gust *et al.*, 2003)
pIJ790	Temperature sensitive plasmid carrying λ-RED genes	(Gust *et al.*, 2003)
pIJ8660	Integrative cloning vector carrying promoterless *eGFP*	(Sun *et al.*, 1999)
pMC153	pIJ8660 + *sIHF*; sIHF-eGFP localization	This work
pIJ6919	pIJ8660 + P_{chpH}-*eGFP*; cytoplasmic localization of GFP	(Elliot *et al.*, 2003)
pET15b	6×His tag protein fusion overexpression vector	Novagen
pMC155	pET15b + *sIHF*; overexpression of sIHF	(Swiercz *et al.*, 2013)
pMC141	pET15b + *srtA*; overexpression of SrtA	(Duong *et al.*, 2012)
pET11a	Protein overexpression vector	Novagen
pAG8744	pET11a + *topA*; overexpression of TopA	(Swiercz *et al.*, 2013)
pMC500	pUC57 derivative with *ermE** promoter	Elliot lab
pRT801	Integrative cloning vector	(Gregory *et al.*, 2003)
pMC158	pRT801+P_{ermE}-*scr1906*; scr1906 overexpression construct	This work
pIJ6902	Integrative cloning vector with thiostrepton inducible promoter (P_{tipA})	(Huang *et al.*, 2005)
pMC157	pIJ6902+*whiG*; *whiG* induction assay	M. A. Elliot, unpublished
pIJ82	Integrative cloning vector	Gift from H. Kieser
pMC156	pIJ82+*whiH*-3× FLAG; WhiH-FLAG to measure expression levels	This work
pMC154	pIJ82 + *sIHF*; Δ*sIHF* complementation plasmid	(Swiercz *et al.*, 2013)
pKT25	Bacterial two-hybrid plasmid; creates fusions to C-terminus of CyaA T25 fragment	(Karimova *et al.*, 1998)
pKNT25	Bacterial two-hybrid plasmid; creates fusions to N-terminus of CyaA T25 fragment	(Karimova *et al.*, 1998)
pUT18	Bacterial two-hybrid plasmid; creates fusions to N-terminus of CyaA T18	(Karimova *et al.*, 1998)

	fragment	
pUT18C	Bacterial two-hybrid plasmid; creates fusions to C-terminus of CyaA T18 fragment	(Karimova *et al.*, 1998)
pMC159	pKT25 + *topA*	This work
pMC160	pKT25 + *sIHF*	This work
pMC161	pKNT25 + *topA*	This work
pMC162	pKNT25 + *sIHF*	This work
pMC163	pUT18 + *sIHF*	This work
pMC164	pUT18C + *topA*	This work
pMC165	pUT18C + *sIHF*	This work
pTZ57R/T	Cloning vector for SELEX DNA	Fermentas
St9C5	Cosmid used for *sIHF* knockout	(Redenbach *et al.*, 1996)

Table 2.4: Oligonucleotides used in sRNA-related studies

Name	Sequence (5′ to 3′)*	Comments
1906-1	CAGGTCGGCGGAACCGACAAGGTGCTC	Northern blot analysis; 5′ RACE
1906-2	GAGCACCTTGTCGGTTCCGCCGACCTG	Northern blot analysis; 3′ RACE
1906-3	GTTGTGCCGGTGACGGGACTCGAACCCGTG	Northern blot analysis
1906-4	GCAACCGTCCGATCAAAGGAAGTATCC	Northern blot analysis
1906-5	GAGTTCAGGTCGGCGGAACC	5′ RACE
1906-6	CCGACAAGGTGCTCTAACCCC	5′ RACE
1906-7	GTAGCTCAGGGGTTAGAGCACC	3′ RACE
3045-1	CCGTGGACGCGCAAGGACGTGGGCGGGC	Northern blot analysis; 3′ RACE
3045-2	GCCCGCCCACGTCCTTGCGCGTCCACGG	Northern blot analysis; 5′ RACE
3045-3	CACGTCCTTGCGCGTCCACGGTCTC	5′ RACE
3045-4	GCAAGGACGTGGGCGGGCAGACGACG	3′ RACE
3124-1	GTGTGGCGCTCCGTTATCGACGCGCTCTT	Northern blot analysis; 5′ RACE
3124-2	AAGAGCGCGTCGATAACGGAGCGCCACAC	Northern blot analysis
3124-3	GGGTACGGCCTTCCTCTCCGAGTAG	5′ RACE
3124-4	CCTCTCCGAGTAGACTGCTGAAG	5′ RACE
3261-1	CGTTCGTACAGTGGCGCGCTCCACC	Northern blot analysis
3261-2	CGCGAACCGACCGCAACCTTCGTCTA	Northern blot analysis
3261-3	TGCCCGCAGTCGGCAACGGCGCCCCTTC	Northern blot analysis
3261-4	GCCCCTTCCGCCCGGTGCCGGCCGATCC	Northern blot analysis
3261-5	GATCCCCCGCCGGAGGCATCCTCTTGTGC	Northern blot analysis
3261-6	CACGCACGCCCCAACGTGCCC	Northern blot analysis; 5′ RACE
3261-7	GGCGTCCAGGTCGTTCGTACAGTG	Northern blot analysis; 5′ RACE
3261-8	CACCCCACGCACGCCCCAACG	Northern blot analysis; 5′ RACE
3261-9	CTCCACCTGGACGCCCTGAACCACGC	5′ RACE
3261-10	GTGGCGCGCTCCACCTGGACGCCCTGAAC	5′ RACE
3261-11	CACCGCGCGAGGTGGACCTGCGGGACTTG	3′ RACE
3261-12	GTTCAGGGCGTCCAGGTGGAGCGCGCCAC	3′ RACE

3558-1	CGATCCGTGACTTCCATGGT	Northern blot analysis
3558-2	CCCGAGAGCCCTCTCAGGCAAACC	Northern blot analysis
3558-3	GGGGAGAGCGGGGGTCGTCTCCAC	Northern blot analysis; 5′ RACE
3558-4	GGGGGAGAGCGGGGGTCGTC	5′ RACE
3558-5	GGAGGAGTCGGACCGGGTTAGCACG	Northern blot analysis; 5′ RACE
3558-6	GGCCGTGGAGACGACCCCCGCTC	3′ RACE
3558-7	CGGGGCCCAGATCGTGAGAAGTGC	Northern blot analysis
3558-8	CCCACCCGGACATGCTGACGACCCCCG	Northern blot analysis
3974-1	TGCTGGCGACGGGGGATGCACCAGC	Northern blot analysis; 5′ RACE
3974-2	GCTGGTGCATCCCCCGTCGCCAGCA	Northern blot analysis; 3′ RACE
3974-3	GGAAAAGACCCGGTTGCTGG	5′ RACE
3974-4	CGACGGGGGATGCACCAGCAAC	5′ RACE
3974-5	CGAGTAGCCCGGTTGCTGGTGC	3′ RACE
3974-6	GTTGCTGGTGCATCCCCCGTCG	3′ RACE
5676-1	TGTGTGCGCGAGGCACGACCAGGTCGA	Northern blot analysis; 5′ RACE
5676-2	TCGACCTGGTCGTGCCTCGCGCACACA	Northern blot analysis; 3′ RACE
5676-3	GGTCGAAGCCGGGGAAGCC	5′ RACE
5676-4	CGTGCCTCGCGCACACAACCGGAG	3′ RACE
M13 forward	GTAAAACGACGGCCAG	Sequencing of cDNA clones
M13 reverse	CAGGAAACAGCTATGAC	Sequencing of cDNA clones, general sequencing
5S	CCCTGCAGTACCATCGGCGCT	Control probe for RNA integrity in northern blots
5′ RACE adapter	GCUGAUGGCGAUGAAUGAACACUGCGUU UGCUGGCUUUGAUGAAA	RNA adapter for RACE experiments
3′ RACE adapter	GCGAGCACAGAATTAATACGACTCACTA TAGGT12VN	RNA adapter for RACE experiments
5′ RACE adapter-1	GCTGATGGCGATGAATGAACACTG	5′ RACE – amplification of cDNA clones
5′ RACE adapter-2	CGCGGATCCGAACACTGCGTTTGCTGGC TTTGATG	5′ RACE – amplification of cDNA clones
3′ RACE adapter-1	GCGAGCACAGAATTAATACGACT	3′ RACE – amplification of cDNA clones
3′ RACE adapter-2	CGCGGATCCGAATTAATACGACTCACTA TAGG	3′ RACE – amplification of cDNA clones

scr1906 upstream	CGAATACAGCGAGTTCACCG	Amplification and overexpression of *scr1906*
scr1906 downstream	CGACAGCAGGTAGAGCTCGG	Amplification and overexpression of *scr1906*
small 1906 upstream	GCCGGTGTAGCTCAGGGGTTAGAGC	Amplification and overexpression of *scr1906*
small 1906 downstream	GGACCTACTTCCACTCATAATGGG	Amplification and overexpression of *scr1906*
small scr1906 plus	AATTCGCCGGTGTAGCTCAGGGGTTAGA GCACCTTGTCGGTTCCGCCGACCTGAAC TCTGGACACCG	Generate dsDNA for small scr1906 insert
small scr1906 minus	GATCCGGTGTCCAGAGTTCAGGTCGGCG GAACCGACAAGGTGCTCTAACCCCTGAG CTACACCGGCG	Generate dsDNA for small scr1906 insert
whiH upstream	CGAGGTCCTGCTGACCCAGTGGC	Creating WhiH-3× FLAG
whiH/XhoI	CAGG**CTCGAG**GTGCTCGCGGGGGG	Creating WhiH-3× FLAG
whiH/stop/ XhoI	CAGG**CTCGAG**TGACCGCCTTCCGCCGG	Creating WhiH-3× FLAG
whiH downstream	AGAGCGTTACGCCCAATCCGCGTGGC	Creating WhiH-3× FLAG
whiH internal	GGACGAGTTGCCCGTGCAGTCC	RT-PCR for checking Δ*whiG* strain
T7 scr1906 plus	TAATACGACTCACTATAGGGCCGGTGTA GCTCAGGGGTTAGAGCACCTTGTCGGTT CCGCCGACCTGAACTCTGGACA	*In vitro* transcription of *scr1906*
T7 scr1906 minus	GTGTCCAGAGTTCAGGTCGGCGGAACCG ACAAGGTGCTCTAACCCCTGAGCTACAC CGGCCCTATAGTGAGTCGTATTA	*In vitro* transcription of *scr1906*
T7 whiH up	TAATACGACTCACTATAGGGCGTGAGTA CCCTTGCGCAC	*In vitro* transcription of *whiH*
T7 whiH dwn	GCTGCTGGACGAGTTGCCCG	*In vitro* transcription of *whiH*
FLAG plus	TCGAAGGCGGCGGCGACTACAAGGACCA CGACGGCGACTACAAGGACCACGACATC GACTACAAGGACGATGACGACAAGC	Create 3× FLAG insert
FLAG minus	TCGAGCTTGTCGTCATCGTCCTTGTAGT CGATGTCGTGGTCCTTGTAGTCGCCGTC GTGGTCCTTGTAGTCGCCGCCGCCT	Create 3× FLAG insert

* Bolded, underlined sequence: *Eco*RI, *Bam*HI, *Kpn*I, *Xba*I, *Nde*I, or *Xho*I restriction enzyme sites

Table 2.5: Oligonucleotides used in sIHF-related studies.

Name	Sequence (5′ to 3′)*	Comments
SCO1480 k/o 1	CGTATCCGACAGTTCGACATCCGAGGTGACGT AGGCGTGATTCCGGGGATCCGTCGACC	Gene knockout
SCO1480 k/o 2	CAGCGATTATTCCAGCAATCCCGGAGTGGTCC GGACTCATGTAGGCTGGAGCTGCTTC	Gene knockout
SCO1480 up	CGTTGCGGACTGCTGCCGACCG	Complementation
SCO1480 down	GCGGCG**GAGCTC**TCCTTGCGCATATGGGCGAC G	Complementation
SCO1480 internal	CTGCTTGGCGCGGACTTTGCCC	Checking gene knockout
SCO1480 Nde	GGGTGC**CATATG**GCTCTTCCGCCCCTTACCC	SCO1480 overexpression
SCO1480 Bam	GGGTGC**GGATCC**TCAGCTGCCGGTGCTGCC	SCO1480 overexpression
Fuse 1	GCATA**GGATCC**CGTTGCGGACTGCTGCCGACC G	SCO1480 fusion to *eGFP*
Fuse 2	CGTAT**CATATG**CTCTGGGCCTGGCAGCTCTGG GCCCGGCAGGCCGCTGCCGGTGCTGCCGAACT CG	SCO1480 fusion to *eGFP*
dsDNA 43 bp 1	ACCAGGTGGTTGCCGATCACCACGAAGCGGGT GGTGTGGCGGG	Protein interaction studies
dsDNA 43 bp 2	CCCGCCACACCACCCGCTTCGTGGTGATCGGC AACCACCTGGT	Protein interaction studies
dsDNA 60 bp 1	CGTACGCGTCGCCACGGCGGCGGCATCGTCCA CGAGAACACCCGCCACACCACCCGCTTC	Protein interaction studies
dsDNA 60 bp 2	GAAGCGGGTGGTGTGGCGGGTGTTCTCGTGGA CGATGCCGCCGCCGTGGCGACGCGTACG	Protein interaction studies
dsDNA 407 bp 1	AACCCACGTTCTGAGGTTCC	Protein interaction studies
dsDNA 407 bp 2	ACCAGGTGGTTGCCGATCAC	Protein interaction studies
dsDNA curved 1	AAAAATCGCGAAAAAAGCGCGAAAAAGCGCGA AAAAATCGCG	Protein interaction studies
dsDNA curved 2	CGCGATTTTTTCGCGCTTTTTCGCGCTTTTTT CGCGATTTTT	Protein interaction studies

dsDNA non-curved 1	TCGAATCGCGCGCTAAGCGCTTCGAACCTCGCGCTAAGCTCG	Protein interaction studies
dsDNA non-curved 2	CGAGCTTAGCGCGAGGTTCGAAGCGCTTAGCGCGCGATTCGA	Protein interaction studies
dsDNA non-curved nick 1a	CTCGAATCGCGCGCTA	Protein interaction studies
dsDNA non-curved nick 1b	GCGCTTCGAACCTCGCGCTAAGCTC	Protein interaction studies
dsDNA FRET control 1	TGGTTGCCGATCACCACGAAGCGGGTGGTGTGG	Protein interaction studies
dsDNA FRET control 2	CCACACCACCCGCTTCGTGGTGATCGGCAACCA	Protein interaction studies
dsDNA FRET 1	Fluorescin – TGGTTGCCGATCACCACGAAGCGGGTGGTGTGG	Protein interaction studies
dsDNA FRET 2	TAMRA – CCACACCACCCGCTTCGTGGTGATCGGCAACCA	Protein interaction studies
SELEX fwd	CGAGCAGTAGACC	Amplifying SELEX DNA
SELEX rev	GCAAGTCGTCGTG	Amplifying SELEX DNA
Motif #1 plus	TCGAAAAATCGGAATCTGGTGCA	SELEX EMSA
Motif #1 minus	TGCACCAGATTCCGATTTTTCGA	SELEX EMSA
Motif #2 plus	TCGAATACGGAAAGCTTTGTGCA	SELEX EMSA
Motif #2 minus	TGCACAAAGCTTTCCGTATTCGA	SELEX EMSA
Motif #3 plus	TCGAAAGGATAGCCTTAGATGCA	SELEX EMSA
Motif #3 minus	TGCATCTAAGGCTATCCTTTCGA	SELEX EMSA
Control motif	GATCGCTAATCTGATGCAAGATG	SELEX EMSA
Control motif	CATCTTGCATCAGATTAGCGATC	SELEX EMSA
M13 forward	GTAAAACGACGGCCAG	Sequencing of SELEX inserts
pKT25 sIHF fwd	CGC**TCTAGA**AGGCGTGGCTCTTCCGC	Ligation of *sIHF* into pKT25
pKT25 sIHF rev	CGC**GGTACC**GACTCAGCTGCCGGTGCT	Ligation of *sIHF* into pKT25
pKT25 topA fwd	CGC**TCTAGA**GAAGTTGTCCCCGACCAG	Creating pKT25 + *topA*

pKT25 topA rev	CGC**GGTACC**GGCTCAGTCCTCCGACGT	Creating pKT25 + *topA*
pUT18(C)/pKNT 25 sIHF fwd	CGC**GGATCC**AGGCGTGGCTCTTCCGC	Creating pUT18, pUT18C and pKNT25 + *sIHF*
pUT18C sIHF rev	CGC**GAATTC**GACTCAGCTGCCGGTGCT	Creating pUT18C + *sIHF*
pUT18(C)/pKNT 25 topA fwd	GCC**GGATCC**GAAGTTGTCCCCGACCAG	Creating pUT18, pUT18C, and pKNT25 + *topA*
pUT18C topA rev	CGC**GAATTC**GGCTCAGTCCTCCGACGT	Creating pUT18C + *topA*
pUT18/pKNT25 sIHF rev	CGG**GAATTC**CGCTGCCGGTGCTGCC	Creating pUT18 and pKNT25 + *sIHF*
pUT18/pKNT25 topA rev	CGGCAATTCCGTCCTCCGACGTCTTCGA	Creating pUT18 and pKNT25 + *topA*
topA1	CGCACT**CATATG**TCCCCGACCAGCGAG	TopA overexpression
topA2	CGCACT**GGATCC**TCAGTCCTCCGACGTCTTCG	TopA overexpression
ftsk up	GATCATCACCAACCCGAAGC	qPCR
ftsK dwn	CGGTTGAAGTCGTCGATGTG	qPCR
hupS up	GGTTCGGGTCAAGAAGACCT	qPCR
hupS dwn	CGCTCACCAGGTCCTTGAA	qPCR
smc up	CCGAGTCCGTTCTACGTGAT	qPCR
smc dwn	TTCTGGTGCGTGATGACGAT	qPCR
parA up	TGGAGCCCTCTCCTATCTGG	qPCR
parA dwn	GTCATAGGTGACGCCCACAC	qPCR
parB up	CCACGCTTCAGCATGTTTCA	qPCR
parB dwn	GTGATGGCGTCGAGTGGAA	qPCR
scpA up	GCTCCTCCAGTTGATCTCCA	qPCR
scpA down	GGATGTGCGCCATGAACTC	qPCR
scpB up	AACAGGTGCGATCCTGTACG	qPCR
scpB dwn	CCATCCGCTCCAGGAAGTAG	qPCR

* Bolded, underlined sequence: *Eco*RI, *Bam*HI, *Kpn*I, *Xba*I, *Nde*I, or *Xho*I restriction enzyme sites

Table 2.6 Standard *Taq* polymerase PCR reaction conditions

Reagent	**Final Concentration**
Taq Reaction Buffer (10×)	1×
Forward Primer (50 µM)	1 µM
Reverse Primer (50 µM)	1 µM
DMSO (100%)	5 %
dNTPS (20 mM)	200 µM (each nucleotide)
Taq Polymerase (5 U/µL)	1.5 U
Template	2-20 ng/ml plasmid DNA or 20-200 ng/ml genomic DNA
Nuclease-free water	-

Table 2.7 Standard *Taq* polymerase PCR cycling conditions

PCR Step	**Temperature (°C)**	**Time**	**Number of Cycles**
1. Denaturation	95	5 minutes	1
2. Denaturation	95	30 seconds	30
3. Primer annealing	T_m - 5	30 seconds	
4. Extension	72	1 min/kb	
5. Final Extension	72	5 minutes	1

Table 2.8 Standard Phusion High-Fidelity DNA polymerase PCR reaction conditions

Reagent	Final Concentration
Phusion Reaction Buffer (5×)	1×
Forward Primer (50 µM)	1 µM
Reverse Primer (50 µM)	1 µM
DMSO (100%)	5 %
dNTPS (20 mM)	200 µM (each nucleotide)
Phusion Polymerase (5 U/µL)	0.02 U
Template	0.02-200 ng/ml plasmid DNA or 1000-5000 ng/ml genomic DNA
Nuclease-free water	-

Table 2.9 Standard Phusion High-Fidelity DNA polymerase PCR cycling conditions

PCR Step	Temperature (°C)	Time	Number of Cycles
1. Denaturation	98	30 seconds	1
2. Denaturation	98	10 seconds	30
3. Primer annealing	$T_m + 3$	30 seconds	
4. Extension	72	30 seconds/kb	
5. Final Extension	72	5 minutes	1

CHAPTER 3

SMALL RNA REGULATORS IN *S. COELICOLOR*

Preface

Work outlined in section 3.2.1 and 3.2.2 has been published in *Nucleic Acids Research* (Swiercz *et al.*, 2008). Figures 3.1, 3.2, 3.3 and Table 3.1 used in this chapter are reproduced or slightly altered from the original manuscript, as *Nucleic Acids Research* allows authors to utilize their published work for thesis preparation. Figure 3.7 was kindly provided by Matthew Moody.

3.1 Introduction

3.1.1 Small RNAs and methods for their discovery

Small RNAs (sRNAs) are important regulators of many cellular processes. Most function by binding to target mRNAs where they influence transcript stability or translation (Storz *et al.*, 2004). Upon sRNA binding, structural changes within the target mRNA can occur, leading to an increase or decrease in transcript stability through altered RNase susceptibility. Alternatively, sRNAs can bind to specific regions within a target mRNA, such as the ribosome-binding site (RBS), where they affect translation, either by blocking the RBS or changing an inhibitory structure to allow ribosome binding. Instead of binding mRNAs, a small subset of characterized sRNAs bind and modulate protein activity (Babitzke and Romeo, 2007; Wassarman, 2007). In the past, sRNAs were largely overlooked as regulatory elements due to their small size, resistance to point mutations, un-translated nature and lack of sequence homology within distant bacterial relatives. The increasing numbers of publically available bacterial genome sequences, which enable comparisons of genomes from closely related species, have facilitated the identification of trans-encoded sRNAs, which are highly conserved sequences within intergenic regions.

Initial systematic searches for sRNAs in bacteria relied heavily on computational screens, and genome comparisons of related species. This comparative genomics approach, pioneered by Wasserman *et al*. (2001), used strong sequence conservation within the noncoding regions of related species as a starting point for identifying candidate sRNA genes. Conserved sequences were then analyzed further for their potential to encode small peptides, their proximity to adjacent coding genes and potential for inclusion within 5′ untranslated regions, or the likelihood that they represented conserved operator regions of adjacent protein-encoding genes. Such sequences were eliminated from the analysis. The remaining sequences were inspected for characteristic elements of sRNAs such as stem loop structures or transcription termination motifs that are typically found at the end of genes. Application of this method led to the successful identification of numerous sRNAs in various bacterial species (Silvaggi *et al.*, 2006; Christiansen *et al.*, 2006; Xiao *et al.*, 2009). However, this technique fails to identify sRNAs encoded within open reading frames with potential *cis*-encoded targets. This method is also limited to identifying sRNAs with sequence similarity in closely related species. In an effort to address some of these shortcomings, searches were adapted to identify sRNA

genes that lacked sequence homology in related species and included searches for 'orphan' promoters and terminator elements that flank a region with no obvious coding potential, as well as conserved structural elements (Wassarman *et al.*, 2001). In all cases, potential sRNAs are verified by demonstrating transcript presence or gene expression experimentally. A common approach to test for sRNA transcripts is northern blot analysis, using total RNA extracts from cells grown on different media and under different conditions, while PCR following a reverse transcription reaction (RT-PCR) of a target RNA or microarray analysis can also be used to confirm gene expression.

An alternative method to the comparative genomics approach for identifying sRNAs is a direct cloning approach. This technique involves creating a cDNA library from size-selected small RNA (*e.g.* those smaller than 100 nucleotides [nt]). This includes the attachment of 5′ and 3′ linkers and reverse transcription using primers to the known linker sequences. The products are amplified and then sequenced using the linker specific primers. A third approach has involved isolating sRNAs based on their interactions with Hfq. Hfq is a RNA-binding chaperone protein to which the majority of sRNAs bind (Zhang *et al.*, 2003; Sharma and Vogel, 2009). Hfq is found in many bacteria with important exceptions, including the chlamydia and actinomycetes. Over the last 5 years, new technologies have been developed (see discussion), and these are now being employed to develop a more comprehensive list of sRNAs expressed by specific bacteria. These methods also have the added benefits of identifying sRNAs that are encoded opposite of protein coding genes, expressed at levels that are not detected with northern blot analysis, and that do not share homology with related species.

3.1.2 Small RNAs in S. coelicolor

At the start of this work, the available genomic sequences of multiple *Streptomyces* and other actinomycete species allowed us to take a comparative genomics approach in searching for potential sRNAs in *S. coelicolor*. The 8-9 Mb *Streptomyces* chromosome is linear and divided into three sections. The middle section, referred to as the "core", extends from ~1.5 Mb to 6.4 Mb (Bentley *et al.*, 2002), carries the essential genes and is well conserved among *Streptomyces* species. The outer sections, referred to as the "arms", harbor conditionally adaptive genes with limited conservation between species. Given that most genetic conservation is confined to the core region, we focused our attention on this area in our comparative search for sRNAs. Out of the 833 intergenic regions that spanned more than 200 bp, 664 had sequences conserved in other streptomycetes. By concentrating on relatively large intergenic regions, it was possible to increase the likelihood of identifying autonomous sRNA sequences. To minimize the chances of identifying conserved promoter or terminator regions associated with flanking protein coding genes, conserved sequences located within 40 bp of a flanking coding gene were excluded from downstream analyses. Sequences that resembled degenerate transposases, tRNAs, rRNAs, predicted riboswitches or other characterized sequences were also excluded from further investigations. The remaining 114 intergenic regions containing sequences that were conserved in at least three *Streptomyces* species, were analyzed using sRNAFinder – a program

designed to identify noncoding genes by evaluating primary sequence and structural conservation by comparative genomics (Tjaden, 2008a). Based on the results from sRNAFinder, 20 conserved sequences were chosen for sRNA validation and preliminary characterization.

3.2 Results

3.2.1 Experimental validation of predicted sRNAs in S. coelicolor

We had identified 20 reasonable sRNA candidates using the criteria outlined above. We were interested in determining whether these sRNAs were expressed, and under what conditions. As the *S. coelicolor* life cycle is defined by distinct developmental stages, we opted to probe sRNA expression at timepoints corresponding to each life cycle stage. Specifically, we tested sRNA expression during vegetative growth, the transition to aerial growth, early sporulation and late sporulation. Differential sRNA expression could indicate sRNA association with a particular developmental stage. In contrast, equivalent sRNA expression at all timepoints could indicate a potential housekeeping function. In addition to testing sRNA expression at different stages of development, we also chose to compare the expression of each sRNA under nutrient limiting and rich growth conditions.

It is also worth noting that for each of our 20 candidate sRNAs, we were unable to predict the directionality of the candidate sRNAs. In other bacteria, putative promoter and terminator sequences can be used as a guide for determining directionality, but *Streptomyces* encodes over 60 sigma factors (Bentley *et al.*, 2002) and thus promoter sequences are highly variable. Furthermore, the identification of rho-independent terminators is also not straightforward due to the extremely high G+C content of the *Streptomyces* genomes (Bentley *et al.*, 2002). To circumvent this problem, we conducted northern blot analyses using two 25-30 nt complementary oligonucleotides as probes; these corresponded to the most highly conserved regions within each predicted sRNA. This would ensure that sRNA presence was detected regardless of the strand from which it was transcribed. The oligonucleotides were individually radiolabelled with ^{32}P and each set was used simultaneously to probe the size-fractionated RNA. Of the initial 20 sRNA candidates, we successfully confirmed transcript presence for six sRNAs (Figure 3.1A).

We next endeavored to determine the strand from which the candidate sRNAs were expressed. Each ^{32}P labeled oligonucleotide was used individually to probe the same size fractionated RNA to establish sRNA orientation relative to its flanking genes (Figure 3.1B). Each confirmed sRNA was given a numerical designation, corresponding to its upstream adjacent gene on the plus strand, and this was prefaced by "scr", for ***S. c****oelicolor* s**R**NA. The remaining 14 sRNA candidates were not detectable using northern blotting.

Out of the six confirmed sRNAs, four (scr3045, scr3558, scr3974 and scr5676) were expressed in RNA isolated from both rich and minimal media-grown cultures (Figure 3.1A). In contrast, scr1906 was only expressed in cultures grown on minimal medium, while scr3261 expression appeared limited to cultures grown on rich medium (Figure 3.1A). Expression levels of scr3045, scr3261 and scr5676 were relatively constitutive during vegetative and aerial hyphae growth (Figure 3.1A).

Higher levels of expression were evident for scr3045 and scr3974 on rich medium and scr5676 on minimal medium (Figure 3.1A). In addition to varying levels of expression, the majority of the sRNAs exhibited varied temporal expression over the time course examined. For example, expression of scr3558 was strongest during sporulation (late development) on both media types, whereas the remainder of the sRNAs showed a decrease in expression levels during this time (Figure 3.1A). scr3974 was expressed at low levels during growth on minimal media, but exhibited a more dynamic profile during growth on rich medium: it was highly expressed during vegetative growth, with transcript levels decreasing to nearly undetectable levels during sporulation (Figure 3.1A). Interestingly, scr1906 was expressed exclusively during aerial hyphae formation and sporulation on minimal medium (Figure 3.1A). In all cases, a 5S RNA control was included for comparison among timepoints to ensure equal RNA sample loading for proper transcript abundance comparisons.

Although northern blot analysis provided approximate sRNA sizes, it was of interest to map the start and end sites of each sRNA, as these would not only allow for identification of promoter and terminator regions, but also provide definitive gene sizes. RNA end sites were mapped using 5′ and 3′ RACE (Table 3.1). When RNA secondary structure prevented end mapping using RACE, northern analyses using overlapping probes were used to map approximate start and end sequences.

3.2.2 sRNA expression analysis in various developmental mutants

The sRNA expression profiles in wild type *S. coelicolor* suggested that transcription of certain sRNAs was developmentally regulated. For example, scr1906 expression appeared to be induced prior to sporulation during growth on minimal medium. Given that, it was of interest to examine sRNA expression patterns in a variety of developmental mutants, including classic *bld* (*bldA*, *bldB*) and *whi* (*whiB*, *whiG*) mutant strains. *bldA* and *bldB* are both defective in antibiotic production and raising of aerial hyphae; however, the 'bald' mutant phenotype of *bldA* is conditional in that the strain is able to raise aerial hyphae when grown on minimal medium (but not rich medium) (Lawlor *et al.*, 1987; Leskiw *et al.*, 1991; Pope *et al.*, 1998; Eccleston *et al.*, 2002). In contrast, *whiB* and *whiG* mutants are blocked during the early stages of sporulation, as discussed in Chapter 1 (Section 1.2.3).

To examine the expression profiles of the six verified sRNAs in different developmental mutants; northern blot analysis was conducted using RNA harvested from each mutant strain grown on minimal or rich media, at similar timepoints as before. Expression profiles of scr3045, scr3261 and scr5676 under all growth conditions were not altered in the mutant strains, relative to the wild type. In contrast, the other three sRNAs displayed varying degrees of transcription. scr3558 exhibited the same expression profiles in the *whi* mutants as compared to wild type *S. coelicolor*, but there was a significant decrease in its expression on both media types in a *bldB* mutant, and a change in transcript abundance compared to normal conditions in a *bldA* mutant (Figure 3.2A). Unlike the other sRNAs, scr3974 transcript levels were higher in a *bldB* mutant during growth on rich medium compared to wild type *S. coelicolor* (Figure 3.2B).

The expression profile of scr1906 was the most dramatically altered in the developmental mutants tested (Figure 3.3A). In wild type strains, scr1906 was expressed during aerial development on minimal medium. Media dependence and temporal regulation were lost in both *bld* mutant strains tested. On minimal medium, scr1906 retained wild type expression levels in both *bld* strains; however, higher levels were observed following growth on rich medium (where little expression was seen in wild type). Although scr1906 expression in the *whiB* mutant was the same as in the wild type strain, there was no detectable scr1906 expression in the *whiG* mutant on either media type. This is of particular interest as it suggests that scr1906 may be completely dependent on σ^{WhiG} for its expression

3.2.3 Characterization of scr1906

From the six confirmed sRNAs examined above, scr1906 was chosen for further characterization due to its unique media dependent expression profile, and its connection to σ^{WhiG}. The late onset of scr1906 expression during the *S. coelicolor* life cycle on minimal medium indicated that it was synthesized under a specific set of growth conditions and in turn implied a potential role in sporulation. From previous northern blot experiments it was known that scr1906 was encoded on the same strand as its two flanking genes: *SCO1905*, encoding a hypothetical protein, and *SCO1906*, encoding a putative secreted protein (Figure 3.1B). In addition to this, northern blot analysis also revealed the presence of two transcripts: one of ~60 nt and another ~200 nt in size. End mapping of the smaller transcript confirmed it to be 61-63 nt. Unexpectedly, mapping of the larger transcript was unsuccessful. It is currently unclear whether the smaller transcript is a separate transcript or a processed product of the larger transcript. Notably, however, it was only the smaller scr1906 transcript that exhibited temporal expression when *S. coelicolor* was grown on minimal medium.

3.2.4 Effects of scr1906 overexpression and deletion

In many cases, overexpression of an sRNA can result in phenotypic changes that provide hints as to sRNA function (Majdalani *et al.*, 1998; Mandin and Gottesman, 2009; Landt *et al.*, 2010). In an attempt to characterize the biological role of scr1906, we designed an overexpression construct that encompassed the sequence of the smaller sRNA, given the media-dependence and temporal accumulation observed for this transcript. This overexpression construct was introduced into wild type *S. coelicolor*, along with a plasmid-only control, and northern blot analysis was conducted to confirm the overexpression of the smaller scr1906 transcript (Figure 3.4). These studies also revealed that the terminator sequence engineered into the overexpression vector remained as a part of the sRNA transcript based on the size difference with scr1906 from wild type using northern blot analysis. This suggested that the native small scr1906 transcript cannot self-terminate and may potentially represent a processed version of the larger scr1906 transcript *in vivo*. Alternatively, the appropriate terminator sequence for proper small scr1906 transcript termination may be within the sequence specific to the larger scr1906 transcript, which was not included in the overexpression construct.

To test whether scr1906 overexpression caused any phenotypic changes, its growth was compared to that of a wild type control strain (containing the empty plasmid) was assessed. During growth on a sporulation-specific medium, the overexpression strain acquired the grey spore-associated pigment approximately a day earlier than the wild type strain. To test whether this was correlated with earlier sporulation, relative spore chain abundance of each strain was assessed. Coverslip impressions were taken from both strains at the time when the overexpression strain developed the grey pigment, and relative spore abundance was determined. Initial trials suggested that the overexpression strain produced more spore chains than wild type based on light microscopy observations; however, these results were not consistently reproducible.

To complement the overexpression analyses, an *scr1906* deletion strain was also constructed by deleting the majority of the intergenic region between *SCO1905* and *SCO1906*. While initial experiments suggested a slight delay in sporulation when compared to the wild type, again, these results were not reproducibly observed. Furthermore, SEM of the *scr1906* deletion strain did not reveal any phenotypic differences for the mutant relative to wild type (Figure 3.5). Consequently, we were unable to draw any definitive conclusions about a developmental role for scr1906 following either its overexpression or deletion based on phenotypic assays.

3.2.5 Regulation of scr1906 expression

The absence of scr1906 expression in a *whiG* mutant prompted us to consider the possibility that scr1906 expression was directly dependent on σ^{WhiG}. To explore this further, scr1906 expression was examined in strains bearing mutations in the only known direct targets of σ^{WhiG}: *whiI* and *whiH*, which are both predicted to encode sporulation-specific transcription factors (Ryding *et al.*, 1998; Aínsa *et al.*, 1999). Expression of the smaller *scr1906* transcript could be detected in both *whiH* and *whiI* mutants (Figure 3.3B) suggesting that expression of the smaller *scr1906* transcript was either directly dependent on σ^{WhiG} or indirectly dependent through the activity of another as-yet-unknown σ^{WhiG} -dependent transcription factor.

To distinguish between these possibilities, we created an inducible *whiG* construct, and used this strain to follow the expression of two direct σ^{WhiG} targets (*whiH* and *whiI*) together with scr1906, following *whiG* induction. The inducible *whiG* construct was created by cloning *whiG* downstream of a thiostrepton-inducible *tipA* promoter (Huang *et al.*, 2005) in an integrating plasmid. This construct was then introduced into a *whiG S. coelicolor* mutant strain (Flärdh *et al.*, 1999). The assay involved extracting RNA every 15 minutes after inducing *whiG* expression. This RNA was then used to examine the expression profiles of *whiI*, *whiH* and scr1906 using northern blot analysis. Previous work has shown that the transcripts of *whiH* and *whiI* can be detected within 15 minutes of *whiG* induction (M. Elliot, personal communication). Therefore, if *scr1906* expression was directly dependent on σ^{WhiG}, scr1906 transcripts would be expected shortly after *whiG* expression (within 15 minutes); however, if *scr1906* was indirectly dependent on σ^{WhiG}, a lag between *whiG* induction and *scr1906* expression would be expected (> 15 minutes), as this would represent the time required for a σ^{WhiG}-dependent regulator(s) to be

transcribed and translated, before acting to promote *scr1906* transcription. As a control, the same strain carrying an empty vector was used.

The results from this experiment were not clear-cut, as *scr1906* expression could be detected in the uninduced control (Figure 3.6A). This suggests that the *tipA* promoter permits a low level of 'leaky' *whiG* expression. As a test, reverse transcription-PCR (RT-PCR) was used to determine whether *whiH* transcripts were also present in induced control RNA samples (Figure 3.6B). Unexpectedly, *whiH* transcripts were detected in RNA samples extracted from an induced control strain lacking a functional WhiG protein. This suggests that the RNA preparations could be contaminated with DNA or that there was an issue with the parent strain, such as a partially functional mutant or a spore stock contamination. This experiment was only completed once and no additional troubleshooting was conducted due to project termination.

3.2.6 Identifying and testing targets of scr1906

TargetRNA (Tjaden, 2008b), a program designed to predict sRNA targets based on calculating sRNA-mRNA optimal hybridization scores, was used to search for potential scr1906 targets. The predicted target with the highest statistically relevant score was the transcript of *whiH*, one of the two known direct targets of σ^{WhiG}. The sRNA-mRNA interaction between scr1906 and *whiH* is predicted to encompass 20 interrupted nucleotides shared by the 5′ end of *whiH* and a region of scr1906 that is contained within the smaller scr1906 transcript. Intriguingly, the *whiH* transcription start site and translation start site are only 2 nucleotides apart, which is unusual, but not uncommon in *S. coelicolor*. The *in silico* prediction raises the possibility that scr1906 may have a role in the regulation of *whiH* expression.

In order to test whether there is any potential interaction between scr1906 and *whiH*, we tested their ability to associate using electrophoretic mobility shift assays (EMSAs), which can be used to confirm RNA-RNA interactions. To this end, radiolabeled scr1906 RNA and increasing concentrations of *whiH* RNA were incubated together and the resulting products were separated on a native polyacrylamide gel. RNA-RNA duplex formation, represented by an upward band shift, was not detected in any of the EMSA trials. The lack of shifted complexes following scr1906 and whiH co-incubation suggested that these RNAs might not interact under the conditions tested. We could not, however, exclude the possibility that the sRNA-mRNA interaction may be transient *in vivo* and/or require a chaperone protein to stabilize this interaction, as is the case for some characterized sRNA-RNA interactions (Valentin-Hansen *et al.*, 2004).

To further probe a potential relationship between scr1906 and *whiH*, we assessed whether there were any changes to the intracellular levels of WhiH in the *scr1906* deletion and overexpression mutant strains. A *whiH* derivative harboring a C-terminal FLAG-tag (DYKDDDDK; (Hopp *et al.*, 1988)) -encoding sequence was created, to facilitate WhiH detection. Prior to immunoblot analysis, the tagged protein was confirmed to be fully functional through complementation of a *whiH* mutant. Protein samples were obtained from the WhiH-FLAG strain of *S. coelicolor* during aerial development and sporulation, the stages at which *whiH* is known to be expressed (Ryding *et al.*, 1998). Initially, a sample of the cytoplasmic protein

fraction was used to conduct immunoblot analysis; however, WhiH-FLAG was not detected. To increase the amount of WhiH-FLAG in the cell-free extracts, protein samples were concentrated. Three different protein-concentration protocols were attempted: TCA-, acetone-, and chloroform-methanol-based protein precipitations; however, the resulting protein pellet in each case was largely insoluble and difficult to resuspend. Immunoblot analysis of the concentrated samples led to successful detection of WhiH-FLAG on two separate occasions using the wild type strain; however, this could not be reproducibly detected, and thus we were unable to draw any conclusions about changes in the level of WhiH-FLAG in response to scr1906 levels.

3.3 Discussion

3.3.1 sRNAs in S. coelicolor

In this work, a comparative genomics approach was used to identify potential sRNAs in *S. coelicolor*. Northern blot analysis of a select set of potential sRNAs confirmed the presence of six sRNAs under two sets of growth conditions. Transcripts were not observed for the remaining predicted sRNAs; however, they could still be detected under different growth conditions, as seen in characterized sRNAs of other bacteria. In *E. coli*, for example, OxyS and RyhB sRNAs are expressed in response to oxidative stress (Altuvia *et al.*, 1997) and iron limiting conditions (Massé and Gottesman, 2002), respectively. It is conceivable that those conserved sequences for which we did not detect transcripts are not sRNAs, but instead represent non-transcribed extended regulatory regions of adjacent genes, despite our attempts to eliminate these from our analysis (discussed later). Additionally it is also possible that these potential sRNAs are expressed at a low level and cannot be detected using northern blot analysis or that the target sequence of the probe used for northern blot analysis could be sequestered in the sRNA structure despite efforts to remove secondary structures. Alternatively, it is plausible that the conserved sequence has unknown significance.

In conjunction with our comparative genomics approach for sRNA identification, we also undertook a complementary strategy, involving a small-scale cDNA cloning experiment. None of the previously predicted sRNAs were isolated in this experiment; however, three of the cloned sequences were validated as novel sRNAs: scr2102 (150 nt), scr4677 (70, 35 nt) and scr3287 (60 nt). These sRNAs would not have been identified as sRNA candidates in our comparative genomics screen due to their locations. For instance, scr3287 has an antisense orientation relative to a protein-coding gene and our search had exclusively focused on sequence conservation within intergenic regions. In contrast, scr2101 and scr4677 were intergenic, but both were also immediately adjacent to a protein-coding gene, and thus would have been excluded from our analyses for this reason. scr2101 and scr4677 also exhibited only fragmented sequence homology to related species. In addition, no obvious sRNA-like secondary structures could be predicted for the scr2101 and scr4677 sequences. The results of the cDNA cloning experiment therefore served to highlight the limitations of our comparative genomics approach in that it could not predict sRNAs that share low sequence conservation among

related species, those expressed in close proximity to promoter or terminator regions of adjacent protein-coding genes, or those expressed as antisense RNAs to protein-coding genes.

Two other groups have taken a similar comparative genomics approach to identifying potential sRNAs in *S. coelicolor* (Pánek *et al.*, 2008) and *S. griseus* (Tezuka *et al.*, 2009). In the work by Pánek *et al.* (2008), putative transcripts were detected for 20 sRNAs using RT-PCR and DNA microarrays in *S. coelicolor*, while in *S. griseus,* 12 sRNAs were confirmed using northern blot analysis. One particular sRNA, scr3974, was identified and confirmed in all three studies, while another sRNA, scr2952, was validated only in the other two studies. Although scr2952 had secondary structure potential, our comparative screen did not identify it as an ideal sRNA candidate due to fragmented sequence conservation among related species and its proximity to an adjacent protein-coding gene. While these three studies used a similar method to identify potential sRNAs, the sRNAs identified in each were, for the most part, distinct. This strongly suggests that the parameters used in sRNA searches could significantly affect the output of predicted sRNAs, and that the final sRNA count in *S. coelicolor* is far from saturated.

Since the time that we conducted our global sRNA search, 'deep sequencing' has proven to be a powerful tool for sRNA discovery in bacteria (van Vliet, 2010; Sharma *et al.*, 2010; Raghavan *et al.*, 2011). RNA-sequencing (RNA-Seq) is a 'deep sequencing' technique that involves sequencing reverse-transcribed total RNA to obtain data about transcripts and their abundance in the cell. Recently, 63 possible sRNAs were identified in *S. coelicolor* using 454 sequencing (Vockenhuber *et al.*, 2011). Of these potential sRNAs, 11 were verified by northern blotting – none of which overlapped with the sRNAs previously identified by our group. It should be noted that the data obtained from this study represents the transcriptome at one timepoint, under a single culture condition. Any sRNAs expressed at other times or under different culture conditions would not be identified; therefore, there are likely more sRNAs to discover in *S. coelicolor*. With this in mind, our lab performed RNA-Seq with three species of *Streptomyces*: *S. coelicolor*, *S. avermitilis* and *S. venezuelae*, during various stages of development (Moody *et al*., 2013). RNA samples were pooled together such that each set contained the RNA of a single species throughout development. By comparing the RNA-Seq data from each species, hundreds of novel antisense RNAs and intergenic sRNAs were identified. Compared to the sRNAs identified in our original search (Swiercz *et al.*, 2008), no transcripts were detected for scr3974 and scr3261 potentially due to the different growth conditions used.

3.3.2 Potential roles of sRNAs from S. coelicolor

Since characterized sRNAs in other bacteria are often expressed in response to a particular stress (Gottesman, 2005), it seems likely that *S. coelicolor* encodes stress responsive sRNAs as well. Given the developmental complexity of *S. coelicolor*, it is also conceivable that it encodes sRNAs involved in the regulatory pathways contributing to vegetative growth, aerial development and sporulation. The high levels of scr3974 expression during vegetative growth on rich medium, and the fact that transcript levels drop significantly by sporulation, imply a potential

role for this sRNA during vegetative hyphae growth on rich medium. In contrast, expression of scr1906 was highest just prior to sporulation on minimal medium, suggesting that it may be involved during the transition from vegetative to reproductive growth (aerial hyphae formation and sporulation) when nutrients are limited.

In addition to predicting general functions for sRNAs based on temporal or media dependent expression, our data on the expression profiles of sRNAs in various developmental mutants also provided insight into their regulation. The expression of three sRNAs (scr3045, scr3261 and scr5676) was unchanged in all developmental mutants tested, suggesting that these sRNAs were not involved in the pathways associated with BldA, BldB, WhiB or WhiG function, and may serve a role that is unrelated to development. Increased expression of scr3974 on rich medium in both *whi* mutants tested might indicate repression (direct or indirect) of *scr3974* by the corresponding Whi proteins.

The existence of sRNAs in *S. coelicolor* is now well established; however, the function of very few has been successfully determined. Studies on only two sRNAs in *S. coelicolor* are available. One of these studies includes the characterization of scr3287: the antisense sRNA (αscr3287) (Hindra *et al.*, 2010) identified in our original sRNA search (Swiercz *et al.*, 2008). αscr3287 is antisense to *SCO3287,* the first protein coding gene within a cluster involved in antibiotic production. As expected for antisense sRNAs, αscr3287 was predicted to modulate transcript stability of its target mRNA by either increasing or decreasing its susceptibility to RNases. αscr3287 overexpression, however, was not correlated with changes in target mRNA abundance. Another group has characterized scr5239, which was identified by RNA-Seq (Vockenhuber *et al.*, 2011). scr5239 repressed its mRNA target, *dagA*, which encodes an extracellular agarase, by direct base pairing to the coding region about 40 nts downstream of the RBS (Vockenhuber and Suess, 2012). Since no *dagA* degradation was detected, scr5239 was proposed to impede translation by ribosome stalling instead of decreasing target stability.

3.3.3 Characterizing scr1906

We selected scr1906 from our library of identified sRNAs for further investigation. Exclusive expression during growth on minimal medium suggested that scr1906 might play a role in the response to nutrient depletion, an environmental signal thought to promote *S. coelicolor* sporulation (Rigali *et al.*, 2008). Additionally, the timing of scr1906 expression - peaking just prior to sporulation - and loss of this expression in a *whiG* mutant, further supported a connection between scr1906 and sporulation. Initial overexpression studies were in agreement with a sporulation role; unfortunately, these results could not be reliably reproduced.

Based on scr1906 expression studies in *whiG* and its two known direct targets, *whiH* and *whiI*, we concluded that scr1906 expression was either directly dependent on $\sigma^{WhiG,}$ or an unknown direct target of σ^{WhiG}. Attempts to distinguish between these two possibilities using a *whiG* induction assay were not fruitful, as it

appeared that the *tipA* promoter governing *whiG* expression was leaky, leading to sufficient levels of σ^{WhiG} to cause expression of its direct targets in the absence of induction. Unfortunately, there are few 'tight' inducible systems available for use in *Streptomyces*. Had the system worked as expected and scr1906 transcripts been detected within 15 minutes of *whiG* induction (as was the case for *whiH* and *whiI*), it would have suggested that *scr1906* was a direct σ^{WhiG} target. Modifying the assay through the use of a different inducible promoter, such as the vancomycin inducible promoter of *vanJ* (Hong *et al.*, 2004), or varying the levels of thiostrepton used for *tipA* induction could be used to troubleshoot the assay in the future.

Computational target searches with TargetRNA (Tjaden, 2008b) suggested that *whiH* was the most probable target for scr1906 regulation. A reciprocal search, where the *whiH* sequence was used as input, revealed scr1906 to be the most statistically significant match. Notably, *whiH* is a direct target of σ^{WhiG}, which in turn is responsible for scr1906 expression. Most intriguingly, scr1906 binding was predicted to occur at the start of the *whiH* leaderless transcript. Leaderless transcripts are not uncommon in the *Streptomyces* and are efficiently translated (Janssen *et al.*, 1989; Bibb *et al.*, 1994; Kieser *et al.*, 2000). Leaderless mRNA translation mechanisms are now starting to be defined in *E. coli* (Grill *et al.*, 2000; Kaberdin and Bläsi, 2006; Kaberdina *et al.*, 2009) where they involve recruiting specialized ribosomes, which can become specific for a subset of mRNAs by changing the heterogeneity in their composition. For example, ribosomes lacking protein S1 are responsible for translating leaderless transcripts (Moll *et al.*, 1998). Additionally, changing the stoichiometry of r-proteins or S6, S21 and L12 proteins can contribute to adjusting ribosome function (Byrgazov *et al.*, 2013). The same mechanisms are less likely in *Streptomyces* as these specialized ribosomes are less important for translation in Gram-positive bacteria (Sorokin *et al.*, 1995). The curious overlap of the *whiH* 5′ end with the center of the scr1906 sequence makes it tempting to speculate that scr1906 could facilitate *whiH* translation in a novel manner.

We were, however, unable to confirm a connection between scr1906 and *whiH*. EMSAs did not reveal an interaction between scr1906 and *whiH* RNA. The lack of RNA-RNA interaction in the EMSA experiments did not completely exclude the possibility of an *in vivo* interaction, as other cellular components may be needed to facilitate the interaction. It is also possible that the experimental conditions used were not optimal for RNA folding or RNA interaction; in the absence of a functional assay, condition optimization becomes very empirical. While there are other techniques, such as the structural probing of scr1906 in the presence and absence of its predicted *whiH* target that could also be used to confirm RNA-RNA interactions, these would also require optimal RNA folding.

As an additional means to link scr1906 to *whiH* as a target, a WhiH-FLAG-tag fusion was created to compare its expression in a wild type and *scr1906* deletion strain. It was expected that if scr1906 were required for proper translation, WhiH levels would be lower in the *scr1906* deletion than in a wild type strain. Unfortunately, the concentrations of WhiH in the cell were too low for reliable detection and as a result no conclusions could be drawn.

Since terminating the scr1906 characterization project, due to complications with WhiH-FLAG detection and whiH-scr1906 RNA interaction testing, we have learned about scr1906 courtesy of our RNA-Seq data. scr1906 appears to be a highly expressed 5′ untranslated region (UTR) of *SCO1905*. A similar situation appears to exist for scr3045 as well. The RNA-Seq expression profile for the *scr1906* region shows that scr1906 transcription continues into *SCO1905,* indicating that scr1906 may not be encoded as a separate entity (Figure 3.7). Recently, structural elements at the 5′ end of mRNA have been shown to be important for transcriptional or translational regulation (Breaker, 2012). Together, this suggests that the 5′ untranslated region regulates *SCO1905*, which encodes a hypothetical protein. *SCO1904*, which encodes a putative transcriptional regulator, is organized in an operon with *SCO1905* (Figure 3.1B) suggesting that *SCO1904* is also likely regulated with *SCO1905.* No connections to these protein-encoding genes have been previously made with a role in sporulation; however, the data presented here suggests that the expression of these genes might be developmentally regulated.

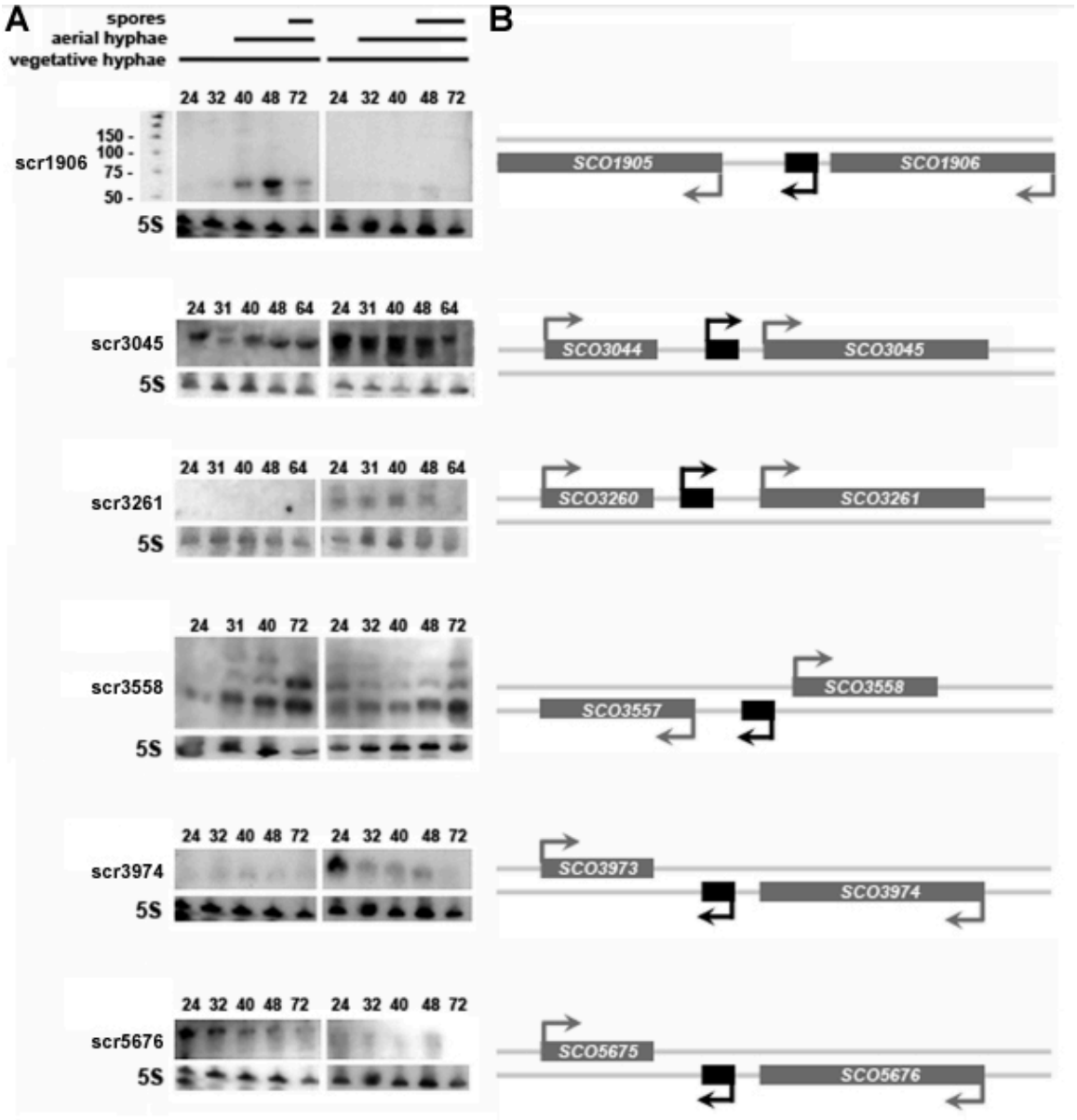

Figure 3.1. **Experimental verification of sRNAs identified using a comparative genomic analysis of intergenic regions**. **(A)** Northern blots probed with labelled DNA oligonucleotides. For northern blot analysis, RNA was harvested from *S. coelicolor* grown on either minimal or rich medium at four or five different timepoints (indicated as hours post-inoculation above each sRNA blot). 5S rRNA was used as a positive control for RNA loading and RNA integrity. For each sRNA, northern blot analysis was carried out using at least three different RNA samples to ensure the reproducibility of expression profiles. **(B)** Diagram indicating the position of each sRNA (shown in black) relative to adjacent protein-coding genes (shown in grey).

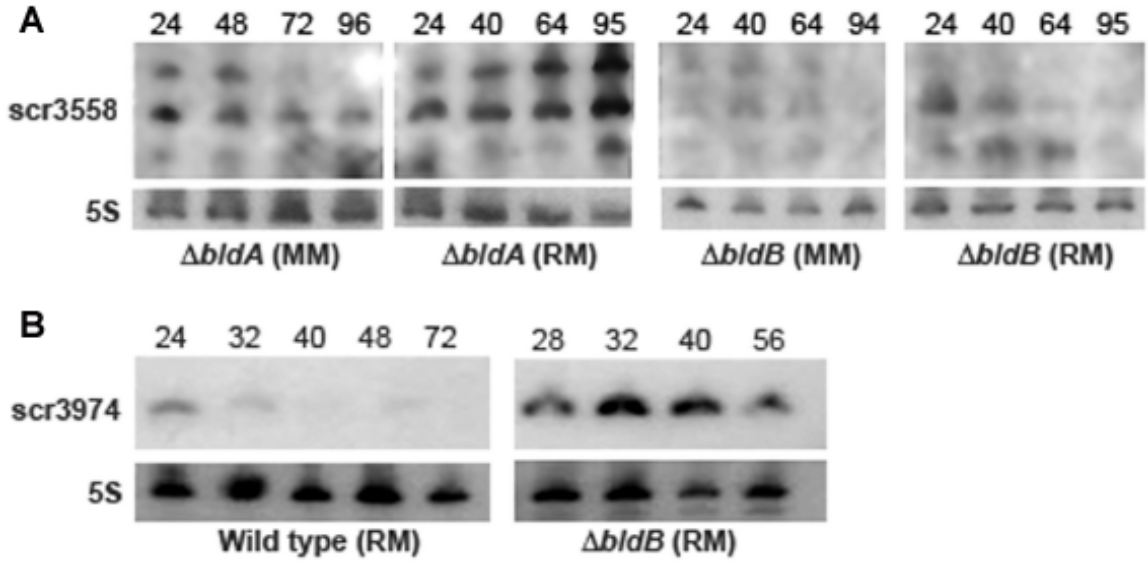

Figure 3.2. **Northern blot analysis showing altered expression profiles of sRNAs in *bld* developmental mutants**. **(A)** scr3558 expression in a *bldA* mutant (left panels), and a *bldB* mutant (right panels) during growth on (rich medium) RM and (minimal medium) MM. **(B)** Expression of scr3974 in a *bldB* mutant (right panel) relative to wild type strain (left panel) on RM. To ensure equivalent comparisons, wild type and mutant RNA samples were transferred to the same membrane after separation by PAGE, and thus were subjected to identical hybridization and washing conditions, and were exposed to X-ray film for the same period of time. Time (in hours) of RNA harvest (post-inoculation) is indicated on the top of each sRNA northern blot. 5S rRNA served as a control for RNA loading and RNA integrity. Northern blot analysis of wild type and mutant RNA samples were repeated at least three times with independent RNA samples.

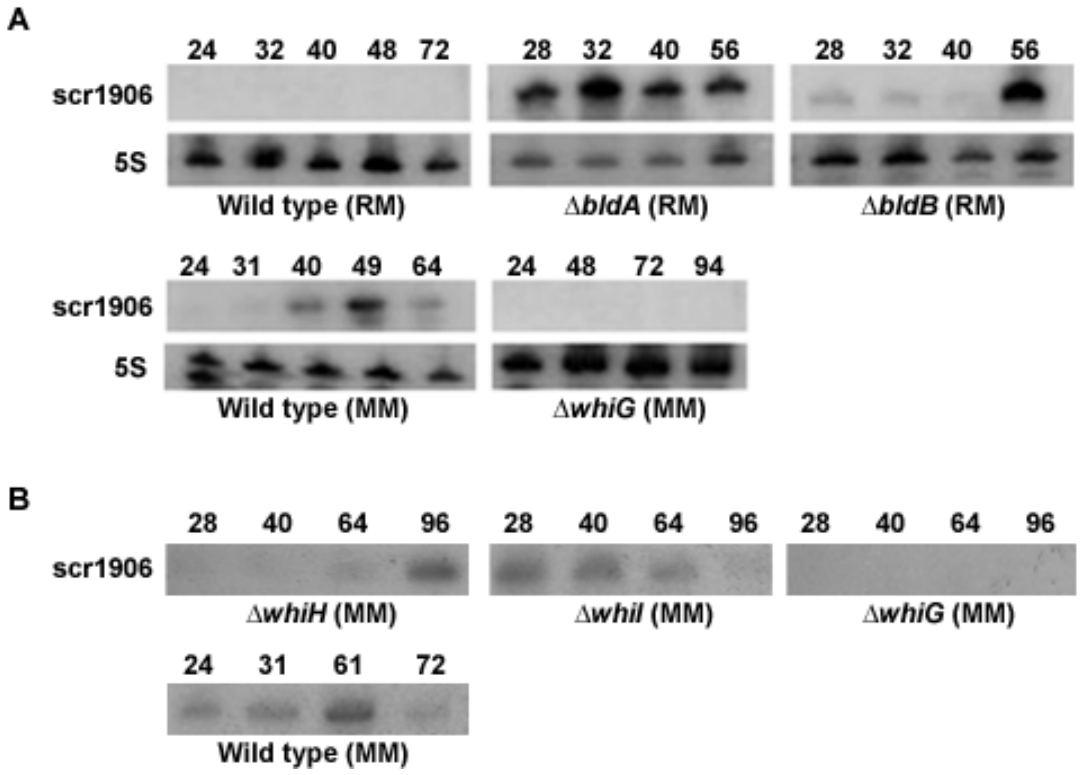

Figure 3.3. **Northern blot analysis showing scr1906 altered expression profiles in *bld* and *whi* developmental mutants**. **(A)** Top panels: comparison of scr1906 expression in *bldA* and *bldB* mutants relative to wild type on rich medium (RM); bottom panels: scr1906 expression in wild type versus *whiG* mutant on minimal medium (MM). 5S rRNA served as a control for RNA loading and RNA integrity. Northern blot analysis of wild type and mutant RNA samples were repeated at least three times with independent RNA samples. **(B)** Comparison of scr1906 expression in *whiH*, *whiI* and *whiG* mutant strains with wild type on minimal medium (MM). For (A) and (B): to ensure equivalent comparisons, wild type and mutant RNA samples were transferred to the same membrane after separation by PAGE, and thus were subjected to identical hybridization and washing conditions, and were exposed to X-ray film for the same period of time. Time (in hours) of RNA harvest (post-inoculation) is indicated on the top of each sRNA northern blot.

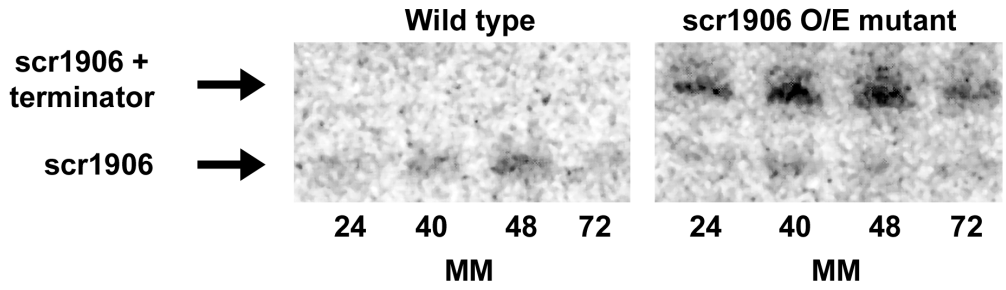

Figure 3.4. **Northern blot analysis of scr1906 levels in wild type and scr1906 overexpression mutant strains**. scr1906 expression in wild type (left panel) and the scr1906 overexpression (O/E) mutant strain (right panel) on minimal medium (MM). To ensure equivalent comparisons, wild type and mutant RNA samples were transferred to the same membrane after separation by PAGE, and thus were subjected to identical hybridization and washing conditions, and were exposed to X-ray film for the same period of time. Time (in hours) of RNA harvest (post-inoculation) is indicated on the bottom of each northern blot.

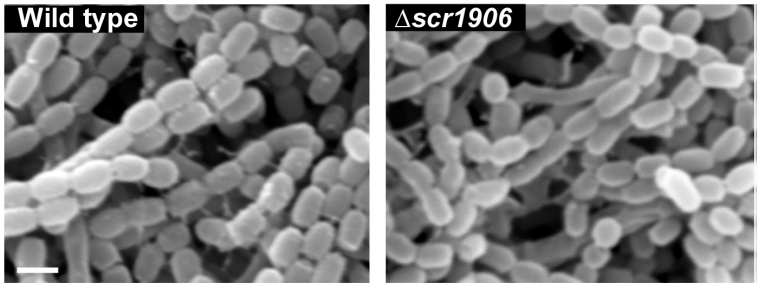

Figure 3.5. **Scanning electron microscopy (SEM) of Δ*scr1906***. SEM image of wild type (left panel) and Δ*scr1906* (right panel) strains after 5 days of growth on minimal medium. No major changes were detected between the spores of the mutant strain compared to wild type. Scale bar represents 1 μm.

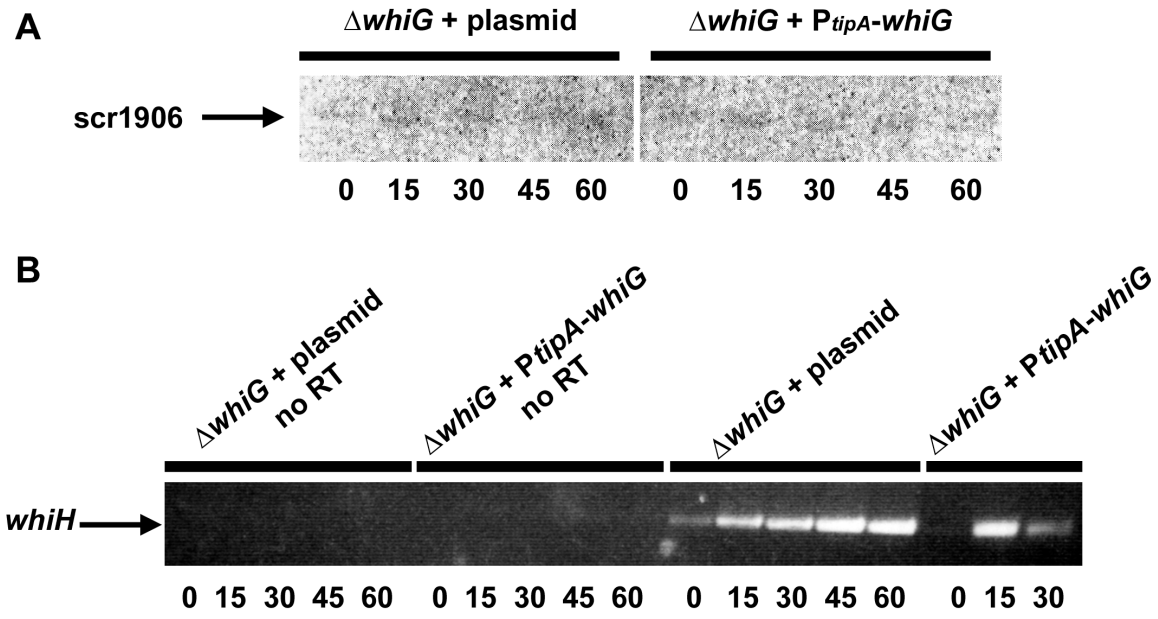

Figure 3.6. **scr1906 expression relative to *whiG* expression induction**. **(A)** Northern blot analysis of scr1906 expression after inducing *whiG* expression (right panel) as compared to the control *whiG* mutant strain (left panel). To ensure equivalent comparisons, RNA samples were transferred to the same membrane after separation by PAGE, and thus were subjected to identical hybridization and washing conditions, and were exposed to X-ray film for the same period of time. Time (in minutes) of RNA harvest (post-*whiG* induction) is indicated on the bottom of the figure. **(B)** Reverse transcription PCR (RT-PCR) of *whiH* before and after *whiG* induction in a *whiG* mutant or carrying an inducible *whiG* (right side of figure), respectively. RT-PCR controls lacking a reverse transcription step from samples of each background strain were used to ensure no DNA contamination and are shown on the left side of the figure. Time (in minutes) of RNA harvest (post-*whiG* induction) is indicated on the bottom of the figure.

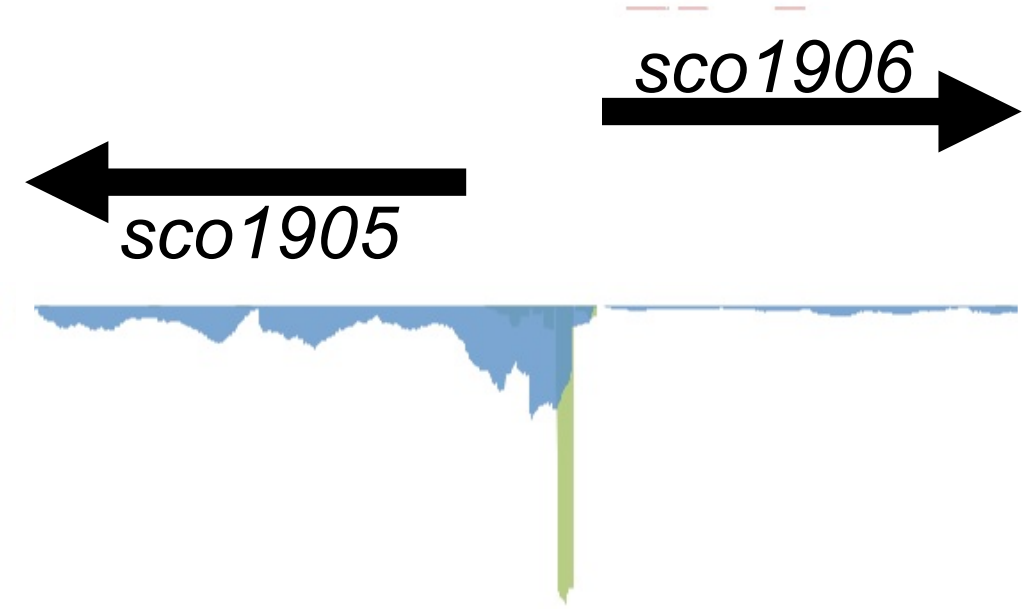

Figure 3.7 RNA-Seq expression profile of scr1906. The y-axis represents the number of RNA-Seq reads aligning at each nucleotide position (i.e. the read coverage). Positive strand coverage is shown above the gene annotation in red (long transcript library); negative strand profiles (below annotation) are shown in blue (long transcript library) and green (sRNA enriched library).

Table 3.1. Mapped and/or estimated 5′ and 3′ ends of sRNAs

sRNA	Start[a]	End[a]	Length (nt)[b]
scr1906	**2, 040, 854**	**2, 040, 91/2/3**	61-63
scr3045	**3, 334, 576** **3, 334, 532**	**3, 334, 819**	244 and 288
scr3261	~3, 610, 382	~3, 610, 566	~185
scr3558	~3, 933, 641 ~3, 933, 612 ~3, 933, 597	~3, 933, 512 ~3, 933, 523 ~3, 933, 531	~130, ~90, ~67
scr3974	**4, 375, 744** **4, 375, 746**	**4, 375, 703**	42 and 44
scr5676	**6, 176, 413**	**6, 176, 230**	184

[a]Bolded values were determined through 5′- or 3′-RACE mapping experiments.

[b]In absence of 5′- or 3′-RACE data, length estimations are based on mapped transcription start site (if determined), approximate transcript size as determined by northern blot analysis, and associated terminator sequences (if appropriate).

CHAPTER 4

sIHF IS A NOVEL NUCLEOID-ASSOCIATED PROTEIN SPECIFIC TO THE ACTINOBACTERIA

Preface

Work outlined in sections 4.2.1 – 4.2.9 and 4.2.11 – 4.2.12, except for the bacterial two-hybrid (B2H) analysis, has been published in *Nucleic Acids Research* (Swiercz *et al.*, 2013). Melanie Gloyd (Department of Biochemistry and Biomedical Sciences, McMaster University) completed the *in vitro* TopA activity assay (section 4.2.12) and Alison Berzins conducted the B2H assay (section 4.2.12). Figures 4.5, 4.7 – 4.13 and 4.20 – 4.23 used in this chapter are reproduced or slightly altered from the original manuscript, as *Nucleic Acids Research* allows authors to utilize their published work for thesis preparation. Figure 4.4 is adapted from the undergraduate final thesis by Kristian Shulist (Elliot lab).

4.1 Introduction

Bacteria encode numerous and diverse nucleoid-associated proteins (NAPs) that compact the chromosome. Cellular levels of individual NAPs can change throughout growth, suggesting that their effects on the nucleoid are growth stage-specific. In *E. coli*, for example, H-NS is present during all growth stages at relatively constant levels, while Fis is only present during the transition from lag to log phase, and Dps becomes most abundant during stationary phase (Dillon and Dorman, 2010). Changes in the levels of a particular NAP can have profound effects on nucleoid dynamics. For example, increases in HU (Kar *et al.*, 2005) or H-NS (Spurio *et al.*, 1992) levels dramatically enhance nucleoid compaction. In addition to organizing chromosomal DNA within cells, nucleoid compaction can also provide a level of DNA protection. For instance, Dps protects DNA by creating highly ordered complexes with DNA that not only contributes to DNA condensation, but also protection during oxidative stress by forming a ferroxidase center between two Dps monomers (Frenkiel-Krispin *et al.*, 2004; Morikawa *et al.*, 2006; Ohniwa *et al.*, 2006). Encoding diverse sets of NAPs likely allows bacteria to fine-tune nucleoid compaction levels depending on growth stage and conditions.

While all bacteria require the activity of NAPs, they don't all use the same collection of proteins. *Chlamydia,* for example, encodes a unique histone-like protein (Hc1) that promotes tight chromosomal compaction at a particular stage in its life cycle. The nucleoid compaction mediated by Hc1 is so severe that expression of this NAP in *E. coli* is lethal (Barry *et al.*, 1992). Highly compacted nucleoids are also found in developed *Bacillus* spores, where the chromosomes are complexed with small acid-soluble proteins (SASPs), which confer DNA protection (Lee *et al.*, 2008). Additional changes to the *Bacillus* nucleoid occur during germination: in *B. megaterium*, nucleoids form ring structures after germination (Ragkousi *et al.*, 2000), and further nucleoid condensation coincides with SASP degradation, before the nucleoids revert to their typical lobed appearance in vegetative cells.

Throughout *S. coelicolor* development, chromosomal DNA is not obviously condensed and instead appears dispersed in the multi-genomic hyphal cells. Prior to

sporulation in the aerial hyphae, a concerted DNA segregation and condensation event takes place, leading to the distribution of equivalent genomic units (often presumed to be a single chromosome) into pre-spore compartments. The arsenal of NAPs that *S. coelicolor* uses to organize its DNA during this process appear conserved in the actinobacteria, but these vary from other bacteria like *E. coli*. In fact, the actinomycetes, which include *S. coelicolor* and *M. tuberculosis*, lack IHF, Fis and H-NS, all of which are found in *E. coli*. This is not to say, however, that functionally equivalent proteins cannot perform the role of these absent NAPs. For instance, Lsr2 has been identified as the H-NS equivalent in mycobacteria (Qu *et al.*, 2013) and current work involves determining if one of the two copies of the *lsr2* genes encoded by most *Streptomyces* species has a similar role (M. Elliot, personal communication). Additionally, Fis is specific to γ-proteobacteria (Ohniwa *et al.*, 2006), whereas an analogous role is played by AbrB in *B. subtilis* (O'Reilly and Devine, 1997).

Apart from Lsr2, another intriguing actinomycetes-specific NAP candidate is one known as mIHF (**m**ycobacterial **i**ntegration **h**ost **f**actor) in *Mycobacterium*. Notably, mIHF bears no sequence or structural similarity to IHF in *E. coli*, but was originally characterized as an integration host factor and shown to facilitate mycobacteria phage DNA integration into the chromosome (Pedulla *et al.*, 1996; Swiercz *et al.*, 2013). Unexpectedly, *mIHF* is essential in both *M. smegmatis* and *M. tuberculosis* (Pedulla *et al.*, 1996; Sassetti *et al.*, 2003) indicating that it must have cellular roles beyond promoting phage DNA integration. Further emphasizing its importance is the fact that it is highly conserved in the actinomycetes. Although *Mycobacterium* and *Streptomyces* are genetically related, sharing a conserved genetic cores harbouring most housekeeping and essential genes (Cole *et al.*, 1998; Bentley *et al.*, 2002; Cerdeño-Tárraga, 2003), their life cycles are very different. Mycobacteria are typically rod shaped, grow by polar tip extension and divide by binary fission, which is in stark contrast to the multicellular life cycle of *Streptomyces* (Figure 1.1). Importantly, because of their differing life cycles, some genes that are essential for viability in the mycobacteria are dispensable in the streptomycetes. Given this, we were interested in determining whether it was possible to manipulate the activity of the mIHF orthologue in *S. coelicolor* (sIHF), in the hopes of elucidating its function.

4.2 Results

4.2.1 sIHF: bioinformatic analysis

sIHF is a small highly basic protein of 107 amino acids (aa): it has a molecular weight of 11.5 kDa and an isoelectric point of 10.4. Sequence analysis revealed sIHF was highly conserved within the streptomycetes with orthologues sharing up to 100% aa sequence identity (Figure 4.1). Outside of the streptomycetes, sequence conservation ranged from 44 – 80% identity within diverse actinobacteria (Figure 4.2). For example, *S. coelicolor* sIHF was 44% identical (60% similar) to its *M. tuberculosi*s counterpart. Few examples of sIHF exist outside of the actinobacteria (Figure 4.3); currently, these exceptions include Firmicutes *Helibacterium modesticaldum* (42% identity and 63% similarity) and *Coprococcus comes* (37%

identity and 57% similarity). In the actinobacteria, sIHF orthologues were not only highly similar, but the surrounding genes were largely syntenous. sIHF was found downstream of *pyrF*, encoding an orotidine 5′-phosphate decarboxylase, an enzyme involved in pyrimidine metabolism, and upstream of *gmk*, encoding a guanylate kinase, which in turn was upstream of *rpoZ*, encoding the omega subunit of RNA polymerase (Figure 4.4).

4.2.2 Expression of sIHF throughout the S. coelicolor life cycle

To determine whether sIHF was required at a specific time during *S. coelicolor* development, sIHF expression was examined at each stage of the life cycle using immunoblot analysis. If sIHF expression were exclusive to a particular growth stage, a role in development could be explored. To conduct the sIHF expression time course, an antibody was generated to a 6×His-sIHF fusion protein, and used to detect sIHF within protein samples from *S. coelicolor* grown on MS (sporulation medium containing a poor carbon source) and R2YE (rich) solid media over a 4 day time course (Figure 4.5A). As a control, a strain lacking sIHF (described below) was used to confirm antibody specificity for sIHF. To ensure equal sample loading for appropriate protein level comparisons, samples were separated on a SDS-PAG and stained with Coomassie Brilliant Blue (Figure 4.5B). Immunoblot analysis revealed that sIHF was detectable throughout the life cycle when grown on either MS or R2YE media. sIHF levels were slightly lower at the later stages of development on MS medium, while levels were fairly consistent on rich medium, apart from a lower level at 72 hours.

4.2.3 Creating an sIHF deletion strain

As mIHF is an essential protein in *Mycobacterium*, we were interested in determining whether it was possible to delete its sIHF orthologue in *S. coelicolor*. To generate this deletion strain, the entire *sIHF*-encoding region was replaced with an apramycin resistance cassette in the *S. coelicolor* chromosome. To eliminate any potential polar effects on the downstream guanylate kinase gene, the antibiotic resistance cassette was excised, generating an in-frame deletion. The deletion strains were confirmed by both PCR (Figure 4.6) and immunoblotting with the sIHF-specific antibody described above (Figure 4.5A). A complementation strain was created by introducing *sIHF,* together with 284 nt of upstream, and 156 nt of downstream sequence, on an integrating vector into the deletion strain. Re-introduction of the wild type *sIHF* gene (but not an empty plasmid control) was sufficient to restore a wild type appearance to the mutant strain, as described below.

4.2.4 Antibiotic production is affected in an sIHF deletion strain

To begin testing the effects of *sIHF* deletion in *S. coelicolor*, the Δ*sIHF* mutant strain and its wild type parent, both carrying an empty integrative plasmid, together with the complemented Δ*sIHF* mutant strain were grown on solid MS and R2YE media for phenotypic observation. When Δ*sIHF* was grown on solid MS medium, neither of the pigmented antibiotics (actinorhodin/blue and undecylprodigiosin/red) were produced; however, enhanced actinorhodin production was observed during growth on rich solid medium (R2YE; Figure 4.7A).

The complemented strain produced these antibiotics at approximately wild type levels. To better quantify the levels of antibiotics produced by Δ*sIHF* and wild type strains, liquid culture time course studies in complex medium (YEME-TSB) were conducted. These revealed a delay and reduction in the production of both pigmented antibiotics by Δ*sIHF* (Figure 4.7B). Calcium-dependent antibiotic (CDA) production was also measured using a plate-based bioassay. Plugs containing the three *S. coelicolor* strains grown for 48 hours were overlaid with soft nutrient agar containing an indicator strain (*Staphylococcus aureus*). After an overnight incubation at 37˚C, zones of indicator strain growth inhibition were measured. Unlike the wild type and complementation strains, no CDA production was observed for the Δ*sIHF* mutant (Figure 4.7C).

4.2.5 Loss of sIHF affects development

In addition to aberrant antibiotic production (above), the phenotypic analysis of Δ*sIHF* revealed that this strain developed more slowly than the wild type or complemented strains on different solid media. The most striking phenotype was observed when the deletion strain was grown on MS medium (Figure 4.8A). Colonies failed to produce the grey spore-associated pigment, appearing white even after extended growth. The complemented strain exhibited partial restoration of grey spore-specific pigmentation.

To investigate this developmental phenotype further, light and scanning electron microscopic investigation of Δ*sIHF* (Figure 4.8B) revealed the presence of spores, indicating that the loss of grey pigment was the result of incomplete spore maturation (with spore pigment deposition representing the final stage of spore maturation [Kelemen *et al.*, 1998]) and not an inability to form spores. Interestingly, Δ*sIHF* spore compartments were irregularly sized and were frequently observed to have an unusual rod-like morphology, as compared to the equally sized, rounded wild type spores. To assess spore size more quantitatively, the lengths of approximately 1000 spore compartments of integrating plasmid-containing wild type and Δ*sIHF* mutant strains, along with the complemented strain, were measured from images captured with a light microscope, using ImageJ software (Abramoff *et al.*, 2004). The majority (>90%) of wild type spores were between 0.6 and 1.4 μm in length, while the distribution of Δ*sIHF* mutant spore sizes was much greater (0.6 to 2.3 μm; Figure 4.8C). Complementation of the Δ*sIHF* mutant strain restored spore length to near wild type levels (0.8 to 1.4 μm for >90% of the spores; Figure 4.8C). The aberrant sizes of the Δ*sIHF* spore compartments suggested a defect in the septation of aerial hyphae during sporulation.

4.2.6 Chromosome segregation and compaction are defective in an sIHF *mutant*

The variable spore sizes of the Δ*sIHF* mutant strain suggested defective septal placement during sporulation. It was of interest to investigate whether chromosome segregation, which occurs concomitantly with septation, was also affected in an Δ*sIHF* mutant strain. To investigate the DNA content of spores, wild type and Δ*sIHF* strains (both containing the integrating plasmid), alongside the complemented strain, were mounted on slides containing 4',6-diamidino-2-phenylindole (DAPI), a fluorescent stain that binds to DNA, and were observed with

a fluorescence microscope (Figure 4.9A,C). DNA content for over 1000 spores per strain was assessed. The data revealed 8.6% of Δ*sIHF* spores were anucleate as compared to 0.3% and 2% for spores produced by the wild type and complemented strains, respectively. The increased occurrence of anucleate spores in Δ*sIHF* suggested a defect in chromosome segregation during sporulation. To further investigate the anucleate phenotype, the DNA content of spores adjacent to anucleate spores was examined. If chromosome segregation was defective in Δ*sIHF*, it would be expected that spore compartments adjacent to anucleate spores would have double the DNA content of a spore flanked by DNA-containing compartments. To test this, the fluorescence emitted from 1000 spore compartments was measured. Due to variation between different images, the emitted fluorescence for each spore was normalized to the average fluorescence of all spores within an image, in order to compare the relative fluorescence of spore compartments. Relative fluorescence from spores adjacent to anucleate spore compartments did not significantly differ from spores flanking chromosome-containing compartments suggesting that the DNA content was largely normal in all spores tested. This suggests that the Δ*sIHF* anucleate spores did not result of entire chromosomes being missegregated into adjacent spore compartments.

While comparing the DNA content of each strain, differences were noted in the levels of nucleoid compaction. The Δ*sIHF* mutant nucleoids appeared more diffuse as compared to the wild type and complemented strains (Figure 4.9A). Nucleoid areas were quantified using ImageJ and revealed that the average nucleoid size for Δ*sIHF* mutant spores was 0.60 μm^2 as compared to 0.33 μm^2 for wild type (Figure 4.9B). When compared with the spore size distribution, the distribution of nucleoid areas followed a similar pattern. The majority of wild type spore nucleoids (>90%) occupied an area between 0.18 and 0.57 μm^2, while the same proportion of Δ*sIHF* spore nucleoids ranged from 0.31 to 0.98 μm^2. The complemented strain showed a more wild type distribution. In addition to nucleoid size, the emitted fluorescence from wild type and Δ*sIHF* spore compartments were compared, as described above, to ensure that the diffuse nucleoid was not the result of multiple chromosomes. The relative emitted fluorescence from each strain was comparable indicating that the spore compartments contained equal amounts of DNA. This, taken together with the diffuse nucleoid phenotype of Δ*sIHF*, suggests that that chromosome compaction is defective in the absence of sIHF.

4.2.7 sIHF associates with the nucleoid

Defects in chromosome condensation and a higher incidence of anucleate spores in an Δ*sIHF* mutant strain, as compared to wild type, were reminiscent of the mutant phenotypes for NAPs in *S. coelicolor* (Ausmees *et al.*, 2007; Dedrick *et al.*, 2009; Kois *et al.*, 2009; Kim *et al.*, 2000; Facey *et al.*, 2009; Salerno *et al.*, 2009). To begin to explore the potential for sIHF to act as a NAP, the cellular localization of sIHF was determined using fluorescence microscopy *in vivo*. A C-terminal translational fusion of *egfp* to *sIHF* within an integrating vector was generated and introduced into the *sIHF* deletion strain. Introducing the *sIHF-egfp* fusion construct restored Δ*sIHF* antibiotic production (Figure 4.10A) and spore size (Figure 4.10B) to

wild type levels, indicating that the protein fusion was functional. The strain containing the protein fusion and a control strain carrying the empty vector with promoterless *egfp*, were fixed on slides and stained with DAPI, prior to visualizing using a fluorescence microscope. sIHF-eGFP appeared to co-localize with the nucleoid within spore compartments (Figure 4.9C). To confirm that this pattern reflected nucleoid-association and to compare it with that of a cytoplasmically localized protein, the sIHF-eGFP fluorescence pattern was compared to that of eGFP under the control of the *chpH* promoter (Figure 4.9C), which is expressed at high levels within spores (Elliot *et al.*, 2003). eGFP, when expressed from the *chpH* promoter, occupied the entire spore compartment area, representing cytoplasmic localization, as compared to the sIHF-eGFP localization, where the localization was more focused, with a gap between the signal and the circumference of the spore membrane (also seen for the DAPI-stained nucleoid) that was not detectable in the cytoplasmic control strain (Figure 4.9C). This suggested that sIHF co-localized with the nucleoid; however, it was still unknown whether this was a direct or indirect interaction.

4.2.8 sIHF binds to DNA

The nucleoid localization of sIHF suggested that it associated with chromosomal DNA. To confirm an association with DNA, sIHF DNA binding activity was tested *in vitro* using electrophoretic mobility shift assays (EMSAs). Initially the affinity of sIHF for DNA hairpins with 11-, 15-, and 19-bp stems was tested. While sIHF bound the 11- and 15-bp hairpin probes, none of the sIHF concentrations tested were sufficient for significant probe shifting and distinct complex formation (Figure 4.11A, B). In contrast, sIHF bound to the GC and AT-rich versions of the 19-bp hairpin probes in a concentration-dependent manner but failed to yield a distinct shifted complex (Figure 4.11C, D). sIHF DNA binding properties were further tested using 40-bp and 60-bp probes. Ten micromolars of sIHF was sufficient to fully shift 0.1 μM of 40- or 60-bp probe, and unlike what was observed with the shorter probes, the sIHF-probe association led to distinct complex formation (Figure 4.12A). Interestingly, when the length of the probe was extended to 407-bp, a lower sIHF concentration (3 μM) was required to fully shift the probe (Figure 4.12B) suggesting that complex formation between sIHF and DNA was DNA length dependent and that sIHF binding may be cooperative. To test sIHF DNA binding specificity, increasing concentrations of unlabeled, non-specific competitor poly [d(I-C)] was incubated with the 407- (Figure 4.12B) or 60-bp probes-containing binding reactions. The ability of this DNA analogue to effectively compete with the labeled probes for sIHF binding suggested that sIHF bound DNA without any obvious specificity.

4.2.9 sIHF binds to DNA of varying conformations

While we had determined that sIHF bound double stranded DNA (dsDNA) non-specifically, there was nothing known about whether sIHF had greater affinity for different forms of DNA. It is well established that different NAPs have varying levels of affinity for DNA with distinct conformations. While there are classic examples of proteins that prefer binding to specific sequences, such as IHF (Hales *et al.*, 1994), other proteins like HU (Castaing *et al.*, 1995; Kamashev *et al.*, 1999;

Kamashev and Rouvière-Yaniv, 2000) prefer binding to distorted DNA (*e.g.* gapped or nicked DNA). To begin probing the affinity of sIHF for different DNA configurations, sIHF binding to single stranded DNA (ssDNA) was compared to dsDNA. sIHF binding to both individual strands of the 60-bp probe, which was previously used to test sIHF binding to dsDNA, was tested. sIHF binding to ssDNA (Figure 4.13) was similar to that of the 19-bp hairpin probe (Figure 4.11C, D), where probe binding was evident but no distinct complex formation was detected, unlike the complexes formed when sIHF bound to the larger dsDNA probes. sIHF binding to curved and gapped DNA, which is preferably bound by HU (Kamashev and Rouvière-Yaniv, 2000), was also tested. The curved DNA probe was 42-bp long and contained repeated stretches of 5-6 A's, while the gapped DNA probe contained a single nucleotide gap within one of the strands, in addition to having a single nucleotide overhang at each 5′ end. sIHF binding to curved DNA was compared to its binding affinity with a probe containing a randomized sequence of the curved probe. sIHF binding to the gapped probe with 5′ overhangs was compared to its binding to the same probe without a gap or overhangs. Unlike HU, sIHF associated with both curved and non-curved probes with equal affinity (Figure 4.14). Similarly, equivalent sIHF binding was observed for the probe containing a gap and 5′ end overhangs relative to a probe without a gap or 5′ overhangs (Figure 4.15). Collectively, sIHF did not appear to have a greater affinity for any of the tested DNA configurations *in vitro*.

4.2.10 sIHF prefers modest DNA sequence preferences in vitro

The above results suggest that sIHF binds to DNA in a non-specific but length dependent manner, without preference for distorted DNA configurations. Although many NAPs bind DNA with little specificity, others – such as IHF in *E. coli* – have greater affinity for specific sequences (Hales *et al.*, 1994) while some other NAPs have multiple consensus sequences, such as Lrp from *E. coli* (Cui *et al.*, 1995; Nou *et al.*, 1995), which binds DNA as a large complex (de los Rios and Perona, 2007) making it difficult to identify its minimal target sequence requirements. This suggests that although sIHF appears to bind DNA non-specifically, this does not exclude the possibility that it preferentially associates with specific sequences relative to random DNA. To test whether sIHF prefers binding to any particular sequences or sequence motifs, a systematic search of DNA-binding sequences was completed using an *in vitro* selection experiment, commonly referred to as SELEX, for **S**ystematic **E**volution of **L**igands by **Ex**ponential Enrichment. The goal of SELEX is to enrich for DNA that is preferred by a protein from a pool of random DNA.

Six rounds of SELEX were completed with sIHF. The sIHF concentration that was used for these rounds was determined by reducing the minimal concentration required to shift a probe, which was a similar size as library DNA, by five fold (Figure 4.16). The DNA extracted following the sixth SELEX round was analyzed for any conserved motifs using MEME (Bailey and Elkan, 1994). To ensure that any motifs identified from the sixth round of selection were enriched for during SELEX, the DNA extracted following the second round was also analyzed and included as a control. MEME did not identify any consensus sequences with the sequences

isolated from the second selection round; however, three potential consensus sequences were identified from the sixth selection round (Figure 4.17). From the 71 sequences that were sequenced from the sixth selection round, eight contained motif #1 (three sets of sequences were duplicates), seven sites contained motif #2 (two sets of sequences were duplicates) and eleven sites contained motif #3 (one set was a duplicate). EMSAs were conducted to test sIHF binding specificity to the identified motifs. Initially, EMSAs were conducted for each enriched probe sequence using increasing concentrations of sIHF; however, no binding preference was observed as compared to a probe with the randomized sequence of one of the SELEX probes (control; Figure 4.18). An additional test was conducted using the SELEX motifs as cold competitor DNA against the curved control probe (used previously; Figure 4.14). Interestingly, increasing concentrations of cold SELEX DNA displaced the complex that was observed with 10 μM sIHF and 0.1 μM control probe suggesting that sIHF preferred to bind to the SELEX motifs over the control probe (Figure 4.19).

4.2.11 DNA structure is affected upon sIHF overexpression

Thus far, sIHF had been shown to bind DNA and impact chromosome compaction. NAPs, such as IHF and HU, contribute to DNA condensation by binding and bending DNA (Pan *et al.*, 1996; Rice *et al.*, 1996; Swinger *et al.*, 2003). To test whether sIHF also bent DNA, fluorescence resonance energy transfer (FRET) was completed. FRET is a useful tool for measuring distances between 10 and 100 Å in DNA to monitor protein-induced bending (Clegg, 1992; Lorenz *et al.*, 1999; Hillisch *et al.*, 2001). It has been used successfully to measure the bending angles of DNA induced by IHF and HU upon binding (Lorenz *et al.*, 1999; Wojtuszewski and Mukerji, 2003; Koh *et al.*, 2008). To this end, a 33-bp DNA molecule, containing fluorescein as a donor and TAMRA as an acceptor on either end, was incubated with sIHF and the efficiency of energy transfer was measured to calculate the end-to-end distance of the bound DNA. At this time no positive control was available for the assay; however, FRET analysis was discontinued because the structure of sIHF bound to DNA was solved at this time revealing that sIHF does not appear to bend DNA (Swiercz *et al.*, 2013).

As an alternative method to further characterize the effects of sIHF on DNA in the presence of other proteins, an inducible system was used to analyze any changes to DNA structure after sIHF overexpression. Briefly, plasmid DNA was examined from *E. coli* grown in the presence and absence of sIHF, where *sIHF* was cloned behind an IPTG-inducible promoter on a multi-copy plasmid. Plasmid DNA, which was extracted 8 hours post sIHF induction, was separated on an agarose gel and compared with a control plasmid preparation, which was prepared from cells that were not subject to IPTG treatment (and therefore did not overexpress sIHF; Figure 4.20). Protein extracts were also generated for these same induced and control cultures, and sIHF overexpression - or lack thereof - was confirmed by analyzing protein extracts separated using SDS-PAGE (Figure 4.21). Plasmid DNA extracted from the sIHF overexpressing strain had a significantly different plasmid topology profile when compared with the control (Figure 4.20). To ensure that differences in plasmid topology were not due to the addition of IPTG or to the overexpression of

any foreign protein in *E. coli*, the experiment was repeated, only overexpressing an unrelated protein that is not involved in DNA binding (SrtA) (Duong *et al.*, 2012). Plasmids isolated from both SrtA-induced and uninduced strains had the same DNA topology (Figure 4.20). This suggested that the change in plasmid topology following sIHF overexpression was due specifically due to the overexpression of sIHF.

4.2.12 sIHF affects topoisomerase activity

Changes to plasmid topology upon sIHF overexpression suggested that sIHF might influence DNA supercoiling/condensation. Based on preliminary small angle x-ray scattering (SAXS) data (A. Guarné, personal communication) and the solved crystal structure of sIHF bound to DNA (Figure 4.22; Swiercz *et al.*, 2013), sIHF does not appear to affect DNA structure in the same way as IHF, HU, H-NS and Fis (among others), which condense DNA by bending, bridging and wrapping DNA (Luijsterburg *et al.*, 2006). To probe the connection between sIHF and DNA supercoiling/condensation, sIHF activity was assessed in conjunction with a key supercoiling determinant: DNA topoisomerase. In *S. coelicolor*, *topA* encodes the sole type I topoisomerase responsible for introducing positive supercoils into chromosomal/plasmid DNA. TopA was overexpressed, purified and incubated with a supercoiled plasmid in the presence and absence of sIHF. sIHF alone did not impact plasmid supercoiling/relaxation and the concentration of sIHF used during the assay was not sufficient to shift the plasmid DNA (Figure 4.23A, B). As expected, TopA relaxed the supercoiled plasmid substrate, as evidenced by the topoisomers that formed in the presence of increasing concentrations of TopA (Figure 4.23A, B). In contrast, increasing concentrations of sIHF appeared to inhibit TopA-induced plasmid DNA relaxation (Figure 4.23A, B). To demonstrate that sIHF was responsible for the reduced DNA relaxation, lysozyme (a small unrelated protein) was substituted for sIHF in the assay. TopA activity, and the accompanying DNA relaxation, were unaffected by lysozyme, suggesting that sIHF specifically inhibited the relaxation activity of TopA (Figure 4.23B). From this data, it appeared that sIHF could influence DNA structure in a topoisomerase-dependent manner.

It was of interest to determine whether sIHF was affecting TopA activity through a direct protein-protein interaction. A B2H assay was used to test whether sIHF and TopA interactions could be detected. *sIHF* and *topA* were cloned upstream or downstream of either *Bortedella pertussis* adenylate cyclase subunits (T25 or T18) to create N- or C-terminal fusions with TopA or sIHF. Combinations of plasmids, such that each adenylate cyclase subunit was combined with TopA or sIHF, were introduced into *E. coli*. Blue/white selection, based on transcription of the *lacZ* reporter gene in the presence of interacting adenylate cyclase subunits via an TopA and sIHF interaction, was used to identify colonies of interest. Although colonies containing combinations of these fusions appeared blue, indicating an interaction between TopA and sIHF, the negative control strains, with just one protein fused to an adenylate cyclase subunit, also appeared a shade of blue. No conclusions from these preliminary results have been made, as the assay needs to be repeated.

4.2.13 sIHF affects the expression of other NAPs

Changes to chromosome dynamics exhibited by NAPs usually coincide with alterations in global gene expression (Dorman and Deighan, 2003; Gama-Castro *et al.*, 2008; Prieto *et al.*, 2011). Since sIHF affects DNA topology, it was of interest to test whether this impacted transcription of other NAPs in the cell. To test this, the expression levels of a select panel of *S. coelicolor* genes encoding proteins involved in DNA organization (namely *parA*, *parB*, *scpA*, *scpB*, *smc*, *ftsK* and *hupS*) were analyzed in Δ*sIHF* and wild type strains using reverse transcription quantitative PCR (RT-qPCR). To begin, RNA was extracted from wild type and Δ*sIHF* strains that were grown on solid MS medium to various stages of development (vegetative growth, aerial development and early and late sporulation). After reverse transcription reactions with gene-specific primers, cDNA was quantified using quantitative PCR (qPCR). Target gene expression levels were normalized to total RNA as a suitable uniformly expressed endogenous reference gene has not been identified under our lab conditions with qPCR (R. St-Onge and Hindra, personal communication). *rpoB*, which encodes the β subunit of RNA polymerase, was included as a reference gene to demonstrate the level of transcript fluctuation throughout development.

qPCR data was analyzed and revealed that transcription levels of the majority of tested genes (*parA*, *smc*, *ftsK* and *rpoB*) were not significantly different between Δ*sIHF* and wild type (Figure 4.24). The transcription levels of *scpA* and *scpB* throughout development were considerably increased in Δ*sIHF* and, intriguingly, *hupS* transcript levels were significantly lower during early and late sporulation in Δ*sIHF*, as compared to wild type (Figure 4.24). Collectively, these results suggest that sIHF influences transcription levels of select NAPs and implies that it could specifically affect transcription of other genes (discussed in Chapter 5).

4.3 Discussion

4.3.1 sIHF is a unique NAP

Although sIHF is not required for the growth or viability of *S. coelicolor*, it affects processes throughout development. Phenotypic characterization of a mutant lacking *sIHF* revealed defects in chromosome segregation and compaction, spore development and antibiotic production. Although the Δ*sIHF* mutant phenotype was unique, it shared characteristics with other *S. coelicolor* mutants that affect chromosomal DNA organization. The increased incidence of anucleate spores in Δ*sIHF* (8.6% as compared to 0.3% in wild type) has also been seen in mutant strains lacking proteins involved in chromosome segregation or compaction. For example, loss of the ParA and ParB proteins, which are involved in chromosome segregation, results in 11.7% more anucleate spores as compared to wild type (Kim *et al.*, 2000). Additionally, deleting chromosome condensation proteins such as SMC or its predicted protein partners, ScpA and ScpB, results in 6.2% and 5% more anucleate spores, respectively, when compared to wild type (Kois *et al.*, 2009). It is possible that the variable spore size and unequal chromosome segregation observed for the *sIHF* mutant was caused by improper septa formation during sporulation. This suggests that sIHF may influence FtsZ and/or SsgA/B localization, where improper localization of these proteins could result in loss of equally spaced septa (Willemse

et al., 2011). The increased occurrence of missegregated chromosomes in conjunction with heterogeneous spore lengths, as observed here, is not unprecedented. This phenotype has also been seen for strains lacking SmeA-Sffa (FtsK-like proteins involved in clearing DNA from septal sites) and DpsA (a nucleoid compaction protein) (Ausmees *et al.*, 2007; Facey *et al.*, 2009).

The loss of nucleoid compaction observed for the Δ*sIHF* mutant strain (Figure 4.9A) has also been observed for Δ*smc,* Δ*hupS* and Δ*dpsA* mutants (Dedrick *et al.*, 2009; Kois *et al.*, 2009; Facey *et al.*, 2009; Salerno *et al.*, 2009), where SMC, HupS and DpsA are all well characterized NAPs found in most bacteria. Δ*sIHF* affected chromosomal DNA similarly to other *S. coelicolor* NAP mutants; however, none of these strains have the same collective phenotype as Δ*sIHF*. For instance, Δ*hupS* spores have reduced spore pigmentation (Kois *et al.*, 2009), like Δ*sIHF* (Figure 4.8A), but spore size and shape and chromosomal segregation are normal (Kois *et al.*, 2009). Interestingly, transcript levels of *hupS* (Figure 4.24), as determined by qPCR, are significantly reduced in Δ*sIHF*, as compared to wild type. This implies that the chromosome condensation defect of the Δ*sIHF* strain may be an indirect one that is mediated through the activity of HupS. It will therefore be interesting to determine whether the loss of sIHF impacts chromosome condensation directly or indirectly as a result of reduced HupS levels (Chapter 5). The effect of reduced ScpA/B levels can also be studied in a similar manner.

In addition to the loss of chromosome segregation, the aberrant antibiotic production by Δ*sIHF* (Figure 4.7A-C) has not been observed in conjunction with mutations in any other *S. coelicolor* NAP-encoding gene. The altered antibiotic production capabilities of Δ*sIHF* could be the result of losing sIHF-mediated regulation of genes involved in antibiotic production. It is not uncommon for NAPs to also function as global transcription factors. In *E. coli*, for example, IHF and HU influence the expression of 150-500 and >900 genes, respectively (Gama-Castro *et al.*, 2008; Prieto *et al.*, 2011). In general, NAP-mediated changes in transcription profiles can be either direct or indirect. This likely depends on whether a NAP binds to a consensus sequence and where these sequences are within the genome. If a NAP binds exclusively upstream of certain promoters, then this can be regarded as a direct effect; however, a NAP that binds DNA non-specifically could change transcription profiles by indirectly influencing the accessibility of transcription factors or RNA polymerase. Based on SELEX results, sIHF exhibits preferential binding to three DNA motifs over random DNA (Figure 4.19). This, coupled with changes in *hupS* and *scpA/B* transcription in Δ*sIHF* relative to wild type (Figure 4.24), suggests that sIHF might bind more readily to specific sites within the chromosome and potentially change the expression of genes directly. Additional studies involving global gene expression and *in vivo* binding site analysis (Chapter 5) will be important to draw definitive conclusions about sIHF binding specificity and transcriptional changes in its presence.

4.3.2 sIHF binds DNA

In collaboration with the group of Dr. Alba Guarné, a crystal structure for sIHF in complex with DNA has been determined (Swiercz *et al.*, 2013). Of 107 residues,

residues 14 to 103 were modeled (likely due to end flexibility) and form five α-helices: a long protruding N-terminal α-helix followed by four shorter α-helices that make up the protein core. sIHF interacts with the minor groove of DNA. The primary DNA binding site in sIHF appears to be an 11-residue lid located between α4 and α5 within the protein core, which exposes positively charged residues that make contact with the DNA phosphate backbone. The conformation of the "lid" domain is very similar to structures found in topoisomerase VI (Corbett and Berger, 2003) and ribosomal protein S13 (Brodersen *et al.*, 2002). A second potential DNA contact site in sIHF exists within the second turn of the helix-two turns-helix (H2TH) motif, which interacts with the minor groove of the DNA. This potential sIHF-DNA interaction site resembles that of ribosome protein S13 with RNA and the H2TH motif of endonuclease VIII with DNA (Zharkov *et al.*, 2002; Gilboa *et al.*, 2002; Fromme and Verdine, 2002). Unfortunately, the structure of topoisomerase VI was not determined while in complex with DNA; and thus the DNA binding properties of this domain have not been assessed. Additionally, the contribution of the H2TH motif in nucleic acid binding for S13 and endonuclease VIII is unknown; however, they are found within larger structures that have defined binding sites and thus only exhibit peripheral binding.

sIHF binding to DNA of various sizes was tested. EMSAs did not reveal any significant binding between sIHF and 11- and 15-bp DNA probes (Figure 4.11A, B) or distinct complex formation between sIHF and 19-bp DNA probes (Figure 4.11C, D). Unlike the larger probes that displayed distinct complex formation with sIHF (Figure 4.12A, B), the 11-, 15- and 19-bp probes were hairpins, which are structurally different compared to duplex DNA. The lack of binding or distinct complex formation with smaller probes is likely not due to probe structure as crystallization studies revealed that sIHF forms a complex with 19-bp duplex DNA (Swiercz *et al.*, 2013) and 8-bp hairpin DNA (A. Guarné, personal communication). EMSAs also revealed that sIHF binding is DNA length dependent (Figure 4.12A, B). A lower sIHF concentration is required to shift larger probes than smaller ones. This could indicate that there is a form of cooperative binding or that sIHF prefers a unique DNA structure that is inherent in larger fragments of DNA.

It is interesting to note that IHF in *E. coli* binds to a consensus sequence with ~1000 fold more affinity than random DNA (Wang *et al.*, 1995), and like sIHF, it does not make any residue-specific contacts with DNA (Rice *et al.*, 1996). HU also does not make any residue-specific contacts with DNA (Swinger *et al.*, 2003), but prefers binding to distorted DNA, including those with gaps, cruciform and phase loops (Balandina *et al.*, 2002; Swinger and Rice, 2007). These observations suggest that IHF and HU may recognize the shape adopted by a particular DNA sequence, but not specific sequences *per se*. sIHF did not exhibit preferential binding to any of the DNA forms tested in this study apart from preferring dsDNA over ssDNA (Figures 4.12A, 4.13-4.15); however, three DNA motifs that were preferably bound by sIHF were identified using SELEX (Figures 4.17, 4.19). It will be interesting to solve and compare the structural changes of sIHF when bound to the SELEX derived sequences, to the current structure, which was solved using a non-specific DNA sequence. While bound to non-specific DNA, the majority of DNA contacts made by

sIHF are with the DNA phosphate backbone (Swiercz *et al.*, 2013) and residues within the 'lid' region of sIHF, including three arginines and a glutamine, associate with the minor groove of DNA; however, specific DNA interactions are not made (Swiercz *et al.*, 2013). Solving the structure of sIHF bound to the SELEX derived sequences will be important to distinguish between sequence versus structural specificity. Major changes to sIHF structure upon binding the preferred DNA sequences are not unprecedented, as this has been demonstrated for other proteins. For example, the structure of the *lac* repressor was solved while bound to non-specific and specific DNA (Kalodimos *et al.*, 2001; Kalodimos *et al.*, 2002; Kalodimos *et al.*, 2004) and these studies revealed that when bound to non-specific DNA, LacI solely interacted with the DNA backbone through electrostatic interactions, but that there were major changes to its structure that lead to specific contacts with a consensus sequence (Kalodimos *et al.*, 2001; Kalodimos *et al.*, 2002; Kalodimos *et al.*, 2004). If no specific contacts are made between sIHF and the SELEX derived sequences it will suggest that sIHF prefers a feature of these sequences, such as groove widening or flexibility.

4.3.3 sIHF alters DNA topology

No changes to DNA structure were observed during sIHF structural studies or FRET-binding assays. In the case of IHF and HU in *E. coli,* the significant DNA bending observed for these proteins requires a key proline residue in its DNA interacting interface; sIHF lacks an analogous proline residue. Intriguingly, the presence of two potential DNA binding sites in sIHF suggests that it could be involved in bridging distinct DNA segments. Since sIHF binds to DNA as a monomer (Swiercz *et al.*, 2013), DNA bridging would occur in a manner different to that of H-NS and Lsr-2, which oligomerize to bridge DNA (Almirón *et al.*, 1992; Chen *et al.*, 2008). It is also possible that sIHF influences DNA structure *in vivo* in conjunction with a protein partner. Some evidence of this exists as plasmid topology dramatically changed upon sIHF overexpression in *E. coli*. It would be important to repeat this experiment with plasmid DNA isolated from Δ*sIHF* and an sIHF overexpression *S. coelicolor* strain to solidify the biological significance of these results.

Given that sIHF profoundly affects plasmid DNA relaxation exhibited by TopA (Figure 4.23), the sole type I topoisomerase in *S. coelicolor* and other actinobacteria, it is tempting to speculate that TopA may be a potential sIHF interacting partner. Alternatively, sIHF could affect the structure of DNA such that it is less accessible to TopA. This has been demonstrated with HU, where increasing concentrations of HU reduced the relaxation activity of topoisomerase I by stabilizing the supercoiled plasmid DNA substrate (Rouvière-Yaniv *et al.*, 1979; Guo and Adhya, 2007). With this in mind, sIHF may contribute to DNA compaction by stabilizing supercoiled DNA or interacting directly with TopA to prevent DNA relaxation; however, mechanisms for either types of activity are still elusive. Preliminary studies to distinguish between these two possibilities have involved testing potential interaction between TopA and sIHF using a B2H. This assay still needs to be repeated to ensure that the results are reproducible. It is tantalizing to speculate that sIHF interacts with a protein-binding partner through its extended N-terminal

α-helix, as it does not appear that this region contributes to DNA binding. This N-terminal domain is highly conserved within sIHF (Figures 4.1, 4.2, 4.3), suggesting that is has an important role in sIHF function.

4.3.4 Summary of findings

Collectively, the chromosome segregation and compaction defects of Δ*sIHF* and the DNA binding properties of sIHF suggest that it is a unique NAP, which binds DNA with preference to three DNA motifs identified through SELEX. Like some NAPs, sIHF also impacts gene expression with significant changes to *hupS* and *scpA/B* expression, relative to their wild type expression. It is possible that sIHF acts as a transcription factor and affects the expression of these genes directly. Alternatively, these could be indirect effects caused by nucleoid compaction changes in Δ*sIHF*, as discussed in Chapter 5. Additional defects in Δ*sIHF*, such as aberrant antibiotic production and defects in spore maturation, contribute to the unique characteristics of sIHF as a NAP. It will be interesting to analyze the expression levels of genes involved in antibiotic production or spore maturation in Δ*sIHF* and wild type, and determine whether the Δ*sIHF* phenotype can be explained by the changes in the expression of genes involved in these pathways. Additionally, uncovering the mechanism of counteracting TopA activity will reveal whether sIHF constrains supercoils or if it interacts with TopA directly to influence its activity. It is possible that sIHF simply constrains supercoiled DNA and prevents TopA activity at a certain concentration, as seen with HU (Rouvière-Yaniv *et al.*, 1979; Guo and Adhya, 2007), but if it interacts with TopA this will suggest a very different mechanism of action.

```
Streptomyces_coelicolor       --VALPPLTPEQRAAALEKAAAARRERAEVKNRLKHSGASLHEVIKQGQE 48
Streptomyces_ghanaensis       --VALPPLTPEQRAAALEKAAAARRERAEVKNRLKHSGASLHEVIKQGQE 48
Streptomyces_albus            --VALPPLTPEQRAAALEKAAAARRERAEVKNRLKHSGASLHEVIKQGQE 48
Streptomyces_clavuligerus     --MALPPLTPEQRAAALEKAAAARRERAEVKNRLKHSGASLHEVIKQGQE 48
Streptomyces_avermitilis      --MALPPLTPEQRAAALEKAAAARRERAEVKNRLKHSGASLHEVIKQGQE 48
Streptomyces_prunicolor       --MALPPLTPEQRAAALEKAAAARRERAEVKNRLKHSGASLHDVIKQGQE 48
Streptomyces_venezuelae       --MALPPLTPEQRAAALEKAAAARRERAEVKNRLKHSGASLHDVIKSGQE 48
Streptomyces_griseus          MPTSLPALTSEQRAEALAKAGRVRKERSEMLGALKAGRLSLLDVLDRG-- 48
                                  :**.**.**** ** **. .*:**:*: . ** .  ** :*:. *

Streptomyces_coelicolor       NDVIGKMKVSALLESLPGVGKVRAKQIMERLGISESRRVRGLGSNQIASL 98
Streptomyces_ghanaensis       NDVIGKMKVSALLESLPGVGKVRAKQIMERLGISESRRVRGLGSNQIASL 98
Streptomyces_albus            NDVIGKMKVSALLESLPGVGKVRAKQIMERLGISESRRVRGLGSNQIASL 98
Streptomyces_clavuligerus     NDVIGKMKVSALLESLPGVGKVRAKQIMERLGISESRRVRGLGSNQIASL 98
Streptomyces_avermitilis      NDVIGKMKVSALLESLPGVGKVRAKQIMERLGISESRRVRGLGSNQIASL 98
Streptomyces_prunicolor       NDVIGKMKVSALLESLPGVGKVRAKQIMERLGISESRRVRGLGSNQIASL 98
Streptomyces_venezuelae       NDVIGKMKVSALLESLPGVGKVRAKQIMERLGISESRRVRGLGSNQIASL 98
Streptomyces_griseus          DDTARQTRALQLLQSLPGVGTVTARRHLVDLGISESRRIQGLGARQRARL 98
                               :*.  : :.  **:******.* *:: :  ********::***:.* * *

Streptomyces_coelicolor       EREFGSTGS 107
Streptomyces_ghanaensis       EREFGSTGS 107
Streptomyces_albus            EREFGGSPA 107
Streptomyces_clavuligerus     EREFGGGPA 107
Streptomyces_avermitilis      EREFGSTAG 107
Streptomyces_prunicolor       EREFGSTGS 107
Streptomyces_venezuelae       EREFGSTGA 107
Streptomyces_griseus          IELFPPQG- 106
                                . *
```

Figure 4.1 Alignment of sIHF orthologues within the streptomycetes. Multiple-sequence alignment of sIHF homologs in several streptomycetes. Identical aa are indicated by "*" and similar aa are indicated by ":".

```
Nocardiopsis alba               -MALPPLTPEQRSAALEKAAKARKERAEVKNKLKNGGISLSEVLADSLKD 49
Thermobifida fusca              -MALPPLTPEQRAAALEKAAKARKERAEVKHRLKHGGISLTEVLKLGQTN 49
Thermomonospora curvata         -MALPPLTPEQRAAALQKAAKARKERAEVKNRLKHGGTSLAEVLKIGQTD 49
Streptomyces coelicolor         -VALPPLTPEQRAAALEKAAAARRERAEVKNRLKHSGASLHEVIKQGQEN 49
Saccharopolyspora erythraea     MVALPQLTEEQRAAALEKAAAARRARAELKERLKRGGTSLAQVLQDADEN 50
Mycobacterium tuberculosis      -VALPQLTDEQRAAALEKAAAARRARAELKDRLKRGGTNLTQVLKDAESD 49
Frankia alni                    -MPLPPLTPEQRAAALEKAALARKQRAELKERLKKAETTLAAVLEQAEAD 49
                                 :.** ** ***: **:*** **: **.:*. **..   *  *:  .  :

Nocardiopsis alba               EVIG-------KMKVSALLESLPGVGKVRAKQIMERLNIAESRRVRGLGT 92
Thermobifida fusca              EVIG-------KMKVSALLESLPGVGKVRAKQIMERLNIAESRRIRGLGA 92
Thermomonospora curvata         DVIG-------KMKVSALLESLPGVGKVRAKQIMERLGIAESRRVRGLGA 92
Streptomyces coelicolor         DVIG-------KMKVSALLESLPGVGKVRAKQIMERLGISESRRVRGLGS 92
Saccharopolyspora erythraea     EVLG-------KMKVSALLEALPGVGKVRAQQIMERLEIANSRRLRGLGE 93
Mycobacterium tuberculosis      EVLG-------KMKVSALLEALPKVGKVKAQEIMTELEIAPTRRLRGLGD 92
Frankia alni                    EVVGKIDEVVGKMKVSAVLESLPGVGRVRAQKIRERLGISPTRRLRGLGA 99
                                :*:*       *****::**::* **:*:*::*  .: *: :**:****

Nocardiopsis alba               NQRAALESEFGDLTK- 107
Thermobifida fusca              NQRAALESEFGGQ--- 105
Thermomonospora curvata         NQRASLEREFGGGANR 108
Streptomyces coelicolor         NQIASLEREFGSTGS- 107
Saccharopolyspora erythraea     RQRKALLAEFSGE--- 106
Mycobacterium tuberculosis      RQRKALLEKFGSA--- 105
Frankia alni                    KQRAALLEEFGTA--- 112
                                .*  :*  .*.
```

Figure 4.2 Alignment of sIHF orthologues within the actinomycetes. Multiple-sequence alignment of sIHF homologs in various actinomycetes outside of the streptomycetes. Identical aa are indicated by "*" and similar aa are indicated by ":".

```
Streptomyces coelicolor          VALPPLTPEQRAAALEKAAAARRERAEVKNRLKHSGASLHEVIKQGQEND 50
Heliobacterium modesticaldum     MAVPTLTAEQKSEALKKAHAVRSQRTQLRNQLKTGAVSVEAVLNR-MDDE 49
Coprococcus comes                MALPNFTPEERAKALEKAAQVRKARKELKENIKSGETDPASVLKTRKDDP 50
                                 :*:* :*.*::: **:**  .*  * ::::.:* .  .   *:.   ::

Streptomyces coelicolor          VIGKMKVSALLESLPGVGKVRAKQIMERLGISESRRVRGLGSNQIASLER 100
Heliobacterium modesticaldum     VVRGMKVLYLLESLPKVGKRTARRIMADIGIDESRRLQGLGSRQRDALVA 99
Coprococcus comes                LVSKMKVKEFLQAIPGIGGAKADKIMHDVDIPGNRRLGGLGIRQAEALLE 100
                                  :  :**  :*:::* :*   *  **  :.*  .**: *** .*   *

Streptomyces coelicolor          EFGSTGS 107
Heliobacterium modesticaldum     KLT---- 102
Coprococcus comes                YLS---- 103
```

Figure 4.3 Alignment of sIHF orthologues outside of the actinomycetes. Multiple-sequence alignment of sIHF homologues outside of the actinomycetes. Identical amino acids (aa) are indicated by "*" and similar aa are indicated by ":".

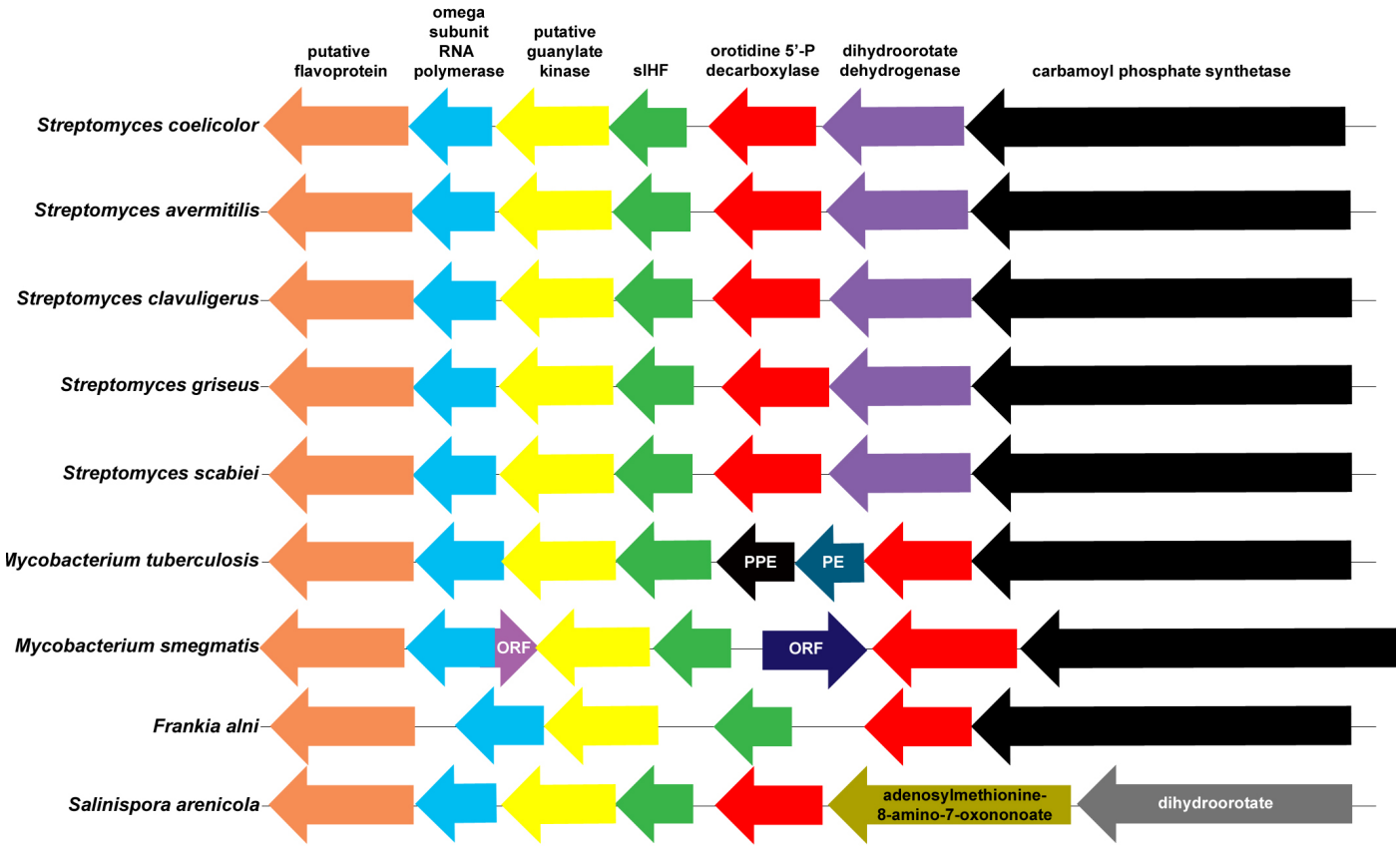

Figure 4.4 Conserved arrangement of the genes surrounding *sIHF* across the actinomycetes. Each colour denotes a different conserved gene. Protein products are listed above each gene or within genes.

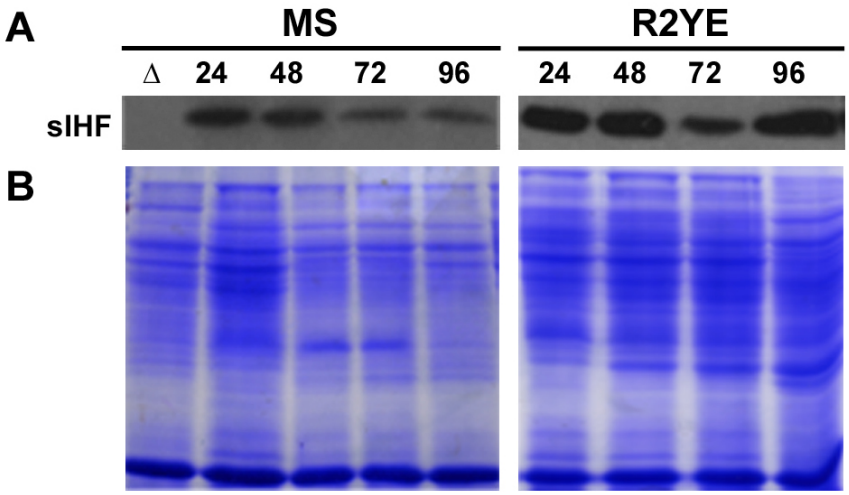

Figure 4.5 Western blot analysis of sIHF production. **(A)** sIHF production is shown in wild type *S. coelicolor* grown on MS or R2YE media. Samples were taken at the indicated times (hours). The Δ*sIHF*-mutant strain (Δ) was used as a negative control. **(B)** Total protein extract loading control for sIHF expression analysis. Samples were taken at the indicated times (hours) as indicated in (A). Protein extracts were separated on a 12.5% polyacrylamide gel and strained with Coomassie Brilliant Blue.

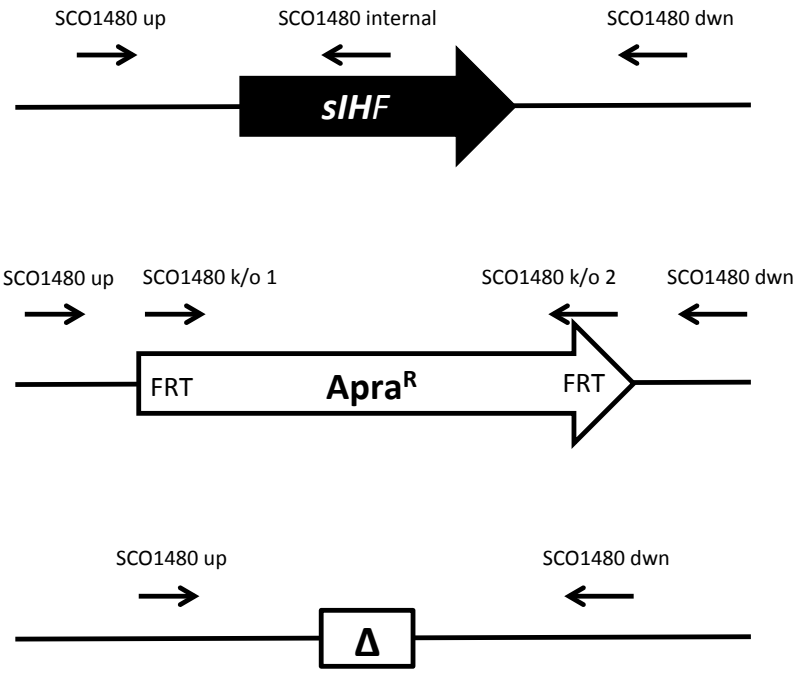

Figure 4.6 Schematic diagram of PCR checks used to confirm loss of *sIHF*. PCR primer combinations SCO1480 up and SCO1480 dwn or SCO1480 up and SCO1480 internal were used to confirm the loss of *sIHF*. The top panel shows the primer-binding sites when the wild type *sIHF* gene is present. The middle panel shows the primer-binding sites when the *sIHF* gene is replaced by the apramycin resistance cassette, which has FRT sites at each end of its sequence. The bottom panel shows the primer-binding sites when the apramycin cassette is removed. The remaining DNA fragment represents the residual FRT site following the removal of the apramycin cassette, which is initially used for creating the deletion. When *sIHF* is deleted the SCO1480 internal primer-binding site is lost and this feature can be used as a diagnostic tool to confirm the loss of *sIHF*. Additionally, replacing the *sIHF* gene with the apramycin cassette permits another set of primers (SCO1480 k/o 1 and 2) to amplify the resistance cassette. This diagram is not to scale.

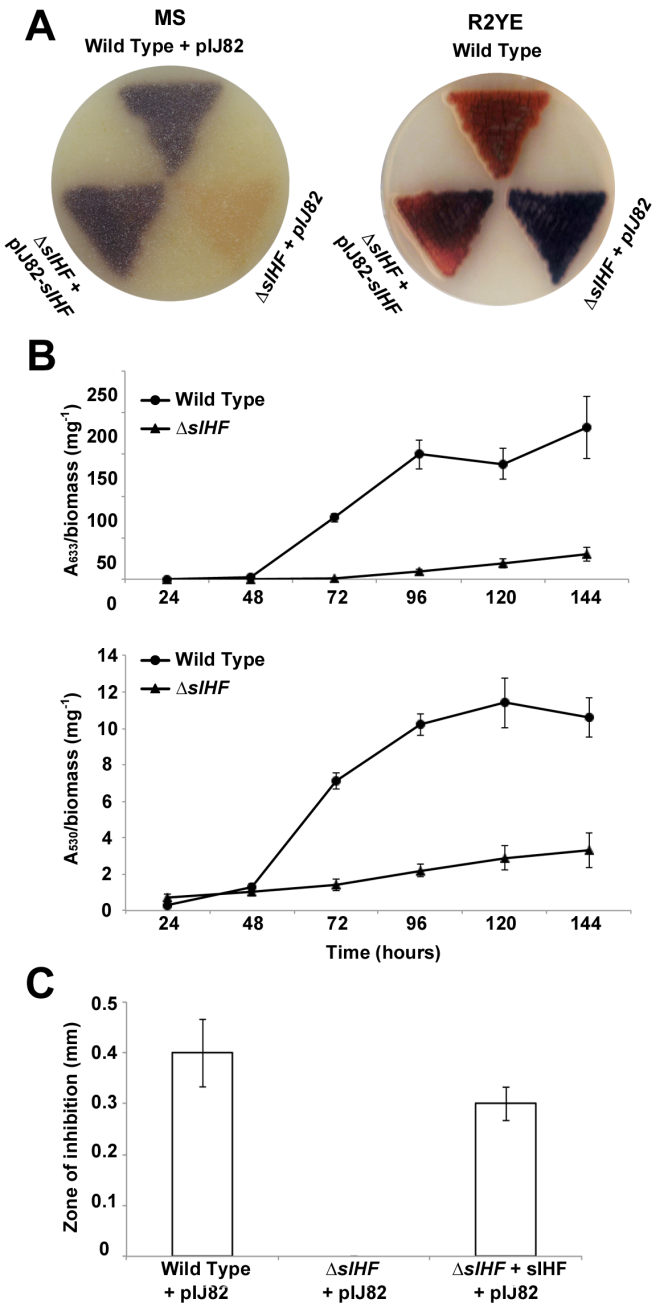

Figure 4.7 *S. coelicolor* antibiotic production in the absence of sIHF. **(A)** Plasmid-containing wild type and Δ*sIHF* in-frame deletion strains, as well as the complemented strain, were grown on MS (left) and R2YE (right) agar media for 5 and 4 days, respectively. Images were taken from the underside of each plate to effectively display antibiotic production. **(B)** Actinorhodin (top) and undecylprodigiosin (bottom) production by wild type and Δ*sIHF* strains in complex liquid YEME-TSB medium over a 6-day time course. **(C)** CDA production assay by plasmid-containing wild type and Δ*sIHF* strains, along with the complemented strain.

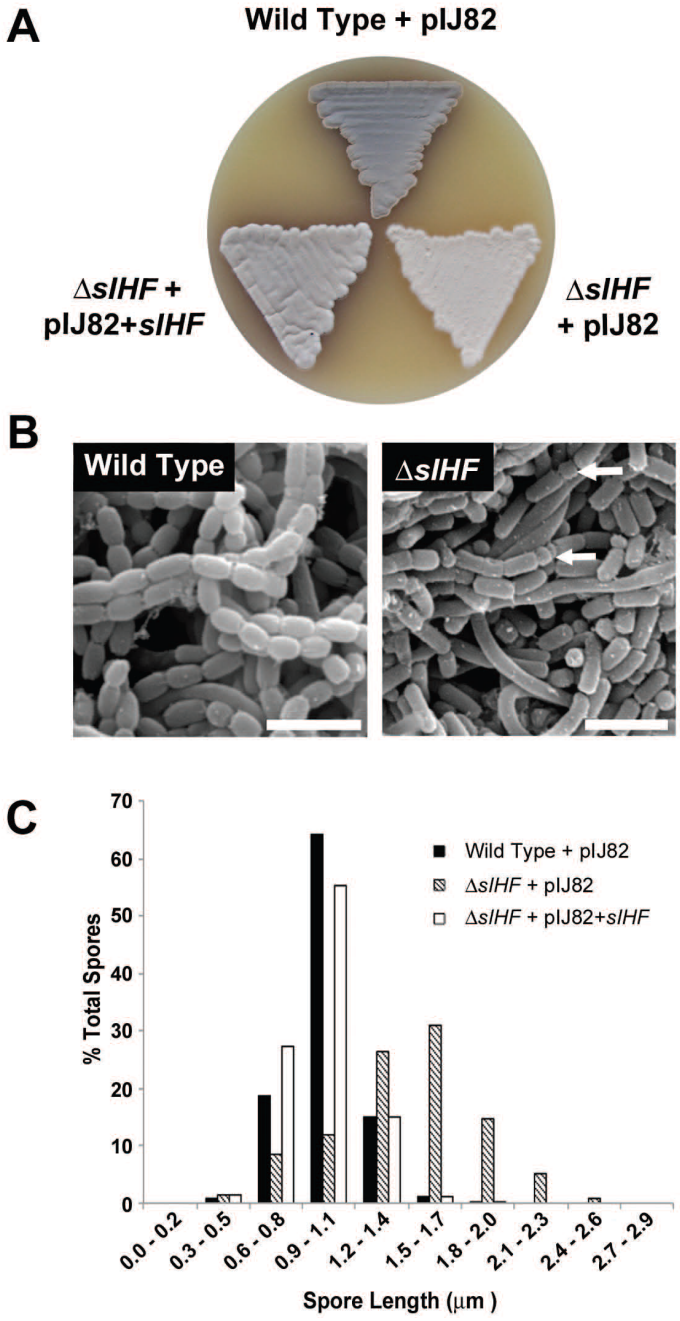

Figure 4.8 Developmental defects of the *S. coelicolor sIHF* deletion mutant. (A) Plasmid-containing wild type and Δ*sIHF* strains, together with the complementation strain, grown on MS agar medium for 5 days. **(B)** SEM images of wild type and Δ*sIHF* spores after 5 days of growths on MS agar. Scale bar represents 2.5 μm (for both images). **(C)** Comparison of spore lengths of wild type, Δ*sIHF* and complementation strains, as determined from light microscopy images. Between 1,000 and 1,100 spores were measured for each strain, and lengths were rounded to the nearest 0.1 μm.

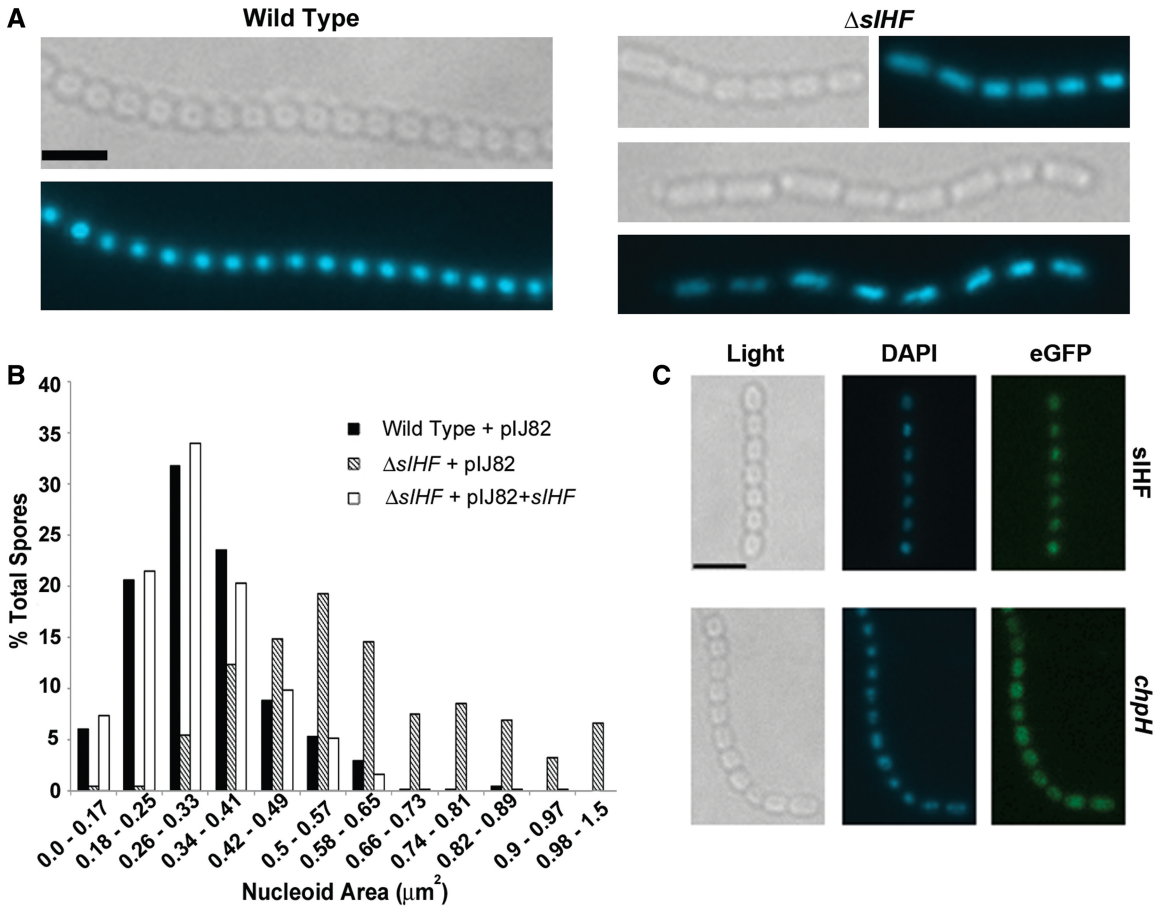

Figure 4.9 sIHF localization within spore compartments relative to chromosomal DNA. **(A)** Light and DAPI fluorescence images of wild type (left panels) and Δ*sIHF* (right panels) strains. Each image set depicts the same spore chain. The scale bar represents 2.6 μm. **(B)** Comparison of nucleoid areas for wild type, Δ*sIHF* and complemented strains, with calculated areas rounded to the nearest 0.01 mm^2. 500–600 spores were examined for each strain. **(C)** Light and fluorescence microscopy (DAPI and GFP) images of wild type spores expressing an sIHF-eGFP translational fusion (top panels) or P_{chpH}-*eGFP* transcriptional fusion (bottom panels). The DAPI panel shows chromosomal DNA localization, while the eGFP panel shows the localization of eGFP when fused to either sIHF or the *chpH* promoter. Scale bar represents 3.2 μm.

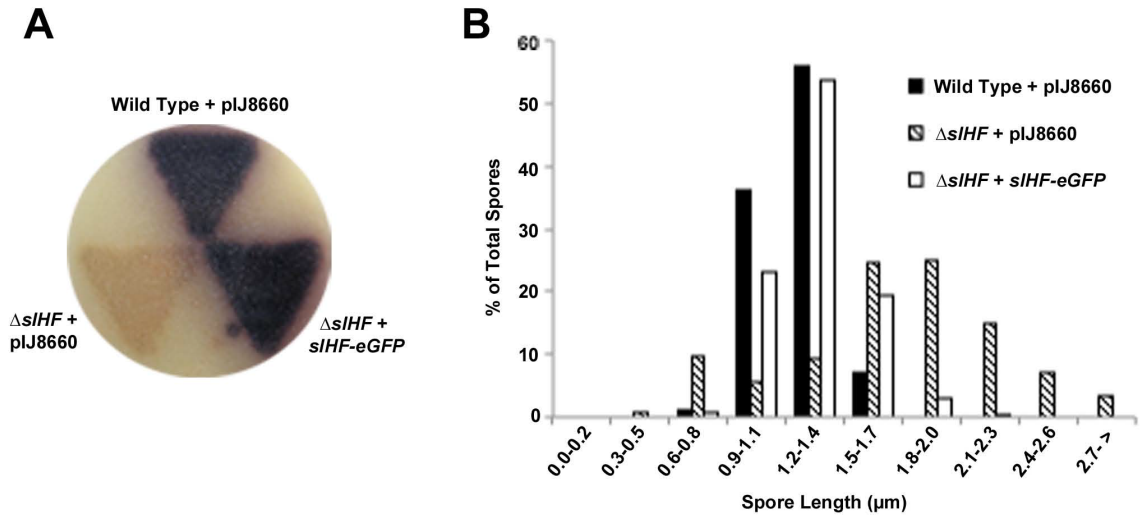

Figure 4.10 Complementation of Δ*slHF* with sIHF-eGFP. **(A)** Wild type, Δ*slHF* (both carrying pIJ8660) and the *slHF-eGFP* complementation strains grown on MS agar for 6 days. Image is taken from the underside of the plate to show the complementation of antibiotic production. **(B)** Spore length measurements of wild type, Δ*slHF* (both carrying pIJ8660) and the *slHF-eGFP* complementation strains. A total of 300 spores were measured for each strain.

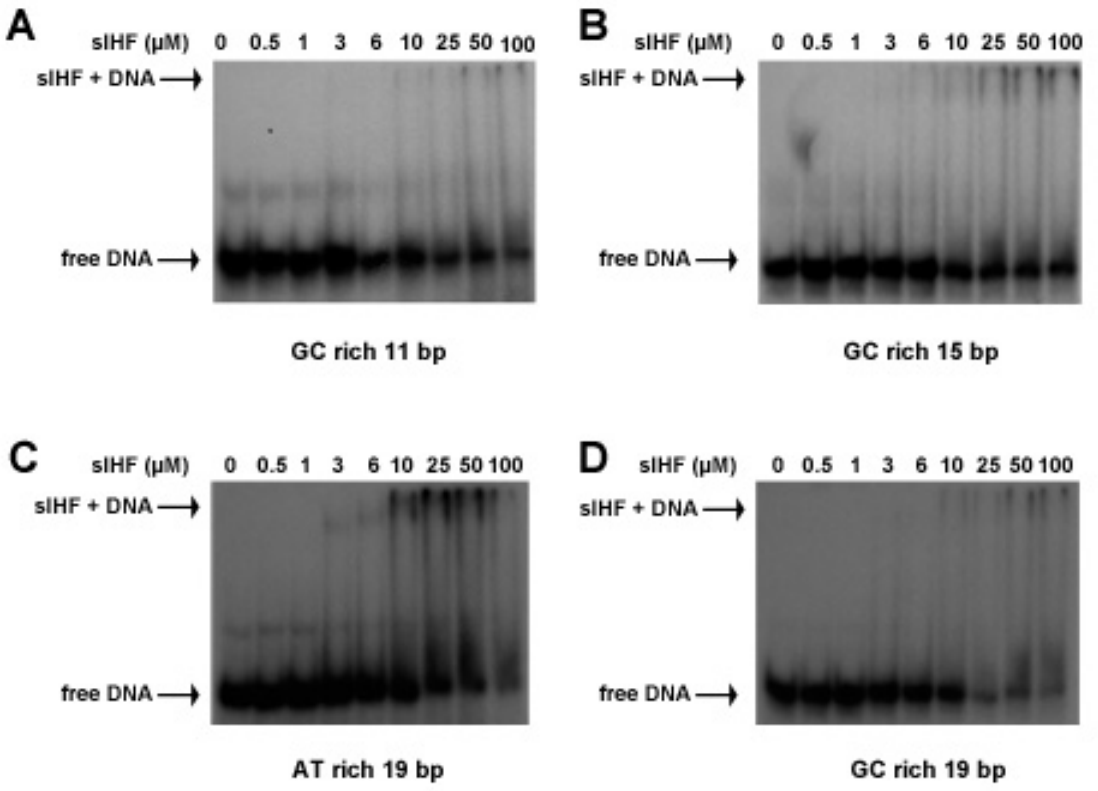

Figure 4.11 sIHF binding to hairpin DNA. EMSAs showing sIHF binding to **(A)** GC rich 11-bp, **(B)** GC rich 15-bp, **(C)** AT rich 19-bp and **(D)** GC rich 19-bp probes. Increasing concentrations of sIHF were added, as indicated, to 0.1 μM of each probe.

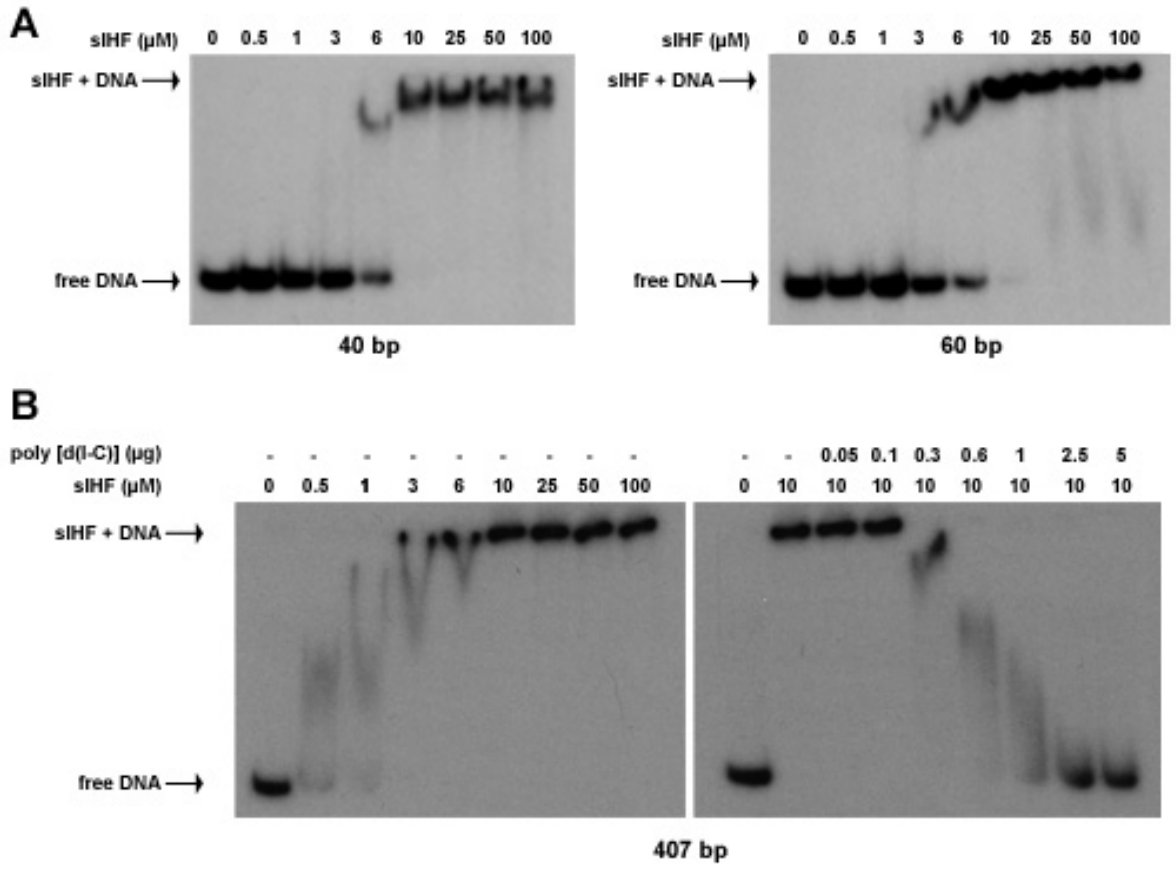

Figure 4.12 sIHF binding to DNA of increasing length. **(A)** EMSAs showing sIHF binding to probes of increasing length. Increasing concentrations of sIHF were added to the indicated DNA probes. Panels represent the binding of sIHF to a 40-bp DNA (left) and a 60-bp DNA probe (right). **(B)** EMSAs showing the binding affinity of sIHF to a 407-bp DNA probe. The left panel shows sIHF-DNA complex formation in the presence of increasing concentrations of sIHF. The right panel shows the effect of increasing poly(dI-dC) concentrations on sIHF-probe complexes.

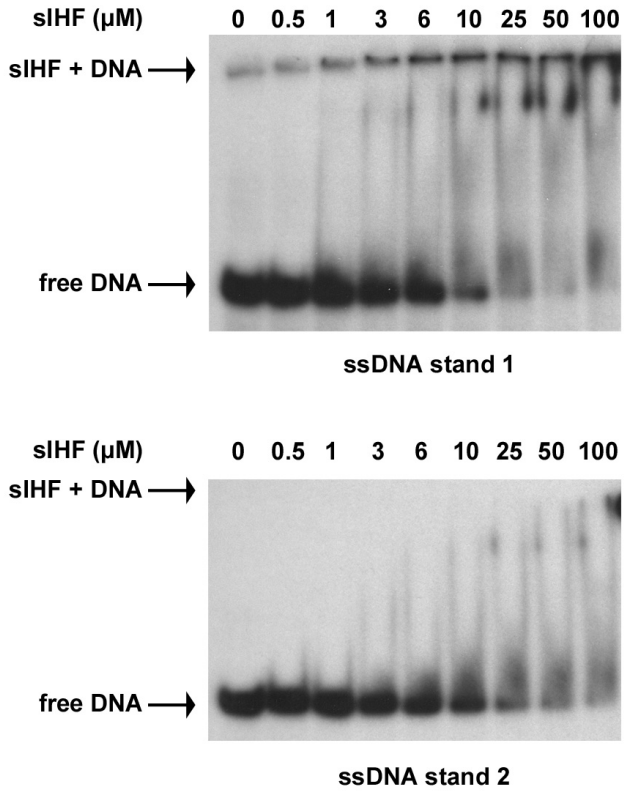

Figure 4.13 sIHF binding to ssDNA. EMSAs showing the binding affinity of sIHF to both single strands of the 60-bp dsDNA probe. Increasing concentrations of sIHF were added, as indicated, to 0.1 μM of each probe.

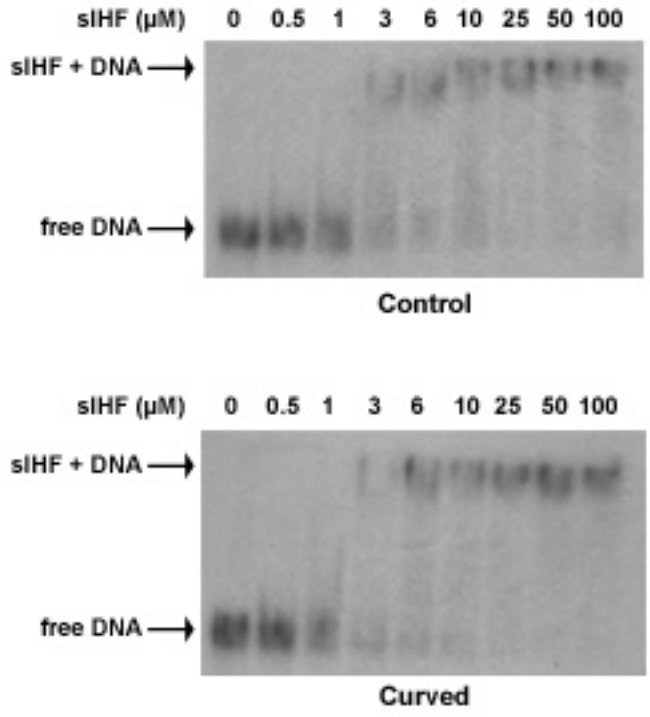

Figure 4.14 sIHF binding to curved DNA. EMSAs showing sIHF binding to curved DNA (bottom panel) as compared to non-curved control DNA (top panel). Increasing concentrations of sIHF were added, as indicated, to 0.1 μM of each probe.

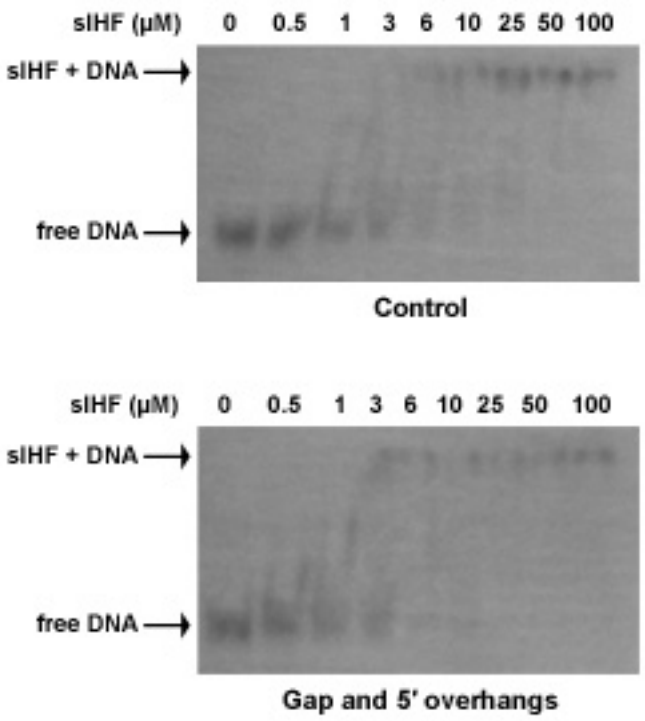

Figure 4.15 sIHF binding to DNA with a gap and 5′ overhangs. EMSAs showing sIHF binding to DNA containing a gap and 5′ overhangs (bottom panel) as compared to control DNA without a gap and 5′ overhangs (top panel). Increasing concentrations of sIHF were added, as indicated, to 0.1 μM of each probe.

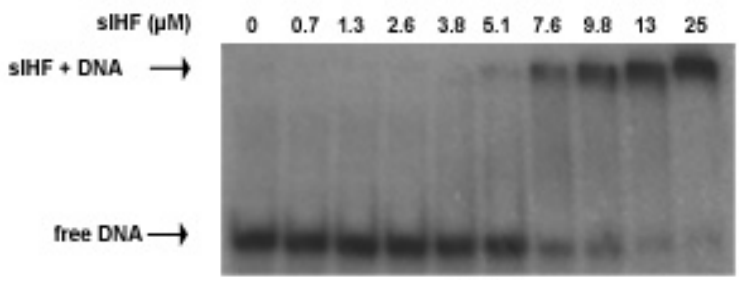

Figure 4.16 Determining sIHF concentration for SELEX via EMSA. Increasing concentrations of sIHF were added to 0.1 μM of a 40-bp probe. The lowest sIHF concentration required to shift the DNA was reduced five fold and used during SELEX rounds. The 40-bp probe was used because it was the closest to the size of the 48 bp DNA library fragments used for SELEX.

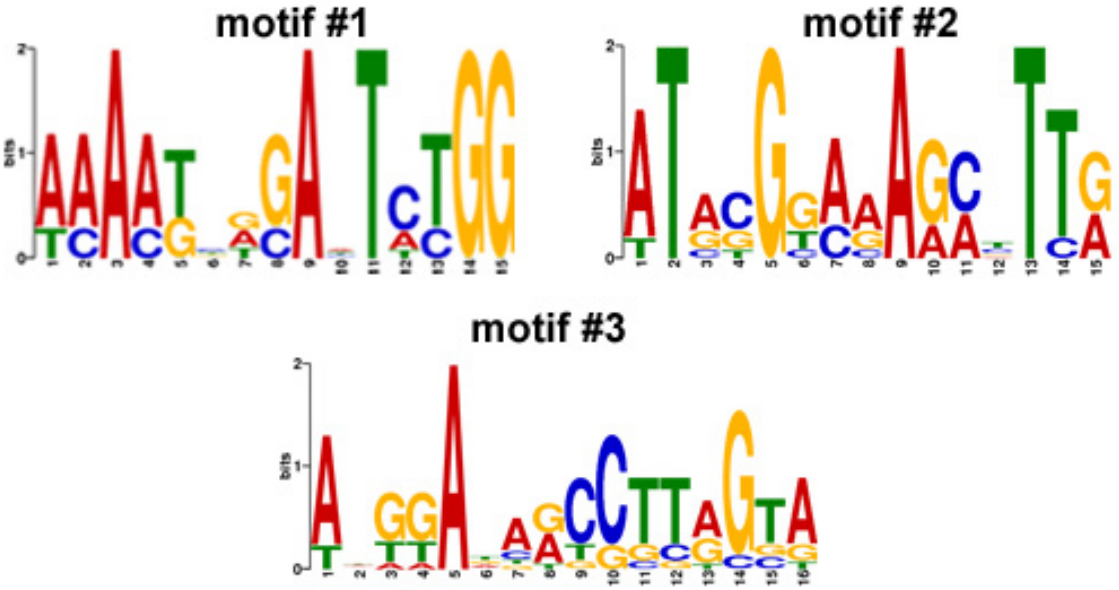

Figure 4.17 Schematic of SELEX sIHF DNA-binding motifs identified by MEME. The DNA sequences, obtained from sequencing the DNA bound by sIHF after the sixth SELEX round, were analyzed using MEME. Three DNA motifs were identified and are represented as 'sequence logos'. The height of each nucleotide represents the probability of finding it at that respective position within the sequence.

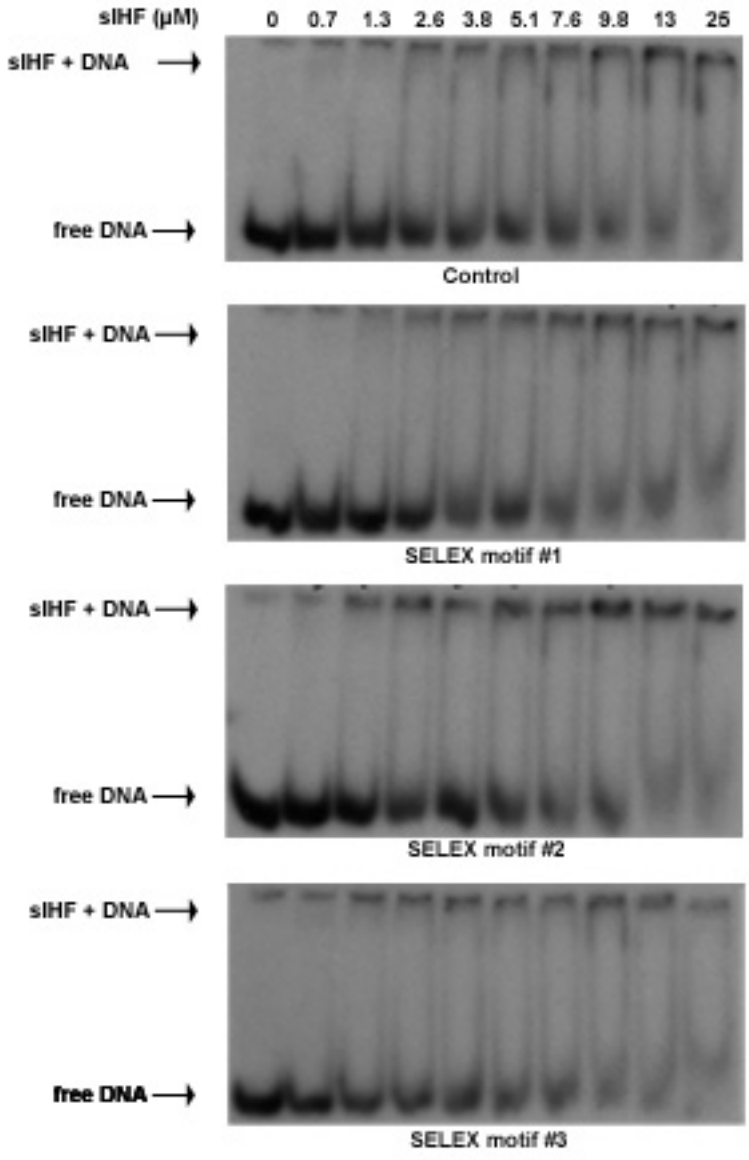

Figure 4.18 EMSAs comparing sIHF binding to SELEX DNA-binding motifs to random DNA. EMSAs showing sIHF binding to probes containing the sequences of the DNA binding motifs identified by SELEX. Increasing concentrations of sIHF were added to 0.1 μM of each probe. The probes used in each case are indicated below each panel. The control was a scrambled sequence of SELEX motif #1.

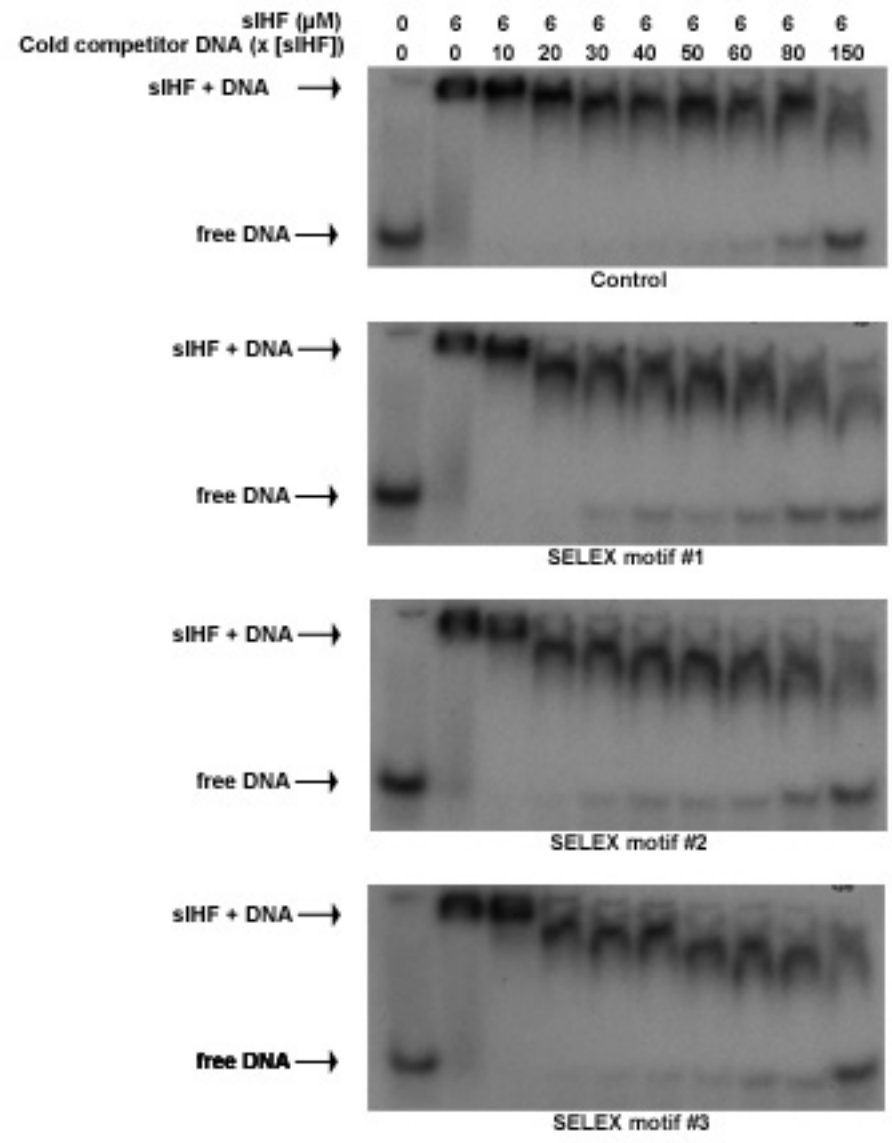

Figure 4.19 Competition EMSAs comparing sIHF preference for SELEX DNA motifs to random DNA. Increasing concentrations of control (sequence randomized) or enriched SELEX DNA binding motifs were added as competitor DNA to EMSA reactions containing constant concentrations of sIHF and 40-bp probe. The level of effective competition was determined by the loss of sIHF-DNA complex formation with the 40-bp probe and increased free DNA concentrations.

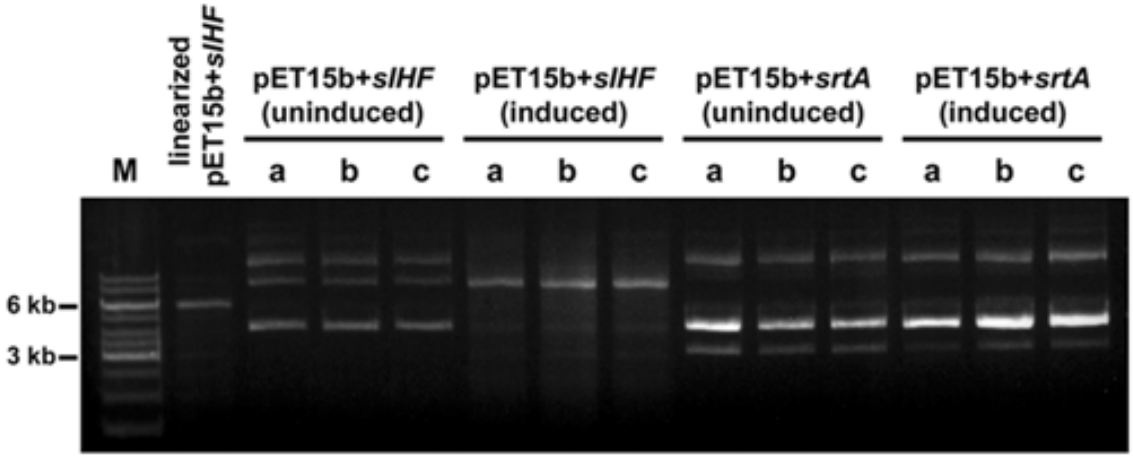

Figure 4.20 Effect of sIHF overexpression on plasmid DNA forms *ex vivo*. pET15b containing either *sIHF* (left) or *srtA* (right), isolated from *E. coli*. IPTG was added to three independent cultures (a, b and c) to induce overexpression of *sIHF* and *srtA*, while three others were grown without induction prior to plasmid harvest. For size comparison, a marker (M) was run alongside linearized (*Nde*I digested) pET15b+*sIHF*.

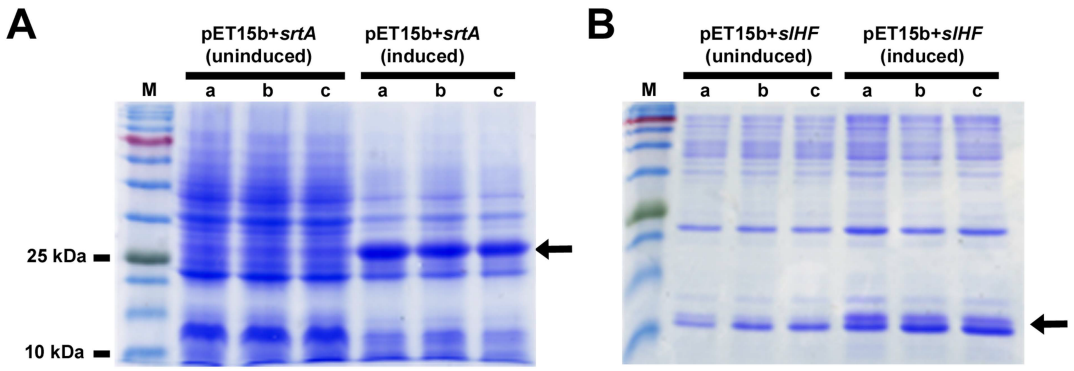

Figure 4.21 SrtA and sIHF expression post-induction. Protein extracts from cultures where SrtA or sIHF expression was either uninduced (control) or induced, were prepared 8 hours post induction. Equivalent amounts of protein extracts from three separate uninduced and induced cultures (a, b, c) were separated on polyacrylamide gels and strained with Coomassie Brilliant Blue to confirm **(A)** SrtA or **(B)** sIHF expression. Arrows indicate the protein band of interest. The first lane of each gel contains a marker (M).

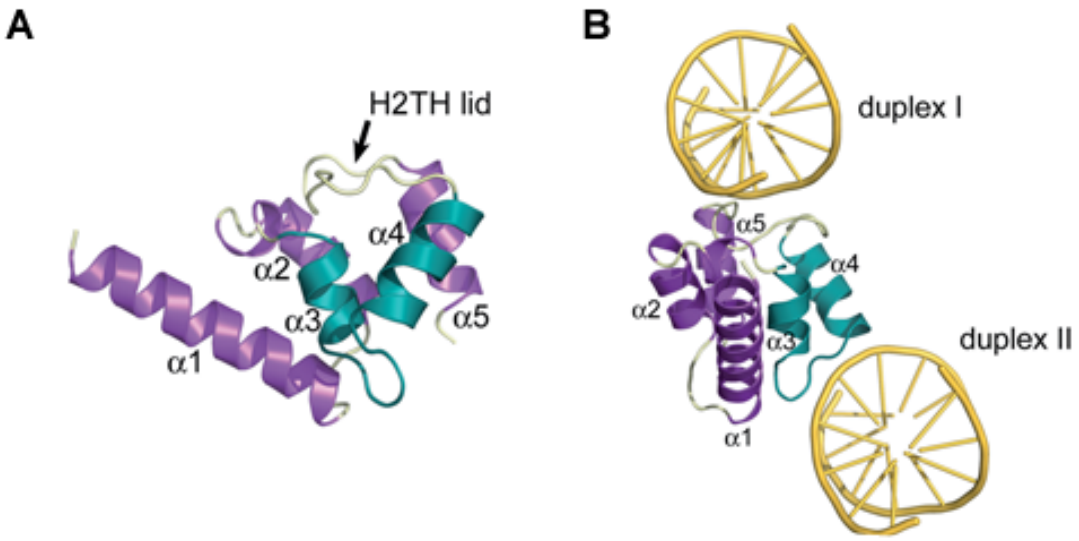

Figure 4.22 Structure of sIHF. **(A)** Ribbon diagram of sIHF with helices shown in purple, loops in cream and the H2TH motif coloured in teal. **(B)** Interaction of sIHF with neighbouring DNA molecules (shown in yellow). The view is rotated 90˚ with respect to the view in panel (A) and the two neighbouring DNA duplexes are labeled for reference.

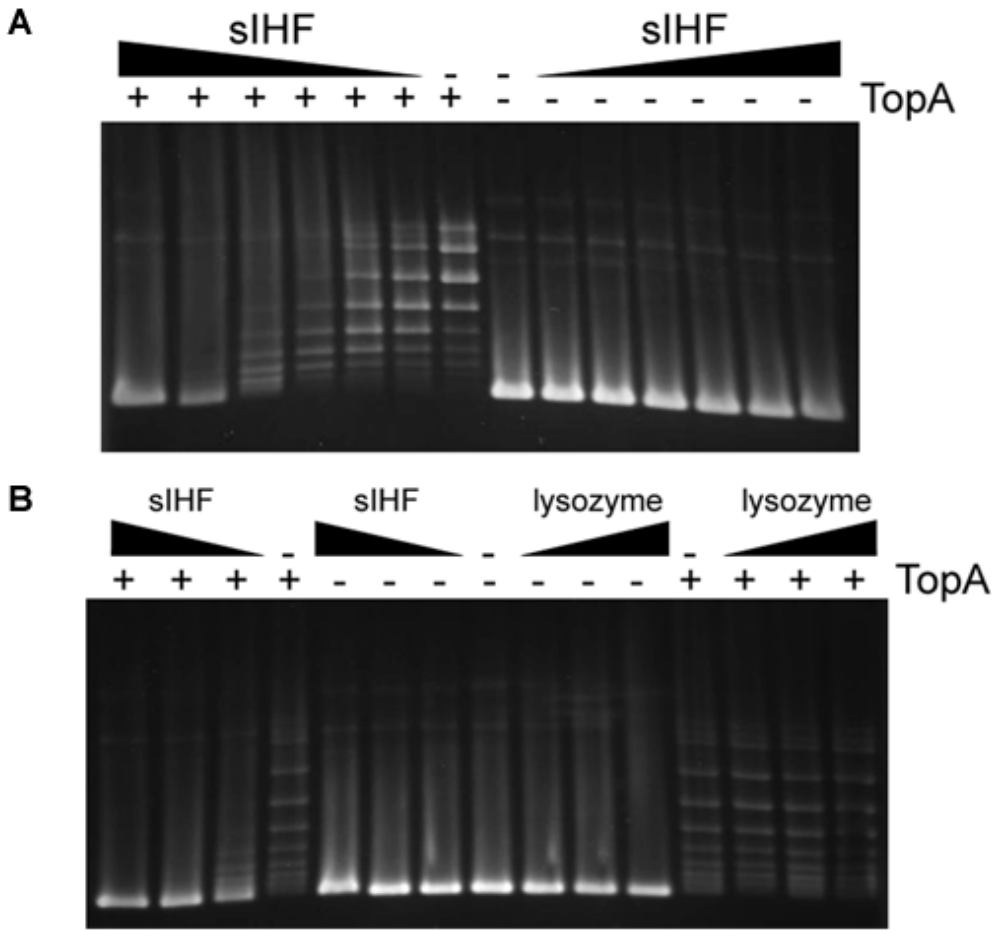

Figure 4.23 Effect of sIHF on plasmid DNA supercoiling. **(A)** The minimal amount of sIHF able to affect TopA activity was assayed by incubating supercoiled pUC19 plasmid DNA with serially diluted sIHF (1:540 to 1:17 [pUC19:sIHF] molar excess) in the presence/absence of TopA. **(B)** Supercoiled pUC19 plasmid DNA was incubated alone, or together with increasing concentrations of either sIHF or lysozyme (at 1:135, 1:270 and 1:540 [DNA:protein] molar excess), in the presence/absence of *S. coelicolor* TopA (8 µg/ml) as indicated.

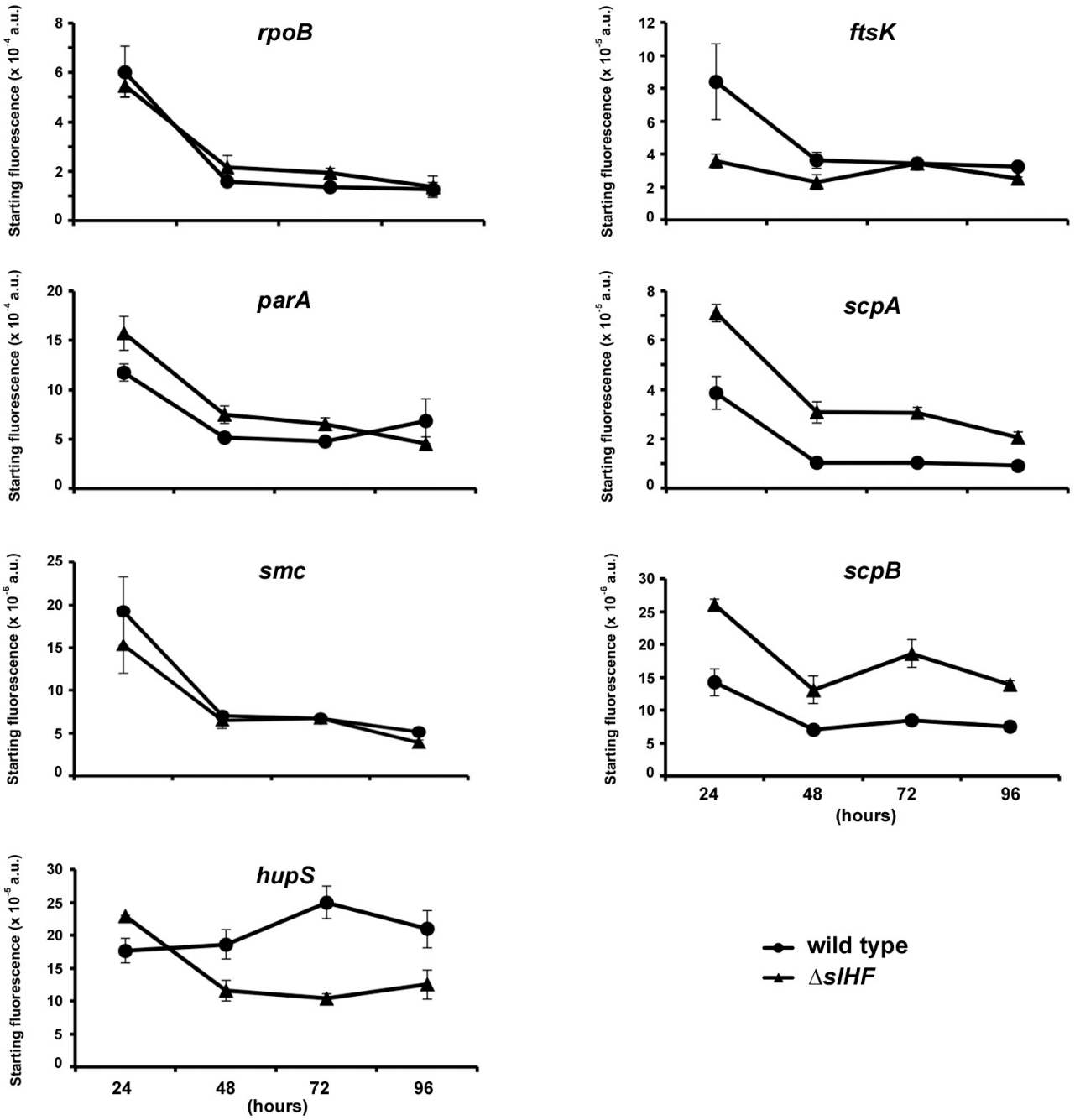

Figure 4.24 Expression of NAPs in Δ*slHF*. Comparison of the expression levels of various genes encoding proteins involved in chromosome organization in wild type and Δ*slHF* as determined by qPCR. RNA was extracted at four different timepoints throughout development (indicated in hours on x-axis). The gene under investigation is indicated above each graph. For all graphs, wild type profiles are marked with closed circles, while Δ*slHF* profiles are indicated with closed triangles.

CHAPTER 5

SUMMARY AND FUTURE DIRECTIONS

5.1 Summary of research

Small RNAs (sRNAs) are known to make important regulatory contributions to numerous cellular processes in a wide variety of bacteria (Gottesman and Storz, 2011). To investigate their importance in *Streptomyces*, we used complementary bioinformatic and experimental approaches and initially identified six novel sRNAs in *S. coelicolor*: scr1906, scr5676, scr3974, scr3558, scr3261 and scr3045 (Swiercz *et al.*, 2008). To explore the role of these sRNAs, we followed their expression throughout the *S. coelicolor* life cycle under differing growth conditions, and compared their expression in previously isolated mutants of *S. coelicolor* that exhibited impairment at different stages of morphological development. Some of the sRNAs appeared to be developmentally regulated, active only during specific stages of the life cycle, while others were constitutively expressed and may have regulatory roles in 'cellular housekeeping' processes.

Among the six sRNAs examined, one in particular, scr1906, appeared to be closely associated with development, as it was only expressed during sporulation. Notably, expression of scr1906 was completely abolished in the sporulation-defective mutant Δ*whiG*, where *whiG* encodes an alternative sigma factor (σ^{WhiG}) that is required for the early stages of sporulation. scr1906 expression was detected in mutants of both known σ^{WhiG} targets (*whiH* and *whiI* – sporulation-specific transcription factors), suggesting a novel link between an sRNA and sporulation. A connection between scr1906 and *whiH* was explored based on the sequence complementarity of scr1906 with the 5′ end of the *whiH* transcript; however, technical difficulties related to detecting cellular levels of WhiH led to this line of investigation to being abandoned.

A second focus of my research was to characterize a NAP, sIHF (SCO1480) from *S. coelicolor*. NAPs are involved in organizing bacterial chromosomes, but many have also been implicated in global gene regulation (Dillon and Dorman, 2010; Prieto *et al.*, 2011). sIHF is an actinobacterial-specific protein, and its homologue in *M. tuberculosis* (mIHF) is essential for viability (Pedulla and Hatfull, 1998). We showed that sIHF associates with the nucleoid and binds to DNA non-specifically, but in a length-dependent manner. *In vitro*, sIHF prevented DNA relaxation by topoisomerase, a function that may explain the nucleoid condensation defect observed for the Δ*sIHF* mutant. In addition, loss of sIHF impacted sporulation septa placement, resulting in aberrantly sized spores. Interestingly, the expression of genes encoding other *S. coelicolor* NAPs (namely *parA*, *scpA*, *scpB* and *hupS*) were also affected in Δ*sIHF*, suggesting that the mutant phenotype could also stem from perturbations in the levels of these proteins. In addition to morphological defects, deletion of *sIHF* also led to abnormal antibiotic biosynthesis, which was not entirely surprising as developmental mutants of *S. coelicolor* often exhibit altered secondary metabolite production (Champness, 1988; Pope *et al.*, 1996; Champness and Chater, 1994).

5.2 Context and foundation for future work

5.2.1 Small RNAs in *S. coelicolor*

Since our initial search for sRNAs in *S. coelicolor*, our group has analyzed the transcriptome of three *Streptomyces* species using RNA-Seq (Moody *et al.*, submitted). This work has led to the discovery of hundreds of predicted sRNAs and provided further insight into scr1906. Intriguingly, the scr1906 region also appears to represent a 5′ untranslated region (UTR) of the downstream gene, *SCO1905* (Figure 3.7). *SCO1905* encodes a hypothetical protein and is organized in an operon with *SCO1904*, encoding a putative transcriptional regulator (Figure 3.1B). Interestingly, a recent study showed that two 5′ untranslated regions not only controlled the expression of their downstream genes, but also functioned *in trans* to act as sRNAs in *Listera monocytogenes* (Loh *et al.*, 2009). Future analysis of the *SCO1905* 5′ UTR could provide insight into the expression and regulation of this two-gene operon, its connection to sporulation and its association with a developmentally controlled sRNA (scr1906).

5.2.2 The role of sIHF in *Streptomyces*

5.2.2.1 Establishing sIHF connections to other nucleoid-associated proteins

The chromosome segregation and condensation defects seen in Δ*sIHF* are reminiscent of *S. coelicolor* NAP mutant phenotypes. Like Δ*sIHF*, deletion of *parA* and/or *parB*, individually or together, produces significantly more anucleate spore compartments than wild type (Kim *et al.*, 2000). This has also been observed for *smc* and *scpA/B* mutants (Kois *et al.*, 2009). The Δ*sIHF* chromosome condensation defect is one shared with *hupS*, *smc* and *scpA/B* mutants (Kois *et al.*, 2009; Salerno *et al.*, 2009). A decrease in grey spore-associated pigment, as seen for the Δ*sIHF* mutant, has also been reported for Δ*hupS* (Salerno *et al.*, 2009). These shared mutant phenotypes suggest that sIHF may be defective in the same or similar pathways as proteins involved in chromosome segregation and condensation and, therefore, indicate that sIHF is involved in these processes. Alternatively, the observed differences in the expression levels of NAP-encoding genes in the Δ*sIHF* mutant strain, as compared to wild type (Figure 4.24), suggest that the resulting collective changes in NAP levels could contribute to the Δ*sIHF* phenotype.

To probe the direct cause of the Δ*sIHF* phenotype, the effects of deleting *sIHF* in conjunction with other NAPs should be assessed. There are multiple possible phenotypic outcomes for creating double deletion mutants, including: an additive effect, a synergistic effect or no effect. Additionally, a double mutant may not be possible to create because it could be lethal. If the double deletion mutant has a frequency of anucleate spore compartments that is additive to what is observed in each individual deletion strain, it will suggest that sIHF is involved in a different pathway responsible for proper DNA segregation during sporulation. Alternatively, a frequency of anucleate spores in the double mutant that is more severe than each individual deletion strain is suggestive of a synergistic effect. This has been observed in a double mutant of *smc* and *parB*, where the number of anucleate spore

compartments was significantly greater in the double mutant than would have been expected from an additive effect of the single mutant (Dedrick *et al.*, 2009). The connection between SMC and ParB has not been determined. Another possibility is that the frequency of anucleate spore compartments between the two strains is comparable. This is the case for a strain lacking both *parB* and *ftsK* (Dedrick *et al.*, 2009), indicating that the double mutant is able to segregate DNA just as well as the most defective single mutant. If this is the case with sIHF, it is conceivable that sIHF functions in the same pathway as the other deleted chromosome organizing protein(s). Given the importance of chromosome segregation to future spore viability, it seems likely that redundant mechanisms may exist in the cell to ensure effective segregation is accomplished. This is supported by observations when *parA* and *parB*, which encode the major components of the only known partitioning apparatus in *S. coelicolor*, are deleted. If no other pathways were involved in chromosome segregation it would be expected that the Δ*parAB* mutant would have a severe defect in chromosome segregation. In contrast, only 11.7% more spores in the double deletion strain are anucleate, as compared to wild type (Kim *et al.*, 2000), indicating that another segregation system must be functional.

In addition to determining the influence that each NAP has on anucleate spore frequency in the presence/absence of sIHF, the effect of each mutation on chromosome condensation could also be assessed. Changes to nucleoid compaction can be assessed in a similar manner as above. Additionally, the effects of restoring the expression levels of condensation proteins that are reduced in Δ*sIHF* (Figure 4.24) could be analyzed. For example, *hupS* levels are significantly lower in Δ*sIHF* as compared to wild type (Figure 4.24), and thus it is possible that the DNA condensation defects seen for the Δ*sIHF* mutant stem from low HupS levels. To test this, *hupS* expression could be increased in Δ*sIHF* to test whether chromosome compaction is restored.

5.2.2.2 Understanding the DNA binding preferences for sIHF

Most characterized bacterial NAPs bind to specific DNA sequences, whether these are consensus sequences, sequences with a particular GC-bias or DNA with a defined structure (discussed in Chapter 4). For example, consensus sequences have been identified for IHF and Lrp (Hales *et al.*, 1994; Cui *et al.*, 1995; Nou *et al.*, 1995), whereas HU preferentially binds to DNA with gaps and nicks (Balandina *et al.*, 2002; Swinger and Rice, 2007) Additionally, H-NS and Fis bind AT-rich DNA sequences (Kahramanoglou *et al.*, 2011).

In the case of sIHF, our initial studies revealed that sIHF prefers dsDNA to ssDNA; however, no binding preferences were found for the other tested DNA forms. Three DNA binding sequences were enriched for sIHF binding during SELEX. Competition EMSAs were used to confirm that sIHF bound to these sequences preferably to control randomized DNA sequences. Future work will involve characterizing the interaction between sIHF and these binding motifs to identify why they are preferred. This will involve protein-DNA complex interaction studies, discussed later, and examining sequence-specific features, such as minor groove widths.

It is possible that sIHF DNA binding preferences change *in vivo*, where possible interactions between sIHF and other cytoplasmic proteins could influence the chromosomal sites bound by sIHF. To determine the *in vivo* DNA-binding characteristics of sIHF, chromatin-immunoprecipitation sequencing (ChIP-Seq) could be performed. This method has successfully identified *in vivo* binding regions and consensus sequences for numerous NAPs, such as Lrp (Cui *et al.*, 1995) and EspR, a NAP encoded by *M. tuberculosis* (Blasco *et al.*, 2012). sIHF binding sites from ChIP-Seq data could then be mapped to the *S. coelicolor* genome and reveal if sIHF, like many other NAPs, such as Fis and H-NS (Grainger *et al.*, 2006; Kahramanoglou *et al.*, 2011), preferentially binds within noncoding regions (promoter regions), where it would have the potential to exert considerable transcriptional regulatory effects. The data obtained from ChIP-Seq-type experiments could also be mined in an effort to determine whether it has any sequence or conformational bias in its chromosome association.

In addition to further investigating the binding specificity of sIHF, it will be of particular interest to correlate *in vivo* sIHF binding sites with changes in global gene expression. A similar approach has already been taken for *E. coli* IHF and HU NAPs (Prieto *et al.*, 2011), which revealed that of the 30% of operons bound by IHF, a third of these displayed changes in expression in the absence of IHF. Such an approach would help to reveal the complete inventory of *S. coelicolor* genes whose expression depends on sIHF activity. To accomplish this, microarray analysis or RNA sequencing could be performed using RNA extracted from cultures grown under the same conditions as for the ChIP-Seq experiments (described above). This will allow correlations to be made between sIHF binding sites and changes in transcription between wild type and the Δ*sIHF* mutant. If sIHF binds to regulatory regions and affects the expression of downstream genes/operons, it would suggest that sIHF may directly control the transcription of these genetic loci. Alternatively, if there is no to low correlation between binding sites and global transcriptional changes it may indicate that changes in global gene expression are an indirect effect of losing sIHF activity and are likely due to rearrangements in nucleoid topology that cause promoter regions to be more/less accessible.

5.2.2.3 Characterizing the role of sIHF and its connection with topoisomerase

sIHF negatively impacts the activity of TopA (the sole topoisomerase I in *S. coelicolor*) *in vitro*; however, there is still much that remains unclear about this relationship. sIHF binds to DNA, but it is not known whether it also interacts directly with TopA to inhibit DNA relaxation. An initial B2H assay investigating the potential interaction between sIHF and TopA did not support such an interaction; however, the assay has not yet been reproduced. Additionally, a lack of an interaction during a B2H assay does not necessarily prove that no interaction occurs; therefore, other methods are needed to unequivocally answer this question. This could include directly testing of purified TopA and sIHF, by determining if complexes of these proteins co-elute following fractionation on a sizing column. A lack of co-elution may suggest that the proteins do not interact or it may mean that their interaction requires the presence of DNA. To account for the latter possibility, DNA could also be included in the reaction.

To study the functional link between sIHF and TopA, the effects of depleting TopA (a *topA* null mutation is lethal) in Δ*sIHF* could be analyzed. If Δ*sIHF* exhibits reduced nucleoid compaction due to increased levels of DNA relaxation by TopA, then a decrease in TopA activity in an Δ*sIHF* mutant should suppress the mutant phenotype, restoring wild type levels of nucleoid compaction. It will be interesting to determine whether such suppression impacts the expression of *hupS*, *scpA* and *scpB*. If the expression of these genes were sensitive to supercoiling, restoring nucleoid compaction to wild type levels would also restore expression of these genes. In contrast, if the supercoil status of the chromosome did not affect the expression of these genes, restoring nucleoid compaction would not have an effect, but may indicate that their expression is directly dependent on sIHF.

The helical core of sIHF is in the primary DNA binding determinant and the function of the N-terminal α-helix is not currently understood. Thus far, we know that the N-terminal α-helix comprises approximately one third of the sIHF sequence, does not make contacts with DNA, protrudes from the more compact core structure (Figure 4.22) and is highly conserved (Figures 4.1, 4.2 and 4.3). This would suggest that the N-terminal helix has an important function, likely independent of DNA binding. This region could interact with TopA or with another protein. Testing the effects of N-terminal truncations would reveal whether it is critical for sIHF function. These N-terminal truncated mutants could be tested for their ability to bind DNA, their capacity to inhibit TopA activity and for their ability to complement an *sIHF* deletion. We do not anticipate that an N-terminal truncation would impact DNA binding, largely because this region does not associate with DNA; however, this sequence may influence the overall structure of the protein, and such alterations could be detrimental for sIHF activity. It is also conceivable that sIHF interacts with other proteins. To identify any potential sIHF-interacting proteins in *S. coelicolor*, we can take advantage of a yeast-two-hybrid library that is available in our lab. Potential interactions would be validated using purified proteins, subjected to co-crystallization, and interacting domains mapped using mutagenesis with the two hybrid system.

5.2.3 sIHF long-term goals

The overall long-term goal is to develop a thorough understanding of how sIHF contributes to nucleoid topology and global gene regulation, and how these affect DNA segregation and condensation. Since sIHF is conserved in the actinomycetes (Figure 4.2), the information from this model can be applied towards understanding these processes within this group of bacteria. It will be interesting to correlate sIHF function to its essential nature in *Mycobacteria* (Pedulla and Hatfull, 1998) and potentially other actinomycetes. Additionally, given that mIHF is essential for mycobacterial viability, understanding how it acts could provide the basis for future drug development, as there is considerable interest in more targeted therapies. Since m/sIHF is not found in all bacteria, targeting it would be not detrimental to the rest of an individual's native microflora, which would reduce potential side effects.

Another intriguing avenue of future study involves elucidating the connection between sIHF and antibiotic production. The Δ*sIHF* mutant exhibits drastic changes in antibiotic production, as compared to wild type. Recently, it has been determined that the metabolite profile of the Δ*sIHF* mutant is vastly different compared to wild type (E. Carlson, personal communication), suggesting that the changes upon losing sIHF function are more drastic than simply altering the production of the three antibiotics we investigated here. It will be fascinating to further investigate the changes in metabolite profiles of other actinomycetes lacking sIHF function. It is possible that global changes in transcription or nucleoid topology when sIHF is lost could result in the activation of cryptic clusters, and could provide a promising new strategy for identifying novel metabolites with medical significance.

REFERENCES

Abramoff, M. D., P. J. Magalhaes & S. J. Ram, (2004) Image processing with ImageJ. *Biophotonics International* **11**: 33–42.

Adams, D. W. & J. Errington, (2009) Bacterial cell division: assembly, maintenance and disassembly of the Z ring. *Nat Rev Microbiol* **7**: 642–653.

Aeling, K. A., M. L. Opel, N. R. Steffen, V. Tretyachenko-Ladokhina, G. W. Hatfield, R. H. Lathrop & D. F. Senear, (2006) Indirect recognition in sequence-specific DNA binding by *Escherichia coli* integration host factor: the role of DNA deformation energy. *J Biol Chem* **281**: 39236–39248.

Aínsa, J. A., H. D Parry & K. F. Chater, (1999) A response regulator-like protein that functions at an intermediate stage of sporulation in *Streptomyces coelicolor* A3 (2). *Mol Microbiol* **34**: 607–619.

Almirón, M., A. J. Link, D. Furlong & R. Kolter, (1992) A novel DNA-binding protein with regulatory and protective roles in starved *Escherichia coli. Genes Dev* **6**: 2646–2654.

Altuvia, S., D. Weinstein-Fischer, A. Zhang, L. Postow & G. Storz, (1997) A small, stable RNA induced by oxidative stress: role as a pleiotropic regulator and antimutator. *Cell* **90**: 43–53.

Atrih, A. & S. J. Foster, (1999) The role of peptidoglycan structure and structural dynamics during endospore dormancy and germination. *Antonie Van Leeuwenhoek* **75**: 299–307.

Ausmees, N., H. Wahlstedt, S. Bagchi, M. A. Elliot, M. J. Buttner & K. Flärdh, (2007) SmeA, a small membrane protein with multiple functions in *Streptomyces* sporulation including targeting of a SpoIIIE/FtsK-like protein to cell division septa. *Mol Microbiol* **65**: 1458–1473.

Babitzke, P. & T. Romeo, (2007) CsrB sRNA family: sequestration of RNA-binding regulatory proteins. *Curr Opin Microbiol* **10**: 156–163.

Bailey, T. L. & C. Elkan, (1994) Fitting a mixture model by expectation maximization to discover motifs in biopolymers. *Proc Int Conf Intell Syst Mol Biol* **2**: 28–36.

Balandina, A., D. Kamashev & J. Rouvière-Yaniv, (2002) The bacterial histone-like protein HU specifically recognizes similar structures in all nucleic acids. *J Biol Chem* **277**: 27622–27628.

Barry, C. E., S. F. Hayes & T. Hackstadt, (1992) Nucleoid condensation in *Escherichia coli* that express a chlamydial histone homolog. *Science* **256**: 377–379.

Bennett, J. A., R. M. Aimino & J. R. McCormick, (2007) *Streptomyces coelicolor* genes *ftsL* and *divIC* play a role in cell division but are dispensable for colony formation. *J Bacteriol* **189**: 8982–8992.

Bennett, J. A., J. Yarnall, A. B. Cadwallader, R. Kuennen, P. Bidey, B. Stadelmaier & J. R. McCormick, (2009) Medium-dependent phenotypes of *Streptomyces coelicolor* with mutations in *ftsI* or *ftsW*. *J Bacteriol* **191**: 661–664.

Bensaid, A., A. Almeida, K. Drlica & J. Rouvière-Yaniv, (1996) Cross-talk between topoisomerase I and HU in *Escherichia coli*. *J Mol Bacteriol* **256**: 292–300.

Bentley, S. D., K. F. Chater, A. M. Cerdeño-Tárraga, G. L. Challis, N. R. Thomson, K. D. James, D. E. Harris, M. A. Quail, H. Kieser, D. Harper, A. Bateman, S. Brown, G. Chandra, C. W. Chen, M. Collins, A. Cronin, A. Fraser, A. Goble, J. Hidalgo, T. Hornsby, S. Howarth, C. H. Huang, T. Kieser, L. Larke, L. Murphy, K. Oliver, S. O'Neil, E. Rabbinowitsch, M. A. Rajandream, K. Rutherford, S. Rutter, K. Seeger, D. Saunders, S. Sharp, R. Squares, S. Squares, K. Taylor, T. Warren, A. Wietzorrek, J. Woodward, B. G. Barrell, J. Parkhill & D. A. Hopwood, (2002) Complete genome sequence of the model actinomycete *Streptomyces coelicolor* A3(2). *Nature* **417**: 141–147.

Bérdy, J., (2005) Bioactive microbial metabolites. *J Antibiot* **58**: 1–26.

Bernhardt, T. G. & P. A. J. de Boer, (2005) SlmA, a nucleoid-associated, FtsZ binding protein required for blocking septal ring assembly over chromosomes in *E. coli*. *Mol Cell* **18**: 555–564.

Bibb, M. J., R. F. Freeman & D. A. Hopwood, (1977) Physical and genetical characterisation of a second sex factor, SCP2, for *Streptomyces coelicolor* A3 (2). *Mol Gen Genet* **154**: 155–166.

Bibb, M. J. & D. A. Hopwood, (1981) Genetic studies of the fertility plasmid SCP2 and its SCP2* variants in *Streptomyces coelicolor* A3 (2). *J Gen Microbiol* **126**: 427–442.

Bibb, M. J., J. White, J. M. Ward & G. R. Janssen, (1994) The mRNA for the 23S rRNA methylase encoded by the *ermE* gene of *Saccharopolyspora erythraea* is translated in the absence of a conventional ribosome-binding site. *Mol Microbiol* **14**: 533–545.

Blasco, B., J. M. Chen, R. Hartkoorn, C. Sala, S. Uplekar, J. Rougemont, F. Pojer & S. T. Cole, (2012) Virulence regulator EspR of *Mycobacterium tuberculosis* is a nucleoid-associated protein. *PLoS Pathog* **8**: e1002621.

Botta, G. A. & J. T. Park, (1981) Evidence for involvement of penicillin-binding protein 3 in murein synthesis during septation but not during cell elongation. *J Bacteriol* **145**: 333–340.

Breaker, R. R., (2012) Riboswitches and the RNA world. *Cold Spring Harb Perspect Biol* **4**: 1–15.

Brodersen, D. E., W. M. Clemons Jr., A. P. Carter, B. T. Wimberly & V. Ramakrishnan, (2002) Crystal structure of the 30 S ribosomal subunit from *Thermus thermophilus*: structure of the proteins and their interactions with 16 S RNA. *J Mol Biol* **316**: 725–768.

Buddelmeijer, N. & J. Beckwith, (2002a) Assembly of cell division proteins at the *E. coli* cell center. *Curr Opin Microbiol* **5**: 553–557.

Buddelmeijer, N., N. Judson, D. Boyd, J. J. Mekalanos & J. Beckwith, (2002b) YgbQ, a cell division protein in *Escherichia coli* and *Vibrio cholerae*, localizes in codependent fashion with FtsL to the division site. *Proc Natl Acad Sci USA* **99**: 6316–6321.

Byrgazov, K., O. Vesper & I. Moll, (2013) Ribosome heterogeneity: another level of complexity in bacterial translation regulation. *Curr Opin Microbiol* **16**: 133–139.

Capstick, D. S., J. M. Willey, M. J. Buttner & M. A. Elliot, (2007) SapB and the chaplins: connections between morphogenetic proteins in *Streptomyces coelicolor*. *Mol Microbiol* **64**: 602–613.

Carballido-López, R. & J. Errington, (2003) The bacterial cytoskeleton: *in vivo* dynamics of the actin-like protein Mbl of *Bacillus subtilis*. *Dev Cell* **4**: 19–28.

Castaing, B., C. Zelwer, J. Laval & S. Boiteux, (1995) HU protein of *Escherichia coli* binds specifically to DNA that contains single-strand breaks or gaps. *J Biol Chem* **270**: 10291–10296.

Cerdeño-Tárraga, A. M., A. Efstratiou, L. G. Dover, M. T. G. Holden, M. Pallen, S. D. Bentley, G. S. Besra, C. Churcher, K. D. James, A. De Zoysa, T. Chillingworth, A. Cronin, L. Dowd, T. Feltwell, N. Hamlin, S. Holroyd, K. Jagels, S. Moule, M. A. Quail, E. Rabbinowitsch, K. M. Rutherford, N. R. Thomson, L. Unwin, S. Whitehead, B. G. Barrell & J. Parkhill, (2003) The complete genome sequence and analysis of *Corynebacterium diphtheriae* NCTC13129. *Nucleic Acids Res* **31**: 6516–6523.

Chakraburtty, R. & M. J. Bibb, (1997) The ppGpp synthetase gene (*relA*) of *Streptomyces coelicolor* A3(2) plays a conditional role in antibiotic production and morphological differentiation. *J Bacteriol* **179**: 5854–5861.

Challis, G. L. & D. A. Hopwood, (2003) Synergy and contingency as driving forces for the evolution of multiple secondary metabolite production by *Streptomyces* species. *Proc Natl Acad Sci USA* **100**: 14555–14561.

Champness, W. C., (1988) New loci required for *Streptomyces coelicolor* morphological and physiological differentiation. *J Bacteriol* **170**: 1168–1174.

Champness, W. C. & K. F. Chater, (1994) Regulation and integration of antibiotic production and morphological differentiation in *Streptomyces* spp. In: Regulation of Bacterial Development. P. J. Piggot, C. P. Moran & P. Youngman (eds.) Washington, D.

C.: American Society for Microbiology, pp. 61-93

Champoux, J. J., (2001) DNA topoisomerases: structure, function, and mechanism. *Annu Rev Biochem* **70**: 369–413.

Chater, K. F., (1993) Genetics of differentiation in *Streptomyces*. *Annu Rev Microbiol* **47**: 685–713.

Chater, K. F., (2001) Regulation of sporulation in *Streptomyces coelicolor* A3 (2): a checkpoint multiplex? *Curr Opin Microbiol* **4**: 667–673.

Chater, K. F., C. J. Bruton, K. A. Plaskitt, M. J. Buttner, C. Mendez & J. D. Helmann, (1989) The developmental fate of *S. coelicolor* hyphae depends upon a gene product homologous with the motility σ factor of *B. subtilis*. *Cell* **59**: 133–143.

Chen, J. M., H. Ren, J. E. Shaw, Y. J. Wang, M. Li, A. S. Leung, V. Tran, N. M. Berbenetz, D. Kocíncová, C. M. Yip, J. M. Reyrat & J. Liu, (2008) Lsr2 of *Mycobacterium tuberculosis* is a DNA-bridging protein. *Nucleic Acids Res* **36**: 2123–2135.

Cherepanov, P. P. & W. Wackernagel, (1995) Gene disruption in *Escherichia coli*: Tc^R and Km^R cassettes with the option of Flp-catalyzed excision of the antibiotic-resistance determinant. *Gene* **158**: 9–14.

Cho, B., E. M. Knight, C. L. Barrett & B. Ø. Palsson, (2008) Genome-wide analysis of Fis binding in *Escherichia coli* indicates a causative role for A-/AT-tracts. *Genome Res* **18**: 900–910.

Chong, P. P., S. M. Podmore, H. M. Kieser, M. Redenbach, K. Turgay, M. Marahiel, D. A. Hopwood & C. P. Smith, (1998) Physical identification of a chromosomal locus encoding biosynthetic genes for the lipopeptide calcium-dependent antibiotic (CDA) of *Streptomyces coelicolor* A3 (2). *Microbiol* **144**: 193–199.

Christiansen, J. K., J. S. Nielsen, T. Ebersbach, P. Valentin-Hansen, L. Søgaard-Andersen & B. H. Kallipolitis, (2006) Identification of small Hfq-binding RNAs in *Listeria monocytogenes*. *RNA* **12**: 1383–1396.

Claessen, D., W. de Jong, L. Dijkhuizen & H. A. B Wösten, (2006) Regulation of *Streptomyces* development: reach for the sky! *Trends Microbiol* **14**: 313–319.

Clegg, R. M., (1992) Fluorescence resonance energy transfer and nucleic acids. *Meth Enzymol* **211**: 353–388.

Cole, S. T., R. Brosch, J. Parkhill, T. Garnier, C. Churcher, D. Harris, S. V. Gordon, K. Eiglmeier, S. Gas, C. E. Barry III, F. Tekaia, K. Badcock, D. Basham, D. Brown, T. Chillingworth, R. Connor, R. Davies, K. Devlin, T. Feltwell, S. Gentles, N. Hamlin, S. Holroyd, T. Hornsby, K. Jagels, A. Krogh, J. McLean, S. Moule, L. Murphy, K. Oliver, J. Osbourne, M. A. Quail, M. A. Rajandream, J. Rogers, S. Rutter, K. Seeger, J. Skelton, R.

Squares, S. Squares, J. E. Sulston, K. Taylor, S. Whitehead & G. Barrell, (1998) Deciphering the biology of *Mycobacterium tuberculosis* from the complete genome sequence. *Nature* **393**: 537–544.

Corbett, K. D. & J. M. Berger, (2003) Structure of the topoisomerase VI-B subunit: implications for type II topoisomerase mechanism and evolution. *EMBO J* **22**: 151–163.

Cui, Y., Q. Wang, G. D. Stormo & J. M. Calvo, (1995) A consensus sequence for binding of Lrp to DNA. *J Bacteriol* **177**: 4872–4880.

Daniel, R. A., A. M. Williams & J. Errington, (1996) A complex four-gene operon containing essential cell division gene *pbpB* in *Bacillus subtilis*. *J Bacteriol* **178**: 2343–2350.

Datsenko, K. A. & B. L. Wanner, (2000) One-step inactivation of chromosomal genes in *Escherichia coli* K-12 using PCR products. *Proc Natl Acad Sci USA* **97**: 6640–6645.

Datta, P., A. Dasgupta, S. Bhakta & J. Basu, (2002) Interaction between FtsZ and FtsW of *Mycobacterium tuberculosis*. *J Biol Chem* **277**: 24983–24987.

Datta, P., A. Dasgupta, A. K. Singh, P. Mukherjee, M. Kundu & J. Basu, (2006) Interaction between FtsW and penicillin-binding protein 3 (PBP3) directs PBP3 to mid-cell, controls cell septation and mediates the formation of a trimeric complex involving FtsZ, FtsW and PBP3 in mycobacteria. *Mol Microbiol* **62**: 1655–1673.

Davis, N. K. & K. F. Chater, (1990) Spore colour in *Streptomyces coelicolor* A3(2) involves the developmentally regulated synthesis of a compound biosynthetically related to polyketide antibiotics. *Mol Microbiol* **4**: 1679–1691.

Davis, N. K. & K. F. Chater, (1992) The *Streptomyces coelicolor whiB* gene encodes a small transcription factor-like protein dispensable for growth but essential for sporulation. *Mol Gen Genet* **232**: 351–358.

de los Rios, S. & J. J. Perona, (2007) Structure of the *Escherichia coli* leucine-responsive regulatory protein Lrp reveals a novel octameric assembly. *J Mol Biol* **366**: 1589–1602.

Dedrick, R. M., H. Wildschutte & J. R. McCormick, (2009) Genetic interactions of *smc*, *ftsK*, and *parB* genes in *Streptomyces coelicolor* and their developmental genome segregation phenotypes. *J Bacteriol* **191**: 320–332.

Del Sol, R., J. G. L. Mullins, N. Grantcharova, K. Flärdh & P. Dyson, (2006) Influence of CrgA on assembly of the cell division protein FtsZ during development of *Streptomyces coelicolor*. *J Bacteriol* **188**: 1540–1550.

Del Sol, R., A. Pitman, P. Herron & P. Dyson, (2003) The product of a developmental

gene, *crgA*, that coordinates reproductive growth in *Streptomyces* belongs to a novel family of small actinomycete-specific proteins. *J Bacteriol* **185**: 6678–6685.

Dillon, S. C. & C. J. Dorman, (2010) Bacterial nucleoid-associated proteins, nucleoid structure and gene expression. *Nat Rev Microbiol* **8**: 185–195.

Ditkowski, B., P. Troć, K. Ginda, M. Donczew, K. F. Chater, J. Zakrzewska-Czerwińska & D. Jakimowicz, (2010) The actinobacterial signature protein ParJ (SCO1662) regulates ParA polymerization and affects chromosome segregation and cell division during *Streptomyces* sporulation. *Mol Microbiol* **78**: 1403–1415.

Dorman, C. J., (2013) Co-operative roles for DNA supercoiling and nucleoid-associated proteins in the regulation of bacterial transcription. *Biochem Soc Trans* **41**: 542–547.

Dorman, C. J. & P. Deighan, (2003) Regulation of gene expression by histone-like proteins in bacteria. *Curr Opin Genet Dev* **13**: 179–184.

Duong, A., D. S. Capstick, C. Di Berardo, K. C. Findlay, A. Hesketh, H. Hong & M. A. Elliot, (2012) Aerial development in *Streptomyces coelicolor* requires sortase activity. *Mol Microbiol* **83**: 992–1005.

Eccleston, M., R. A. Ali, R. Seyler, J. Westpheling & J. R. Nodwell, (2002) Structural and genetic analysis of the BldB protein of *Streptomyces coelicolor*. *J Bacteriol* **184**: 4270–4276.

Eccleston, M., A. Willems, A. Beveridge & J. R. Nodwell, (2006) Critical residues and novel effects of overexpression of the *Streptomyces coelicolor* developmental protein BldB: evidence for a critical interacting partner. *J Bacteriol* **188**: 8189–8195.

Elliot, M. A., M. J. Buttner & J. R. Nodwell, (2008) Multicellular development in *Streptomyces*. In: Myxobacteria: Multicellularity and differentiation. D. E. Whitworth (ed). Washington, D. C.: American Society for Microbiology Press, pp. 419-438.

Elliot, M. A., N. Karoonuthaisiri, J. Huang, M. J. Bibb, S. N. Cohen, C. M. Kao & M. J. Buttner, (2003) The chaplins: a family of hydrophobic cell-surface proteins involved in aerial mycelium formation in *Streptomyces coelicolor*. *Genes Dev* **17**: 1727–1740.

Elliot, M. A. & N. J. Talbot, (2004) Building filaments in the air: aerial morphogenesis in bacteria and fungi. *Curr Opin Microbiol* **7**: 594–601.

Enoch, D. A., J. M. Bygott, M. Daly & J. A. Karas, (2007) Daptomycin. *J Infect* **55**: 205–213.

Errington, J., R. A. Daniel & D. Scheffers, (2003) Cytokinesis in bacteria. *Microbiol Mol Biol Rev* **67**: 52–65

Facey, P. D., M. D. Hitchings, P. Saavedra-Garcia, L. Fernandez-Martinez, P. J. Dyson & R. Del Sol, (2009) *Streptomyces coelicolor* Dps-like proteins: differential dual roles in response to stress during vegetative growth and in nucleoid condensation during reproductive cell division. *Mol Microbiol* **73**: 1186–1202.

Fender, A., J. Elf, K. Hampel, B. Zimmermann & E. G. H. Wagner, (2010) RNAs actively cycle on the Sm-like protein Hfq. *Genes Dev* **24**: 2621–2626.

Flärdh, K., (2003a) Essential role of DivIVA in polar growth and morphogenesis in *Streptomyces coelicolor* A3(2). *Mol Microbiol* **49**: 1523–1536.

Flärdh, K., (2003b) Growth polarity and cell division in *Streptomyces*. *Curr Opin Microbiol* **6**: 564–571.

Flärdh, K., K. C. Findlay & K. F. Chater, (1999) Association of early sporulation genes with suggested developmental decision points in *Streptomyces coelicolor* A3(2). *Microbiol* **145**: 2229–2243.

Flärdh, K., E. Leibovitz, M. J. Buttner & K. F. Chater, (2000) Generation of a non-sporulating strain of *Streptomyces coelicolor* A3(2) by the manipulation of a developmentally controlled *ftsZ* promoter. *Mol Microbiol* **38**: 737–749.

Fogel, M. A. & M. K. Waldor, (2006) A dynamic, mitotic-like mechanism for bacterial chromosome segregation. *Genes Dev* **20**: 3269–3282.

Frenkiel-Krispin, D., I. Ben-Avraham, J. Englander, E. Shimoni, S. G. Wolf & A. Minsky, (2004) Nucleoid restructuring in stationary-state bacteria. *Mol Microbiol* **51**: 395–405.

Fromme, J. C. & G. L. Verdine, (2002) Structural insights into lesion recognition and repair by the bacterial 8-oxoguanine DNA glycosylase MutM. *Nat Struct Biol* **9**: 544–552.

Gama-Castro, S., V. Jiménez-Jacinto, M. Peralta-Gil, A. Santos-Zavaleta, M. I. Peñaloza-Spinola, B. Contreras-Moreira, J. Segura-Salazar, L. Muñiz-Rascado, I. Martínez-Flores, H. Salgado, C. Bonavides-Martínez, C. Abreu-Goodger, C. Rodríguez-Penagos, J. Miranda-Ríos, E. Morett, E. Merino, A. M. Huerta, L. Treviño-Quintanilla & J. Collado-Vides, (2008) RegulonDB (version 6.0): gene regulation model of *Escherichia coli* K-12 beyond transcription, active (experimental) annotated promoters and Textpresso navigation. *Nucleic Acids Res* **36**: D120–124.

Gilboa, R., D. O. Zharkov, G. Golan, A. S. Fernandes, S. E. Gerchman, E. Matz, J. H. Kycia, A. P. Grollman & G. Shoham, (2002) Structure of formamidopyrimidine-DNA glycosylase covalently complexed to DNA. *J Biol Chem* **277**: 19811–19816.

Gonzalez, M. D., E. A. Akbay, D. Boyd & J. Beckwith, (2010) Multiple interaction domains in FtsL, a protein component of the widely conserved bacterial FtsLBQ cell

division complex. *J Bacteriol* **192**: 2757–2768.

Goodfellow, M. & S. T. Williams, (1983) Ecology of actinomycetes. *Annu Rev Microbiol* **37**: 189–216.

Gordon, B. R. G., Y. Li, A. Cote, M. T. Weirauch, P. Ding, T. R. Hughes, W. W. Navarre, B. Xia & J. Liu, (2011) Structural basis for recognition of AT-rich DNA by unrelated xenogeneic silencing proteins. *Proc Natl Acad Sci USA* **108**: 10690–10695.

Gottesman, S., (2005) Micros for microbes: non-coding regulatory RNAs in bacteria. *Trends Genet* **21**: 399–404.

Gottesman, S. & G. Storz, (2011) Bacterial small RNA regulators: versatile roles and rapidly evolving variations. *Cold Spring Harb Perspect Biol* **3**: 1–16.

Grainger, D. C., D. Hurd, M. D. Goldberg & S. J. W. Busby, (2006) Association of nucleoid proteins with coding and non-coding segments of the *Escherichia coli* genome. *Nucleic Acids Res* **34**: 4642–4652.

Grantcharova, N., U. Lustig & K. Flärdh, (2005) Dynamics of FtsZ assembly during sporulation in *Streptomyces coelicolor* A3(2). *J Bacteriol* **187**: 3227–3237.

Graumann, P. L., (2000) *Bacillus subtilis* SMC is required for proper arrangement of the chromosome and for efficient segregation of replication termini but not for bipolar movement of newly duplicated origin regions. *J Bacteriol* **182**: 6463–6471.

Gregory, M. A., R. Till & M. C. Smith, (2003) Integration site for *Streptomyces* phage φBT1 and development of site-specific integrating vectors. *J Bacteriol* **185**: 5320–5323.

Grill, S., C. O. Gualerzi, P. Londei & U. Bläsi, (2000) Selective stimulation of translation of leaderless mRNA by initiation factor 2: evolutionary implications for translation. *EMBO J* **19**: 4101–4110.

Guo, F. & S. Adhya, (2007) Spiral structure of *Escherichia coli* HUαβ provides foundation for DNA supercoiling. *Proc Natl Acad Sci USA* **104**: 4309–4314.

Gust, B., G. L. Challis, K. Fowler, T. Kieser & K. F. Chater, (2003) PCR-targeted *Streptomyces* gene replacement identifies a protein domain needed for biosynthesis of the sesquiterpene soil odor geosmin. *Proc Natl Acad Sci USA* **100**: 1541–1546.

Guzman, L. M., J. J. Barondess & J. Beckwith, (1992) FtsL, an essential cytoplasmic membrane protein involved in cell division in *Escherichia coli*. *J Bacteriol* **174**: 7716–7728.

Haiser, H. J., F. V. Karginov, G. J. Hannon & M. A. Elliot, (2008) Developmentally regulated cleavage of tRNAs in the bacterium *Streptomyces coelicolor*. *Nucleic Acids*

Res **36**: 732–741.

Haiser, H. J., M. R. Yousef & M. A. Elliot, (2009) Cell wall hydrolases affect germination, vegetative growth, and sporulation in *Streptomyces coelicolor*. *J Bacteriol* **191**: 6501–6512.

Hales, L. M., R. I. Gumport & J. F. Gardner, (1994) Determining the DNA sequence elements required for binding integration host factor to two different target sites. *J Bacteriol* **176**: 2999–3006.

Hanahan, D., (1983) Studies on transformation of *Escherichia coli* with plasmids. *J Mol Biol* **166**: 557–580.

Haneishi, T., A. Terahara, M. Arai, T. Hata & C. Tamura, (1974) New antibiotics, methylenomycins A and B. *J Antibiot* **27**: 393–399.

Harz, C. O., (1877) Ueber eine neue Pilzkrankheit beim Rinde *Centralbl Med Wissensch* **15**: 481–485.

Hempel, A. M., S. Cantlay, V. Molle, S. B. Wang, M. J. Naldrett, J. L. Parker, D. M. Richards, Y. G. Jung, M. J. Buttner & K. Flärdh, (2012) The Ser/Thr protein kinase AfsK regulates polar growth and hyphal branching in the filamentous bacteria *Streptomyces*. *Proc Natl Acad Sci USA* **109**: e2371–2379.

Henriques, A. O., P. Glaser, P. J. Piggot & C. P. Moran, (1998) Control of cell shape and elongation by the *rodA* gene in *Bacillus subtilis*. *Mol Microbiol* **28**: 235–247.

Hillisch, A., M. Lorenz & S. Diekmann, (2001) Recent advances in FRET: distance determination in protein-DNA complexes. *Curr Opin Struct Biol* **11**: 201–207.

Hindra, P. Pak & M. A. Elliot, (2010) Regulation of a novel gene cluster involved in secondary metabolite production in *Streptomyces coelicolor*. *J Bacteriol* **192**: 4973–4982.

Hirano, T., (1998) SMC protein complexes and higher-order chromosome dynamics. *Curr Opin Cell Biol* **10**: 317–322.

Ho, T. F., C. J. Ma, C. H. Lu, Y. T. Tsai, Y. H. Wei, J. S. Chang, J. K. Lai, P. J. Cheuh, C. T. Yeh, P. C. Tang, J. T. Chang, J. L. Ko, F. S. Liu, H. E. Yen & C. C. Chang, (2007) Undecylprodigiosin selectively induces apoptosis in human breast carcinoma cells independent of p53. *Toxicol Appl Pharmacol* **225**: 318–328.

Hong, H. J., M. I. Hutchings, J. M. Neu, G. D. Wright, M. S. B. Paget & M. J. Buttner, (2004) Characterization of an inducible vancomycin resistance system in *Streptomyces coelicolor* reveals a novel gene (*vanK*) required for drug resistance. *Mol Microbiol* **52**: 1107–1121.

Hopkins, J. F., S. Panja & S. A. Woodson, (2011) Rapid binding and release of Hfq from ternary complexes during RNA annealing. *Nucleic Acids Res* **39**: 5193–5202.

Hopp, T. P., K. S. Prickett, V. L Price, R. T. Libby, C. J. March, D. P. Cerretti, D. L. Urdal & P. J. Conlon, (1988) A short polypeptide marker sequence useful for recombinant protein identification and purification. *Biotechnol* **6**: 1204–1210.

Hopwood, D. A., (1999) Forty years of genetics with *Streptomyces*: from *in vivo* through *in vitro* to *in silico*. *Microbiol* **145**: 2183–2202.

Hopwood, D. A., (2007a) *Streptomyces in nature and medicine: the antibiotic makers*. Oxford University Press, Oxford; New York.

Hopwood, D. A., (2007b) Therapeutic treasures from the deep. *Nat Chem Biol* **3**: 457–458.

Hopwood, D. A., M. J. Bibb, K. F. Chater, T. Kieser, C. J. Bruton, H. M. Kieser, D. J. Lydiate, C. P. Smith, J. M. Ward & H. Schrempf, (1985) Genetic manipulation of *Streptomyces* - A laboratory manual, Norwich, U. K.: The John Innes Foundation.

Hopwood, D. A., K. F. Chater & M. J. Bibb, (1995) Genetics of antibiotic production in *Streptomyces coelicolor* A3(2), a model streptomycete. *Biotechnol* **28**: 65–102.

Huang, J., J. Shi, V. Molle, B. Sohlberg, D. Weaver, M. J. Bibb, N. Karoonuthaisiri, C. J . Lih, C. M. Kao, M. J. Buttner & S. N. Cohen, (2005) Cross-regulation among disparate antibiotic biosynthetic pathways of *Streptomyces coelicolor*. *Mol Microbiol* **58**: 1276–1287.

Hwang, W., V. Arluison & S. Hohng, (2011) Dynamic competition of DsrA and *rpoS* fragments for the proximal binding site of Hfq as a means for efficient annealing. *Nucleic Acids Res* **39**: 5131–5139.

Itoh, T. & J. Tomizawa, (1980) Formation of an RNA primer for initiation of replication of ColE1 DNA by ribonuclease H. *Proc Natl Acad Sci USA* **77**: 2450–2454.

Iyer, L. M., K. S. Makarova, E. V. Koonin & L. Aravind, (2004) Comparative genomics of the FtsK-HerA superfamily of pumping ATPases: implications for the origins of chromosome segregation, cell division and viral capsid packaging. *Nucleic Acids Res* **32**: 5260–5279.

Jakimowicz, D., K. Chater & J. Zakrzewska-Czerwínska, (2002) The ParB protein of *Streptomyces coelicolor* A3(2) recognizes a cluster of *parS* sequences within the origin-proximal region of the linear chromosome. *Mol Microbiol* **45**: 1365–1377.

Jakimowicz, D., S. Mouz, J. Zakrzewska-Czerwińska & K. F. Chater, (2006) Developmental control of a *parAB* promoter leads to formation of sporulation-associated ParB complexes in *Streptomyces coelicolor*. *J Bacteriol* **188**: 1710–1720.

Jakimowicz, D., P. Żydek, A. Kois, J. Zakrzewska-Czerwińska & K. F. Chater, (2007) Alignment of multiple chromosomes along helical ParA scaffolding in sporulating *Streptomyces* hyphae. *Mol Microbiol* **65**: 625–641.

Janssen, G. R. & M. J. Bibb, (1993) Derivatives of pUC18 that have *Bgl*II sites flanking a modified multiple cloning site and that retain the ability to identify recombinant clones by visual screening of *Escherichia coli* colonies. *Gene* **124**: 133–134.

Janssen, G. R., J. M. Ward & M. J. Bibb, (1989) Unusual transcriptional and translational features of the aminoglycoside phosphotransferase gene (*aph*) from *Streptomyces fradiae*. *Genes Dev* **3**: 415–429.

Jones, D., H. J. Metzger, A. Schatz & S. A. Waksman, (1944) Control of gram-negative bacteria in experimental animals by streptomycin. *Science* **100**: 103–105.

Kaberdin, V. R. & U. Bläsi, (2006) Translation initiation and the fate of bacterial mRNAs. *FEMS Microbiol Rev* **30**: 967–979.

Kaberdina, A. C., W. Szaflarski, K. H. Nierhaus & I. Moll, (2009) An unexpected type of ribosomes induced by kasugamycin: a look into ancestral times of protein synthesis? *Mol Cell* **33**: 227–236.

Kahramanoglou, C., A. S. N. Seshasayee, A. I. Prieto, D. Ibberson, S. Schmidt, J. Zimmermann, V. Benes, G. M. Fraser & N. M. Luscombe, (2011) Direct and indirect effects of H-NS and Fis on global gene expression control in *Escherichia coli. Nucleic Acids Res* **39**: 2073–2091.

Kaiser, B. K. & B. L. Stoddard, (2011) DNA recognition and transcriptional regulation by the WhiA sporulation factor. *Sci Rep* **1**: 1–9.

Kalodimos, C. G., N. Biris, A. M. J. J. Bonvin, M. M. Levandoski, M. Guennuegues, R. Boelens & R. Kaptein, (2004) Structure and flexibility adaptation in nonspecific and specific protein-DNA complexes. *Science* **305**: 386–389.

Kalodimos, C. G., A. M. J. J. Bonvin, R. K. Salinas, R. Wechselberger, R. Boelens & R. Kaptein, (2002) Plasticity in protein-DNA recognition: *lac* repressor interacts with its natural operator *O1* through alternative conformations of its DNA-binding domain. *EMBO J* **21**: 2866–2876.

Kalodimos, C. G., G. E. Folkers, R. Boelens & R. Kaptein, (2001) Strong DNA binding by covalently linked dimeric Lac headpiece: evidence for the crucial role of the hinge helices. *Proc Natl Acad Sci USA* **98**: 6039–6044.

Kamashev, D., A. Balandina & J. Rouvière-Yaniv, (1999) The binding motif recognized by HU on both nicked and cruciform DNA. *EMBO J* **18**: 5434–5444.

Kamashev, D. & J. Rouvière-Yaniv, (2000) The histone-like protein HU binds

specifically to DNA recombination and repair intermediates. *EMBO J* **19**: 6527–6535.

Kang, S. G., W. Jin, M. Bibb & K. J. Lee, (1998) Actinorhodin and undecylprodigiosin production in wild-type and *relA* mutant strains of *Streptomyces coelicolor* A3(2) grown in continuous culture. *FEMS Microbiol Lett* **168**: 221–226.

Kar, S., R. Edgar & S. Adhya, (2005) Nucleoid remodeling by an altered HU protein: reorganization of the transcription program. *Proc Natl Acad Sci USA* **102**: 16397–16402.

Karimova, G., N. Dautin & D. Ladant, (2005) Interaction network among *Escherichia coli* membrane proteins involved in cell division as revealed by bacterial two-hybrid analysis. *J Bacteriol* **187**: 2233–2243.

Karimova, G., J. Pidoux, A. Ullmann & D. Ladant, (1998) A bacterial two-hybrid system based on a reconstituted signal transduction pathway. *Proc Natl Acad Sci USA* **95**: 5752–5756.

Keijser, B. J., E. E. Noens, B. Kraal, H. K. Koerten & G. P. Wezel, (2003) The *Streptomyces coelicolor ssgB* gene is required for early stages of sporulation. *FEMS Microbiol Lett* **225**: 59–67.

Kelemen, G. H., P. Brian, K. Flärdh, L. Chamberlin, K. F. Chater & M. J. Buttner, (1998) Developmental regulation of transcription of *whiE*, a locus specifying the polyketide spore pigment in *Streptomyces coelicolor* A3 (2). *J Bacteriol* **180**: 2515–2521.

Kelemen, G. H. & M. J. Buttner, (1998) Initiation of aerial mycelium formation in *Streptomyces*. *Curr Opin Microbiol* **1**: 656–662.

Kieser, T., M. J. Bibb, M. J. Buttner, K. F. Chater & D. A. Hopwood, (2000) *Practical Streptomyces genetics*. The John Innes Foundation, Norwich, United Kingdom.

Kim, H. J., M. J. Calcutt, F. J Schmidt & K. F Chater, (2000) Partitioning of the linear chromosome during sporulation of *Streptomyces coelicolor* A3(2) involves an *oriC*-linked *parAB* locus. *J Bacteriol* **182**: 1313–1320.

Kirby, R., (2011) Chromosome diversity and similarity within the *Actinomycetales*. *FEMS Microbiol Lett* **319**: 1–10.

Klein, R. J., Z. Misulovin & S. R. Eddy, (2002) Noncoding RNA genes identified in AT-rich hyperthermophiles. *Proc Natl Acad Sci USA* **99**: 7542–7547.

Kleinschnitz, E. M., A. Heichlinger, K. Schirner, J. Winkler, A. Latus, I. Maldener, W. Wohlleben & G. Muth, (2011) Proteins encoded by the *mre* gene cluster in *Streptomyces coelicolor* A3(2) cooperate in spore wall synthesis. *Mol Microbiol* **79**: 1367–1379.

Koh, J., R. M. Saecker & M. T. Record, (2008) DNA binding mode transitions of *Escherichia coli* HUαβ: evidence for formation of a bent DNA-protein complex on intact, linear duplex DNA. *J Mol Biol* **383**: 324–346.

Kois, A., M. Swiatek, D. Jakimowicz & J. Zakrzewska-Czerwińska, (2009) SMC protein-dependent chromosome condensation during aerial hyphal development in *Streptomyces*. *J Bacteriol* **191**: 310–319.

Krinke, L. & D. L. Wulff, (1987) OOP RNA, produced from multicopy plasmids, inhibits lambda cII gene expression through an RNase III-dependent mechanism. *Genes Dev* **1**: 1005–1013.

Kugel, J. F., (2008) Using FRET to measure the angle at which a protein bends DNA: TBP binding a TATA box as a model system. *Biochem Mol Biol Educ* **36**: 341–346.

Laemmli, U. K., (1970) Cleavage of structural proteins during the assembly of the head of bacteriophage T4. *Nature* **227**: 680–685.

Lakey, J. H., E. J. A. Lea, B. A. M. Rudd, H. M. Wright & D. A. Hopwood, (1983) A new channel-forming antibiotic from *Streptomyces coelicolor* A3(2) which requires calcium for its activity. *J Gen Microbiol* **129**: 3565–3573.

Landt, S. G., J. A. Lesley, L. Britos & L. Shapiro, (2010) CrfA, a small noncoding RNA regulator of adaptation to carbon starvation in *Caulobacter crescentus*. *J Bacteriol* **192**: 4763–4775.

Lawlor, E. J., H. A. Baylis & K. F. Chater, (1987) Pleiotropic morphological and antibiotic deficiencies result from mutations in a gene encoding a tRNA-like product in *Streptomyces coelicolor* A3(2). *Genes Dev* **1**: 1305–1310.

Lee, K. S., D. Bumbaca, J. Kosman, P. Setlow & M. J. Jedrzejas, (2008) Structure of a protein-DNA complex essential for DNA protection in spores of *Bacillus* species. *Proc Natl Acad Sci USA* **105**: 2806–2811.

Lenz, D. H., K. C. Mok, B. N. Lilley, R. V. Kulkarni, N. S. Wingreen & B. L. Bassler, (2004) The small RNA chaperone Hfq and multiple small RNAs control quorum sensing in *Vibrio harveyi* and *Vibrio cholerae*. *Cell* **118**: 69–82.

Leonard, T. A., J. Møller-Jensen & J. Löwe, (2005) Towards understanding the molecular basis of bacterial DNA segregation. *Phil Trans R Soc B* **360**: 523–535.

Leskiw, B. K., E. J. Lawlor, J. M. Fernández-Abalos & K. F. Chater, (1991) TTA codons in some genes prevent their expression in a class of developmental, antibiotic-negative, *Streptomyces* mutants. *Proc Natl Acad Sci USA* **88**: 2461–2465.

Levin, P. A. & R. Losick, (1994) Characterization of a cell division gene from *Bacillus subtilis* that is required for vegetative and sporulation septum formation. *J Bacteriol*

176: 1451–1459.

Loh, E., O. Dussurget, J. Gripenland, K. Vaitkevicius, T. Tiensuu, P. Mandin, F. Repoila, C. Buchrieser, P. Cossart & J. Johansson, (2009) A *trans*-acting riboswitch controls expression of the virulence regulator PrfA in *Listeria monocytogenes*. *Cell* **139**: 770–779.

Lorenz, M., A. Hillisch, S. D. Goodman & S. Diekmann, (1999) Global structure similarities of intact and nicked DNA complexed with IHF measured in solution by fluorescence resonance energy transfer. *Nucleic Acids Res* **27**: 4619–4625.

Lucchini, S., G. Rowley, M. D. Goldberg, D. Hurd, M. Harrison & J. C. D. Hinton, (2006) H-NS mediates the silencing of laterally acquired genes in bacteria. *PLoS Pathog* **2**: 746–752.

Luijsterburg, M. S., M. C. Noom, G. J. L. Wuite & R. T. Dame, (2006) The architectural role of nucleoid-associated proteins in the organization of bacterial chromatin: a molecular perspective. *J Struct Biol* **156**: 262–272.

Majdalani, N., C. Cunning, D. Sledjeski, T. Elliott & S. Gottesman, (1998) DsrA RNA regulates translation of RpoS message by an anti-antisense mechanism, independent of its action as an antisilencer of transcription. *Proc Natl Acad Sci USA* **95**: 12462–12467.

Maki, K., T. Morita, H. Otaka & H. Aiba, (2010) A minimal base-pairing region of a bacterial small RNA SgrS required for translational repression of *ptsG* mRNA. *Mol Microbiol* **76**: 782–792.

Mandin, P. & S. Gottesman, (2009) A genetic approach for finding small RNAs regulators of genes of interest identifies RybC as regulating the DpiA/DpiB two-component system. *Mol Microbiol* **72**: 551–565.

Margolin, W., (2005) FtsZ and the division of prokaryotic cells and organelles. *Nat Rev Mol Cell Biol* **6**: 862–871.

Massé, E. & S. Gottesman, (2002) A small RNA regulates the expression of genes involved in iron metabolism in *Escherichia coli*. *Proc Natl Acad Sci USA* **99**: 4620–4625.

Mazza, P., E. E. Noens, K. Schirner, N. Grantcharova, A. M. Mommaas, H. K. Koerten, G. Muth, K. Flärdh, G. van Wezel, (2006) MreB of *Streptomyces coelicolor* is not essential for vegetative growth but is required for the integrity of aerial hyphae and spores. *Mol Microbiol* **60**: 838–852.

McCormick, J. R., E. P. Su, A. Driks & R. Losick, (1994) Growth and viability of *Streptomyces coelicolor* mutant for the cell division gene *ftsZ*. *Mol Microbiol* **14**: 243–254.

McVittie, A., (1974) Ultrastructural studies on sporulation in wild-type and white colony mutants of *Streptomyces coelicolor*. *J Gen Microbiol* **81**: 291–302.

Mendez, C. & K. F. Chater, (1987) Cloning of *whiG*, a gene critical for sporulation of *Streptomyces coelicolor* A3(2). *J Bacteriol* **169**: 5715–5720.

Merrick, M. J., (1976) A morphological and genetic mapping study of bald colony mutants of *Streptomyces coelicolor*. *J Gen Microbiol* **96**: 299–315.

Miguélez, E. M., B. Rueda, C. Hardisson & M. B. Manzanal, (1998) Nucleoid partitioning and the later stages of sporulation septum synthesis are closely associated events in the sporulating hyphae of *Streptomyces carpinensis*. *FEMS Microbiol Lett* **159**: 59–62.

Miller, J. H., (1972) Experiments in molecular genetics, p. xvi, 466 p. Cold Spring Harbor Laboratory, Cold Spring Harbor, N. Y.

Mistry, B. V., R. Del Sol, C. Wright, K. Findlay & P. Dyson, (2008) FtsW is a dispensable cell division protein required for Z-ring stabilization during sporulation septation in *Streptomyces coelicolor*. *J Bacteriol* **190**: 5555–5566.

Mizuno, T., M. Y. Chou & M. Inouye, (1983) Regulation of gene expression by a small RNA transcript (micRNA) in *Escherichia coli* K12. *Proc Japan Acad Ser B: Phys Biol Sci* **59**: 335–338

Mizuno, T., M. Y. Chou & M. Inouye, (1984) A unique mechanism regulating gene expression: translational inhibition by a complementary RNA transcript (micRNA). *Proc Natl Acad Sci USA* **81**: 1966–1970.

Mohl, D. A. & J. W. Gober, (1997) Cell cycle-dependent polar localization of chromosome partitioning proteins in *Caulobacter crescentus*. *Cell* **88**: 675–684.

Moll, I., A. Resch & U. Bläsi, (1998) Discrimination of 5′-terminal start codons by translation initiation factor 3 is mediated by ribosomal protein S1. *FEBS Lett* **436**: 213–217.

Molle, V., W. J. Palframan, K. C. Findlay & M. J. Buttner, (2000) WhiD and WhiB, homologous proteins required for different stages of sporulation in *Streptomyces coelicolor* A3(2). *J Bacteriol* **182**: 1286–1295.

Moody, M. J., R. A. Young, S. E. Jones & M. A. Elliot, (2013) Comparative analysis of non-coding RNAs in the antibiotic producing *Streptomyces* bacteria. *BMC Genomics*, submitted.

Morikawa, K., R. L. Ohniwa, J. Kim, A. Maruyama, T. Ohta & K. Takeyasu, (2006) Bacterial nucleoid dynamics: oxidative stress response in *Staphylococcus aureus*. *Genes Cells* **11**: 409–423.

Nair, S. & S. E. Finkel, (2004) Dps protects cells against multiple stresses during stationary phase. *J Bacteriol* **186**: 4192–4198.

Navarre, W. W., S. Porwollik, Y. Wang, M. McClelland, H. Rosen, S. J. Libby & F. C. Fang, (2006) Selective silencing of foreign DNA with low GC content by the H-NS protein in *Salmonella*. *Science* **313**: 236–238.

Nett, M., H. Ikeda & B. S. Moore, (2009) Genomic basis for natural product biosynthetic diversity in the actinomycetes. *Nat Prod Rep* **26**: 1362–1384.

Nguyen, K. T., J. Tenor, H. Stettler, L. T. Nguyen, L. D. Nguyen & C. J. Thompson, (2003) Colonial differentiation in *Streptomyces coelicolor* depends on translation of a specific codon within the *adpA* gene. *J Bacteriol* **185**: 7291–7296.

Noens, E. E. E., V. Mersinias, B. A. Traag, C. P. Smith, H. K. Koerten & G. P. van Wezel, (2005) SsgA-like proteins determine the fate of peptidoglycan during sporulation of *Streptomyces coelicolor*. *Mol Microbiol* **58**: 929–944.

Nou, X., B. Braaten, L. Kaltenbach & D. A. Low, (1995) Differential binding of Lrp to two sets of pap DNA binding sites mediated by Pap I regulates Pap phase variation in *Escherichia coli*. *EMBO J* **14**: 5785–5797.

O'Reilly, M. & K. M. Devine, (1997) Expression of AbrB, a transition state regulator from *Bacillus subtilis*, is growth phase dependent in a manner resembling that of Fis, the nucleoid binding protein from *Escherichia coli*. *J Bacteriol* **179**: 522–529.

Ohniwa, R. L., K. Morikawa, J. Kim, T. Ohta, A. Ishihama, C. Wada & K. Takeyasu, (2006) Dynamic state of DNA topology is essential for genome condensation in bacteria. *EMBO J* **25**: 5591–5602.

Omer, C. A., D. Stein & S. N. Cohen, (1988) Site-specific insertion of biologically functional adventitious genes into the *Streptomyces lividans* chromosome. *J Bacteriol* **170**: 2174–2184.

Oshima, T., S. Ishikawa, K. Kurokawa, H. Aiba & N. Ogasawara, (2006) *Escherichia coli* histone-like protein H-NS preferentially binds to horizontally acquired DNA in association with RNA polymerase. *DNA Res* **13**: 141–153.

Paget, M. S. B., L. Chamberlin, A. Atrih, S. J. Foster & M. J. Buttner, (1999) Evidence that the extracytoplasmic function sigma factor σ^E is required for normal cell wall structure in *Streptomyces coelicolor* A3(2). *J Bacteriol* **181**: 204–211.

Pan, C. Q., S. E. Finkel, S. E. Cramton, J. A. Feng, D. S. Sigman & R. C. Johnson, (1996) Variable structures of Fis-DNA complexes determined by flanking DNA-protein contacts. *J Mol Biol* **264**: 675–695.

Pan, C. Q., J. A. Feng, S. E. Finkel, R. Landgraf, D. Sigman & R. C. Johnson, (1994)

Structure of the *Escherichia coli* Fis-DNA complex probed by protein conjugated with 1,10-phenanthroline copper(I) complex. *Proc Natl Acad Sci USA* **91**: 1721–1725.

Pánek, J., J. Bobek, K. Mikulík, M. Basler & J. Vohradský, (2008) Biocomputational prediction of small non-coding RNAs in *Streptomyces*. *BMC Genomics* **9**: 217.

Pease, P. J., O. Levy, G. J. Cost, J. Gore, J. L. Ptacin, D. Sherratt, C. Bustamante & N. R. Cozzarelli, (2005) Sequence-directed DNA translocation by purified FtsK. *Science* **307**: 586–590.

Pedulla, M. L. & G. F. Hatfull, (1998) Characterization of the *mIHF* gene of *Mycobacterium smegmatis*. *J Bacteriol* **180**: 5473–5477.

Pedulla, M. L., M. H. Lee, D. C. Lever & G. F. Hatfull, (1996) A novel host factor for integration of mycobacteriophage L5. *Proc Natl Acad Sci USA* **93**: 15411–15416.

Peirson, S. N., J. N. Butler & R. G. Foster, (2003) Experimental validation of novel and conventional approaches to quantitative real-time PCR data analysis. *Nucleic Acids Res* **31**: e73

Piret, J. M. & K. F. Chater, (1985) Phage-mediated cloning of *bldA*, a region involved in *Streptomyces coelicolor* morphological development, and its analysis by genetic complementation. *J Bacteriol* **163**: 965–972.

Pope, M. K., B. D. Green & J. Westpheling, (1996) The *bld* mutants of *Streptomyces coelicolor* are defective in the regulation of carbon utilization, morphogenesis and cell-cell signalling. *Mol Microbiol* **19**: 747–756.

Pope, M. K., B. Green & J. Westpheling, (1998) The *bldB* gene encodes a small protein required for morphogenesis, antibiotic production, and catabolite control in *Streptomyces coelicolor*. *J Bacteriol* **180**: 1556–1562.

Potúcková, L., G. H. Kelemen, K. C. Findlay, M. A. Lonetto, M. J. Buttner & J. Kormanec, (1995) A new RNA polymerase sigma factor, σ^F, is required for the late stages of morphological differentiation in *Streptomyces* spp. *Mol Microbiol* **17**: 37–48.

Prieto, A. I., C. Kahramanoglou, R. M. Ali, G. M. Fraser, A. S. N. Seshasayee & N. M. Luscombe, (2011) Genomic analysis of DNA binding and gene regulation by homologous nucleoid-associated proteins IHF and HU in *Escherichia coli* K12. *Nucleic Acids Res* 40: 3524–3537.

Ptacin, J. L., S. F. Lee, E. C. Garner, E. Toro, M. Eckart, L. R. Comolli, W. E. Moerner & L. Shapiro, (2010) A spindle-like apparatus guides bacterial chromosome segregation. *Nat Cell Biol* **12**: 791–798.

Qu, Y., C. J. Lim, Y. R. Whang, J. Liu & J. Yan, (2013) Mechanism of DNA organization by *Mycobacterium tuberculosis* protein Lsr2. *Nucleic Acids Res* **41**: 5263–5272.

Raghavan, R., E. A. Groisman & H. Ochman, (2011) Genome-wide detection of novel regulatory RNAs in *E. coli*. *Genome Res* **21**: 1487–1497.

Ragkousi, K., A. E. Cowan, M. A. Ross & P. Setlow, (2000) Analysis of nucleoid morphology during germination and outgrowth of spores of *Bacillus species. J Bacteriol* **182**: 5556–5562.

Redenbach, M., H. M. Kieser, D. Denapaite, A. Eichner, J. Cullum, H. Kinashi & D. A. Hopwood, (1996) A set of ordered cosmids and a detailed genetic and physical map for the 8 Mb *Streptomyces coelicolor* A3(2) chromosome. *Mol Microbiol* **21**: 77–96.

Rice, P. A., S. W. Yang, K. Mizuuchi & H. A. Nash, (1996) Crystal structure of an IHF-DNA complex: a protein-induced DNA U-turn. *Cell* **87**: 1295–1306.

Rigali, S., F. Titgemeyer, S. Barends, S. Mulder, A. W. Thomae, D. A. Hopwood & G. P. van Wezel, (2008) Feast or famine: the global regulator DasR links nutrient stress to antibiotic production by *Streptomyces*. *EMBO Rep* **9**: 670–675.

Romeo, T., (1998) Global regulation by the small RNA-binding protein CsrA and the non-coding RNA molecule CsrB. *Mol Microbiol* **29**: 1321–1330.

Rouvière-Yaniv, J., M. Yaniv & J. E. Germond, (1979) *E. coli* DNA binding protein HU forms nucleosome-like structure with circular double-stranded DNA. *Cell* **17**: 265–274.

Ryding, N. J., G. H. Kelemen, C. A. Whatling, K. Flärdh, M. J. Buttner & K. F. Chater, (1998) A developmentally regulated gene encoding a repressor-like protein is essential for sporulation in *Streptomyces coelicolor* A3 (2). *Mol Microbiol* **29**: 343–357.

Salerno, P., J. Larsson, G. Bucca, E. Laing, C. P. Smith & K. Flärdh, (2009) One of the two genes encoding nucleoid-associated HU proteins in *Streptomyces coelicolor* is developmentally regulated and specifically involved in spore maturation. *J Bacteriol* **191**: 6489–6500.

Sambrook, J. & D. W. Russell, (2001) *Molecular cloning: a laboratory manual*. Cold Spring Harbor Laboratory Press, Cold Spring Harbor, N. Y.

Sassetti, C. M., D. H. Boyd & E. J. Rubin, (2003) Genes required for mycobacterial growth defined by high density mutagenesis. *Mol Microbiol* **48**: 77–84.

Sawitzke, J. A. & S. Austin, (2000) Suppression of chromosome segregation defects of *Escherichia coli muk* mutants by mutations in topoisomerase I. *Proc Natl Acad Sci USA* **97**: 1671–1676.

Schmitt-John, T. & J. W. Engels, (1992) Promoter constructs for efficient secretion expression in *Streptomyces lividans*. *Applied Micriobiol Biotechnol* **36**: 493–498.

Schwedock, J., J. R. McCormick, E. R. Angert, J. R. Nodwell & R. Losick, (1997) Assembly of the cell division protein FtsZ into ladder-like structures in the aerial hyphae of *Streptomyces coelicolor*. *Mol Microbiol* **25**: 847–858.

Sharma, C. M., S. Hoffmann, F. Darfeuille, J. Reignier, S. Findeiß, A. Sittka, S. Chabas, K. Reiche, J. Hackermüller, R. Reinhardt, P. F. Stadler & J. Vogel, (2010) The primary transcriptome of the major human pathogen *Helicobacter pylori*. *Nature* **464**: 250–255.

Sharma, C. M. & J. Vogel, (2009) Experimental approaches for the discovery and characterization of regulatory small RNA. *Curr Opin Microbiol* **12**: 536–546.

Sievers, J. & J. Errington, (2000) The *Bacillus subtilis* cell division protein FtsL localizes to sites of septation and interacts with DivIC. *Mol Microbiol* **36**: 846–855.

Silvaggi, J. M., J. B. Perkins & R. Losick, (2006) Genes for small, noncoding RNAs under sporulation control in *Bacillus subtilis*. *J Bacteriol* **188**: 532–541.

Soppa, J., (2001) Prokaryotic structural maintenance of chromosomes (SMC) proteins: distribution, phylogeny, and comparison with MukBs and additional prokaryotic and eukaryotic coiled-coil proteins. *Gene* **278**: 253–264.

Sorokin, A., P. Serror, P. Pujic, V. Azevedo & S. D. Ehrlich, (1995) The *Bacillus subtilis* chromosome region encoding homologues of the E*scherichia coli mssA* and *rpsA* gene products. *Microbiol* **141**: 311–319.

Spurio, R., M. Dürrenberger, M. Falconi, A. La Teana, C. L. Pon & C. O. Gualerzi, (1992) Lethal overproduction of the *Escherichia coli* nucleoid protein H-NS: ultramicroscopic and molecular autopsy. *Mol Gen Genet* **231**: 201–211.

Stackebrandt, E. & C. R. Woese, (1981) Towards a phylogeny of the actinomycetes and related organisms. *Curr Microbiol* **5**: 197–202.

Stella, S., D. Cascio & R. C. Johnson, (2010) The shape of the DNA minor groove directs binding by the DNA-bending protein Fis. *Genes Dev* **24**: 814–826.

Storz, G., J. A. Opdyke & A. Zhang, (2004) Controlling mRNA stability and translation with small, noncoding RNAs. *Curr Opin Microbiol* **7**: 140–144.

Sun, J., G. H. Kelemen, J. M. Fernández-Abalos & M. J. Bibb, (1999) Green fluorescent protein as a reporter for spatial and temporal gene expression in *Streptomyces coelicolor* A3(2). *Microbiol* **145**: 2221–2227.

Swiercz, J. P. & M. A. Elliot, (2012) *Streptomyces* sporulation. In: Bacterial Spores: Current Research and Applications. E. Abel-Santos (ed.) Norfolk, U.K. Horizon Scientific Press, pp. 39–56

Swiercz, J. P., Hindra, J. Bobek, H. J. Haiser, C. Di Berardo, B. Tjaden & M. A. Elliot, (2008) Small non-coding RNAs in *Streptomyces coelicolor*. *Nucleic Acids Res* **36**: 7240–7251.

Swiercz, J. P., T. Nanji, M. Gloyd, A. Guarné & M. A. Elliot, (2013) A novel nucleoid-associated protein specific to the actinobacteria. *Nucleic Acids Res* **41**: 4171–4184.

Swinger, K. K., K. M. Lemberg, Y. Zhang & P. A. Rice, (2003) Flexible DNA bending in HU-DNA cocrystal structures. *EMBO J* **22**: 3749–3760

Swinger, K. K. & P. A. Rice, (2007) Structure-based analysis of HU-DNA binding. *J Mol Biol* **365**: 1005–1016.

Takano, E., M. Tao, F. Long, M. J. Bibb, L. Wang, W. Li, M. J. Buttner, M. J. Bibb, Z. W. Deng & K. F. Chater, (2003) A rare leucine codon in *adpA* is implicated in the morphological defect of *bldA* mutants of *Streptomyces coelicolor*. *Mol Microbiol* **50**: 475–486.

Takayama, K. M., N. Houba-Herin & M. Inouye, (1987) Overproduction of an antisense RNA containing the oop RNA sequence of bacteriophage lambda induces clear plaque formation. *Mol Gen Genet* **210**: 184–186.

Tezuka, T., H. Hara, Y. Ohnishi & S. Horinouchi, (2009) Identification and gene disruption of small noncoding RNAs in *Streptomyces griseus*. *J Bacteriol* **191**: 4896–4904.

Thanbichler, M. & L. Shapiro, (2006) Chromosome organization and segregation in bacteria. *J Struct Biol* **156**: 292–303.

Tjaden, B., (2008)a Prediction of small, noncoding RNAs in bacteria using heterogeneous data. *J Math Biol* **56**: 183–200.

Tjaden, B., (2008b) TargetRNA: a tool for predicting targets of small RNA action in bacteria. *Nucleic Acids Res* **36**: W109–113.

Traag, B. A. & G. P. van Wezel, (2008) The SsgA-like proteins in actinomycetes: small proteins up to a big task. *Antonie Van Leeuwenhoek* **94**: 85–97.

Travers, A. & G. Muskhelishvili, (2005) Bacterial chromatin. *Curr Opin Genet Dev* **15**: 507–514.

Trotochaud, A. E. & K. M. Wassarman, (2004) 6S RNA function enhances long-term cell survival. *J Bacteriol* **186**: 4978–4985.

Trotochaud, A. E. & K. M. Wassarman, (2005) A highly conserved 6S RNA structure is required for regulation of transcription. *Nat Struct Mol Biol* **12**: 313–319.

Tsui, H. C. T., H. C. E. Leung & M. E. Winkler, (1994) Characterization of broadly

pleiotropic phenotypes caused by an *hfq* insertion mutation in *Escherichia coli* K-12. *Mol Microbiol* **13**: 35–49.

Tu, K. C. & B. L. Bassler, (2007) Multiple small RNAs act additively to integrate sensory information and control quorum sensing in *Vibrio harveyi*. *Genes Dev* **21**: 221–233.

Valentin-Hansen, P., M. Eriksen & C. Udesen, (2004) MicroReview: The bacterial Sm-like protein Hfq: a key player in RNA transactions. *Mol Microbiol* **51**: 1525–1533.

van den Ent, F., L. A. Amos & J. Löwe, (2001) Prokaryotic origin of the actin cytoskeleton. *Nature* **413**: 39–44.

van Wezel, G. P., J. Van Der Meulen, S. Kawamoto, R. G. M. Luiten, H. K. Koerten, B. Kraal, (2000) *ssgA* is essential for sporulation of *Streptomyces coelicolor* A3(2) and affects hyphal development by stimulating septum formation. *J Bacteriol* **182**: 5653–5662.

van Vliet, A. H. M., (2010) Next generation sequencing of microbial transcriptomes: challenges and opportunities. *FEMS Microbiol Lett* **302**: 1–7.

Vanderpool, C. K. & S. Gottesman, (2004) Involvement of a novel transcriptional activator and small RNA in post-transcriptional regulation of the glucose phosphoenolpyruvate phosphotransferase system. *Mol Microbiol* **54**: 1076–1089.

Vockenhuber, M. P., C. M. Sharma, M. G. Statt, D. Schmidt, Z. Xu, S. Dietrich, K. Liesegang, D. H. Matthews & B. Suess, (2011) Deep sequencing-based identification of small non-coding RNAs in *Streptomyces coelicolor*. *RNA Biol* **8**: 468–477.

Vockenhuber, M. P. & B. Suess, (2012) *Streptomyces coelicolor* sRNA scr5239 inhibits agarase expression by direct base pairing to the *dagA* coding region. *Microbiol* **158**: 424–435.

Vogel, J. & K. Papenfort, (2006) Small non-coding RNAs and the bacterial outer membrane. *Curr Opin Microbiol* **9**: 605–611.

Wang, S., R. Cosstick, J. F. Gardner & R. I. Gumport, (1995) The specific binding of *Escherichia coli* integration host factor involves both major and minor grooves of DNA. *Biochem* **34**: 13082–13090.

Wang, L., Y. Yu, X. He, X. Zhou, Z. Deng, K. F. Chater & M. Tao, (2007) Role of an FtsK-like protein in genetic stability in *Streptomyces coelicolor* A3(2). *J Bacteriol* **189**: 2310–2318.

Wassarman, K. M. (2007) 6S RNA: a small RNA regulator of transcription. *Curr Opin Microbiol* **10**: 164–168.

Wassarman, K. M., F. Repoila, C. Rosenow, G. Storz & S. Gottesman, (2001) Identification of novel small RNAs using comparative genomics and microarrays. *Genes Dev* **15**: 1637–1651.

Weilbacher, T., K. Suzuki, A. K. Dubey, X. Wang, S. Gudapaty, I. Morozov, C. S. Baker, D. Georgellis, P. Babitzke & T. Romeo, (2003) A novel sRNA component of the carbon storage regulatory system of *Escherichia coli*. *Mol Microbiol* **48**: 657–670.

Wilderman, P. J., N. A. Sowa, D. J. FitzGerald, P. C. FitzGerald, S. Gottesman, U. A. Ochsner & M. L. Vasil, (2004) Identification of tandem duplicate regulatory small RNAs in *Pseudomonas aeruginosa* involved in iron homeostasis. *Proc Natl Acad Sci USA* **101**: 9792–9797.

Willemse, J., J. W. Borst, E. de Waal, T. Bisseling & G. P. van Wezel, (2011) Positive control of cell division: FtsZ is recruited by SsgB during sporulation of *Streptomyces*. *Genes Dev* **25**: 89–99.

Willins, D. A., C. W. Ryan, J. V. Platko & J. M. Calvo, (1991) Characterization of Lrp, and *Escherichia coli* regulatory protein that mediates a global response to leucine. *J Biol Chem* **266**: 10768–10774.

Wojtuszewski, K. & I. Mukerji, (2003) HU binding to bent DNA: a fluorescence resonance energy transfer and anisotropy study. *Biochem* **42**: 3096–3104.

Wright, G. D., (2007) The antibiotic resistome: the nexus of chemical and genetic diversity. *Nat Rev Microbiol* **5**: 175–186.

Wu, L. J. & J. Errington, (2004) Coordination of cell division and chromosome segregation by a nucleoid occlusion protein in *Bacillus subtilis*. *Cell* **117**: 915–925.

Xiao, B., W. Li, G. Guo, B. Li, Z. Liu, K. Jia, Y. Guo, X. Mao & Q. Zou, (2009) Identification of small noncoding RNAs in *Helicobacter pylori* by a bioinformatics-based approach. *Curr Microbiol* **58**: 258–263.

Yanisch-Perron, C., J. Vieira & J. Messing, (1985) Improved M13 phage cloning vectors and host strains: nucleoid sequences of the M13mp18 and pUC19 vectors. Gene **33**: 103–119.

Zhang, A., K. M. Wassarman, C. Rosenow, B. C. Tjaden, G. Storz & S. Gottesman, (2003) Global analysis of small RNA and mRNA targets of Hfq. *Mol Microbiol* **50**: 1111–1124.

Zharkov, D. O., G. Golan, R. Gilboa, A. S. Fernandes, S. E. Gerchman, J. H. Kycia, R. A. Rieger, A. P. Grollman & G. Shoham, (2002) Structural analysis of an *Escherichia coli* endonuclease VIII covalent reaction intermediate. *EMBO J* **21**: 789–800.